

**GROUND REFERENCE POINTS ADJUSTMENT
SCHEME
FOR BIPED WALKING ON UNEVEN TERRAIN**

WU NING

NATIONAL UNIVERSITY OF SINGAPORE

2014

**GROUND REFERENCE POINTS ADJUSTMENT SCHEME
FOR BIPED WALKING ON UNEVEN TERRAIN**

WU NING

(B. Eng) SCU

A THESIS SUBMITTED

**FOR THE DEGREE OF DOCTOR OF PHILOSOPHY
DEPARTMENT OF MECHANICAL ENGINEERING**

NATIONAL UNIVERSITY OF SINGAPORE

2014

DECLARATION

I hereby declare that the thesis is my original work and it has been written by me in its entirety. I have duly acknowledged all the sources of information which have been used in the thesis.

This thesis has also not been submitted for any degree in any university previously.

A handwritten signature in blue ink, appearing to be the Chinese characters '吴宁' (Wu Ning), is positioned above a horizontal line.

Wu Ning

08 January 2014

Acknowledgements

I want to express my most sincere gratitude to my supervisors, Associate Professor Chew Chee-Meng and Professor Poo Aun Neow. I want to thank them for their motivation, support, and critique about the work. Their depth of knowledge, insight and untiring work ethic has been and will continue to be a source of inspiration to me.

I have also benefitted from discussion with many of seniors and colleagues. In particular Li Renjun, Shen Bingquan, Albertus Hendrawan Adiwahono, Huang Weiwei, Yang Lin, Tan Boon Hwa and others in the Control and Mechatronics Lab.

I also would like to thank National University of Singapore for offering me research scholarship and research facilities. I benefitted from the abundant professional books and technical Journal collection at NUS library.

Finally, I would like to devote the thesis to my family for their love and understanding.

Table of Content

Acknowledgements	i
Table of Content.....	ii
Summary.....	v
List of Tables	vii
List of Figures.....	vii
List of Abbreviations	x
Nomenclature	xi
Chapter 1 Introduction.....	1
1.1 Background and Motivation	1
1.2 Research Objectives and Contributions	3
1.3 Simulation Tools.....	5
1.4 Organization of the Thesis	6
Chapter 2 Literature Review	8
2.1 Overview of Bipedal Robot Walking	8
2.2 Stability of Bipedal Robot Walking.....	11
2.2.1 Poincaré Return Map	12
2.2.2 Gait Sensitive Norm.....	12
2.2.3 Zero Moment Point (ZMP)	13
2.2.4 Capturability	14
2.3 Bipedal Robot Walking on Uneven Terrains.....	14
2.3.1 Walking on Known Terrain	15
2.3.2 Walking on Unknown Terrain	16
2.4 Summary	17
Chapter 3 Moving Ground Reference Map.....	18
3.1 Introduction.....	18
3.2 Dynamic Model of Biped Robot.....	19

3.2.1	Linear Inverted Pendulum Mode	20
3.2.2	The Natural Stepping Time for the LIPM.....	22
3.3	Ground Reference Point in Different Models	23
3.3.1	Point Foot Biped	23
3.3.2	Finite-Size Foot Biped: Zero Moment Point	24
3.4	Moving Ground Reference Map	27
3.4.1	Moving Ground Reference Map for Next Step.....	28
3.4.1.1	Selection of the Weighting Factors	32
3.4.1.2	Optimization Tools	33
3.4.2	Moving Ground Reference Map for Current Step	37
3.5	Discussion	40
3.5.1	Comparison with Capture Point.....	40
3.5.1.1	Orbit Energy	41
3.5.1.2	Relationship with Capture Point	43
3.6	Summary	45

Chapter 4 Biped Robot Walking Algorithm Based on Proposed

Moving Ground Reference Map.....	47
4.1 Introduction.....	47
4.2 Motivation.....	47
4.3 Bipedal Robot Walking Based on Preview control	49
4.3.1 Background.....	49
4.3.2 Control Architecture of Bipedal Robot Walking	53
4.3.3 Online Preview Control	55
4.3.4 Simulation Environment	58
4.3.5 Simulation Results	59
4.4 Walking on Uneven Terrain with Unknown Disturbance	63
4.4.1 Example 1: with Unknown Staircase	63
4.4.2 Example 2: with Unknown Staircase and Slope	67
4.5 Summary	72

Chapter 5	Biped Robot Walking Algorithm Based on Proposed Moving Ground Reference Map with Genetic Algorithm Adjustment	73
5.1	Introduction.....	73
5.2	Walking Pattern Generation on Uneven Terrain	74
5.2.1	Dynamics of Bipedal Robot Walking on Uneven Terrain.....	74
5.2.2	Overall Strategy of Bipedal Robot Walking on Uneven Terrain.....	77
5.3	Bipedal Locomotion on Slope Terrain.....	79
5.4	Bipedal Locomotion on Stair Terrain	87
5.5	Summary	94
Chapter 6	Conclusions.....	95
6.1	Summary of Results	95
6.2	Discussion of Practical Implementation	96
6.3	Contribution of the Research	100
6.4	Limitations and Future Work.....	101
	Bibliography	103
	Appendix I: Realistic humanoid robot model details	107
A.1	Dimensions.....	107
A.2	Dynamic of Model	107
	Appendix II: Description of NUSBIP-III ASLAN	112
B.1	Brief History.....	112
B.2	Current Development	112
B.3	Potential future plans.....	116

Summary

In this thesis, we propose an optimized approach for humanoid robot trajectory generation in complex environments, especially uneven terrain. This online model based walking trajectory generation and optimization considers both current robot state and the constraints of landing location. Different terrain walking can be realized by choosing different weighting factors.

There are mainly two categories for bipedal robot walking over uneven terrain. One is to plan the robot motion based on the terrain profile. This category focuses on the accuracy of tracking the predefined trajectories. However, the robustness of this approach may be poor since it could not handle unknown disturbance. The other is to prevent robot from falling due to unknown disturbance. This category put more focus on the online walking motion generation to achieve robust performance with strong disturbance rejection ability. For rough terrain such as steep staircase and large slope, further control approaches should be developed. Therefore, the aim of this research was to synthesize the terrain profile with online optimized stabilization to achieve robust walking performance.

We presented a novel approach called Moving Ground Reference Map, which is continuously adjusted in real time based on the robot's actual dynamics during locomotion to maintain stable walking in face of external disturbance. The moving ground reference map and preview control presented in this thesis were considerably important since they not only improved the disturbance rejection ability but also avoided the falling due to visible unevenness by containing the terrain profiles. The moving ground reference map was used to stabilize the bipedal robot walking by adjusting the ground reference points. The preview controller was presented to generate the walking pattern with consideration of terrain profiles.

Dynamic simulation software Webots has been used to verify the effectiveness of the controller. A clearer explanation for the bipedal robot walking on uneven terrain was presented. The proposed approach was verified using a simple linear-inverted pendulum model. Based on the sensor reading, the online modification of the pre-defined geometric footstep map with constraint was realized. Given an uneven terrain, the robot could walk following the pre-defined map and automatically modify the motion to be more stable. Finally, the results showed that it could significantly improve walking stability, and also minimize the error in tracking the pre-defined trajectory.

In conclusion, this study can achieve an excellent performance for bipedal robot walking, especially over uneven terrain. The technique is very general and can be applied to a wide variety of humanoid robots.

List of Tables

Table 4.1 Simulated humanoid robot parameters	58
Table 5.1 GA Set-up for the generation of optimization of weighting factors	81
Table 5.2 GA Set-up for the generation of optimization of weighting factors	88
Table 6.1 Root-Mean-Square (RMS) power consumption in both legs	97
Table 6.2 Peak power (Max) in both legs	97
Table A.1 Simulated bipedal robot model	108
Table B.1 Specification of NUSBIP-III ASLAN	114

List of Figures

Figure 1.1 User interface of Webots [8]	6
Figure 2.1 Fully actuated biped robots: ASIMO, HRP, HUBO[11-13]	9
Figure 2.2 Biped robot walking on varied terrain[37]	15
Figure 3.1 2D Linear Inverted Pendulum	20
Figure 3.2 Transition of linear inverted pendulum	21
Figure 3.3 Foot placement point in the point foot LIPM	24
Figure 3.4 ZMP in finite-size foot based on 3D linear inverted pendulum mode	25
Figure 3.5 2D Dynamic analysis of linear inverted pendulum mode	26
Figure 3.6 Comparison between pre-planned and actual walking process	30
Figure 3.7 Stability Region of the Finite-Size Foot	38
Figure 3.8 2D Orbit Energy	42
Figure 3.9 3D Orbit Energy	43
Figure 4.1 Requirements of stable walking on uneven terrain	48

Figure 4.2 2D Cart-Table Model[1].....	50
Figure 4.3 Block Diagram of Preview Control.....	52
Figure 4.4 The Error of Support Foot Position and ZMP Reference.....	53
Figure 4.5 Simulation Structure of Bipedal Robot Walking on Uneven Terrain	54
Figure 4.6 Degrees of freedom for simulated humanoid robot.....	58
Figure 4.7 Foot structure with force sensors.....	59
Figure 4.8 Gain of Preview Action	60
Figure 4.9 The walking on flat terrain trajectories of CoM, ZMP and foot in x direction	61
Figure 4.10 The walking on flat terrain trajectories of CoM, ZMP in y direction	61
Figure 4.11 Joints trajectories of walking on flat terrain in right leg	62
Figure 4.12 Joints trajectories of walking on flat terrain in left leg.....	62
Figure 4.13 Walking on the flat terrain with unknown staircase with the proposed approach	63
Figure 4.14 Walking on terrain containing step trajectories in x direction	64
Figure 4.15 Walking without disturbance.....	65
Figure 4.16 Walking on the step	66
Figure 4.17 Walking down from the step	66
Figure 4.18 Terrain profiles in horizontal plane	67
Figure 4.19 Walking performance with the proposed approach.....	67
Figure 4.20 Walking performance without the proposed approach.....	68
Figure 4.21 CoM and ZMP trajectories of biped walking on step and 2 degree slope in x direction.....	69
Figure 4.22 Zoomed in of CoM and ZMP trajectories of biped walking on step and 2 degree slope in x direction	70
Figure 4.23 CoM and ZMP trajectories of biped walking on step and 2 degree slope in y direction.....	70

Figure 4.24 The ground projection of the real CoM and the real ZMP trajectories on the uneven terrain.....	71
Figure 5.1 3D Dynamic Model of Bipedal Robot Walking on Uneven Terrain	74
Figure 5.2 Structure of bipedal robot walking on uneven terrain	78
Figure 5.3 Biped walking on the slope without online ZMP reference adjustment.....	79
Figure 5.4 Biped walking on the slope with Moving Ground Reference Map	80
Figure 5.5 CoM and ZMP trajectories walking on the slope in x direction with the GA optimal weighting factors.....	81
Figure 5.6 CoM and ZMP trajectories in x direction with not optimal weighting factors.....	83
Figure 5.7 CoM and ZMP trajectories walking on the slope in y direction with the GA optimal weighting factors.....	84
Figure 5.8 The stick diagram of the biped walking on the slope.	84
Figure 5.9 The ground projection of the real CoM and the real ZMP trajectories on the 8 degree slope.....	85
Figure 5.10 CoM and ZMP trajectories in x direction with sudden change due to the external force when 6s.	86
Figure 5.11 Terrain Profile in Side View.....	87
Figure 5.12 Stable Walking on Stair with unknown variations heights	88
Figure 5.13 CoM and ZMP trajectories of biped walking on various heights stairs in x direction with the GA optimized weighting	90
Figure 5.14 CoM and ZMP trajectories of biped walking on various heights stairs in x direction with $R=0$, $p=1$	90
Figure 5.15 CoM and ZMP trajectories of biped walking on various heights stairs in x direction with $R=I$; $p=0$	91
Figure 5.16 Comparison of difference adjusted ZMP reference of biped walking on various heights stairs in x direction.....	91
Figure 5.17 CoM and ZMP trajectories of biped walking on various heights stairs in y direction.....	93

Figure 5.18 The stick diagram of the biped walking on the stairs	93
Figure 6.1 Left leg joints velocity, the sub-plots represent the joint velocity of: Hip Roll, Hip Pitch, Knee, Ankle Pitch, and Ankle Roll, respectively.	98
Figure 6.2 Right leg joints velocity, the sub-plots represent the joint velocity of: Hip Roll, Hip Pitch, Knee, Ankle Pitch, and Ankle Roll, respectively.....	98
Figure 6.3 Right leg joints torque, the sub-plots represent the joint torque of: Hip Roll, Hip Pitch, Knee, Ankle Pitch, and Ankle Roll, respectively.	99
Figure 6.4 Left leg joints torque, the sub-plots represent the joint torque of: Hip Roll, Hip Pitch, Knee, Ankle Pitch, and Ankle Roll, respectively.	99
Figure A.1 Simulated bipedal robot dimensions (mm).....	107
Figure B.1 Mechanical drawing and realization of NUSBIP-III ASLAN.....	113
Figure B.2 NUSBIP-III ASLAN legs.	115
Figure B.3: NUSBIP-III ASLAN torso design.	115
Figure B.4: NUSBIP-III ASLAN kicking for goal in ROBOCUP 2010 finale.	116

List of Abbreviations

SSP	Single Support Point
ZMP	Zero Moment Point
LIPM	Linear Inverted Pendulum Mode
CoM	Center of Mass
GA	Genetic Algorithm

Nomenclature

$F(N)$	Force
$F_{GF}(N)$	Ground reaction force
$[F_x \ F_y \ F_z]^T$	Ground reaction force in x, y, z axes
$m(kg)$	Mass of CoM
$g(m/s^2)$	Gravitational acceleration
$r(m)$	Leg length
$p = [p_x \ p_y \ p_z]^T (m)$	Position of Zero Moment Point
$p^{ref} = [p_x^{ref} \ p_y^{ref} \ p_z^{ref}]^T (m)$	Reference of Zero Moment Point
$\theta(rad)$	Degree of inclination angle
$[x \ y \ z]^T (m)$	Position of CoM
$[\dot{x} \ \dot{y} \ \dot{z}]^T (m/s)$	Velocity of CoM
$[\ddot{x} \ \ddot{y} \ \ddot{z}]^T (m/s^2)$	Acceleration of CoM
$z_c(m)$	Constant height of CoM
$x_0^{(n)}(m)$	Initial position of CoM of the n^{th} step
$\dot{x}_0^{(n)}(m/s)$	Initial velocity of CoM of the n^{th} step
$x_T^{(n)}(m)$	Final position of CoM of the n^{th} step
$\dot{x}_T^{(n)}(m/s)$	Final velocity of CoM of the n^{th} step

$s^{(n)}(m)$	Planned step length of the n^{th} step
$\hat{s}^{(n)}(m)$	Actual step length of the n^{th} step
$x_f^{(n)}(m)$	Actual foot landing position of the n^{th} step

Chapter 1

Introduction

1.1 Background and Motivation

Humanoid robots are anthropomorphic robot systems. Generally, humanoid robots move their body by manipulating two legs with respect to the environment. Many researchers anticipate that the humanoid robot industry will be one of the leading industries in the future. It is quite possible, as happened with the personal computer; the day may soon come when there is a robot in every home. Since humanoid robots have similar physical characteristics as humans, they are naturally well-suited to operate in environments designed for humans. The human environment is characterized by discontinuous ground support, such as flights of stairs, uneven terrains, or ladders. Undoubtedly, legs are the most versatile and appropriate tools for locomotion on these uneven terrains. In addition, humanoid robots, like humans, have a very small footprint and can operate in environments which other form of robots cannot easily operate in, for example environments with stairs or other small obstacles. These factors validate the importance and necessity of ongoing research in the domain of humanoid robotics.

There are several motivations for humanoid robot research. Humanoid robots can replace humans in performing dangerous tasks, such as firefighting, space exploration and working in environments with dangerous nuclear radiation. They can also collaborate with humans in the same work place and even use the same tools to increase human productivity and relieve strenuous physical efforts. Moreover, to achieve a better understanding of human walking, the humanoid robot is widely used as a platform to analyze the dynamics and locomotion of humans. Doctors and physiotherapists can then use this

knowledge to improve on the human rehabilitation procedures. It would be difficult to accomplish this well without a deep understanding of the mechanics of human walking motion.

Humans are very versatile and adaptable and can easily handle different ground conditions, reject disturbances while walking and move naturally so as to consume the minimum of energy. The biggest challenge in humanoid robot research is then to develop technologies to control the robot to walk as well as humans do. Achieving this requires several difficult problems to be overcome. Firstly, there is an un-actuated degree of freedom formed by the contact of the foot with the ground surface. This feature distinguishes the walking robots from the robotic arms that use traditional control methods since these arms are fixed to bases. Secondly, the bipedal machine involves non-linear, multi-variable dynamics that make it a difficult problem to find a general analytical solution. Thirdly, walking is not a continuous motion and involves the robot having to switch the support leg during locomotion. Finally, walking on uneven terrains or walking with an unexpected external push, while easily handled by humans, is very challenging for the robot.

To achieve a robust walking behavior, many approaches for bipedal robot walking on the uneven terrains have been proposed. Kajita [1], et al. proposed the preview control approach in which the robot is made to track a pre-defined trajectory. The walking motion of a biped robot is realized by executing the pre-defined trajectories, but in this paper the position of the step adjustment and the current robot state are not mentioned. Based on this approach, several research [2-6] were proposed, which included applying model predictive control to realize online walking motion generation with automatic foot step placement. In the other area, Manchester, et al. [7] proposed a constructive control design for stabilization of non-periodic trajectories of under-actuated robots, which can walk on the uneven, but known terrains without any unexpected disturbances. However, these outcomes are still far from our expectation since the robot may not be able to walk in a stable manner when it lands on an unexpected terrain features, such as a small pothole, and a small

object etc. Therefore, it is necessary to have the capability for online adjustment of the walking pattern to achieve stable bipedal robot walking on an unknown variations of uneven terrain.

The subsequent sections provide the motivation of this thesis and the organization of the thesis. A more detailed discussion of past and ongoing research on humanoid robots will be presented in Chapter 2.

1.2 Research Objectives and Contributions

Achieving stable and reliable bipedal robot walking on uneven terrains remains a challenge. It is desirable for a biped robot to have human-like ability to walk on uneven terrains. When a biped robot is moving on an uneven terrain, it should be able to detect the nature of the terrain just ahead of it and to modify its walking trajectory accordingly. The objective is to avoid premature landing of the swing foot or a wrong foot placement which may lead to a fall. The main research gaps in current bipedal robot walking approaches are identified as follows:

- Most bipedal robot control schemes for the task of walking on uneven terrains rely on walking patterns generated from offline pre-planned trajectories. As a result, these control schemes lack robustness against unexpected and unknown disturbances, which is very common in real world environments.
- Two capabilities are important to achieve reliable and stable walking on uneven terrains. These are tracking of the pre-planned foot location trajectory and disturbance rejection or management. However, most researches focused only on either one of these, while a few others have pursued a tradeoff between the two.

To achieve a robust uneven terrain walking, the main objective of this thesis is to generate a walking pattern that considers both the terrain profile and disturbance resulting from unknown unevenness. More specifically, the objectives of this study are to:

- propose a hybrid hierarchical controller to improve the walking performance;
- propose a moving ground reference map for online adjustment of the foot step positions based on the current state of the robot;

In this thesis, the bipedal robot walking on uneven terrain with unknown unevenness will be presented. An approach, called the moving ground reference map, is proposed to improve the stable walking performance of the robot on such terrains. In this thesis, in order to study the effect of ground reference point adjustment, it considers step time is the constant. The pre-planned foot placements are adjusted online and in real-time using both the current state of the robot and known future terrain information in order to enhance the disturbance rejection ability and to improve stable walking performance. Applying the preview control with the moving ground reference map is shown to improve significantly the robot's walking performance.

The contributions of this thesis are as follows:

- Synthesis of general control architecture for bipedal robot walking over uneven terrain;
- Systematic descriptions of the uneven terrain walking challenge;
- Establishment of a moving ground reference map for improving the stability of locomotion;
- Application of the preview control architecture by using moving ground reference map for generating a robust walking algorithm;
- Verification of the effect of weighting factors in moving ground reference map on bipedal robot walking and Genetic Algorithm is used to optimize the weighting factors.

The algorithm developed in this research is for a fully actuated bipedal robot (6 degrees of freedom at each leg) walking over uneven terrains. The details of the assumptions that are used in the algorithm will be discussed in the

following chapters. The next section describes the simulation tools used in this research.

1.3 Simulation Tools

In this research, the robotics dynamic simulation software Webots [8-10] is used to study the effectiveness of the proposed algorithms. Webots is dynamic simulation software developed by Cyberbotics [10]. It is a development environment used to model, program and simulate robots. Webots relies on ODE, the Open Dynamics Engine, for rigid body dynamics simulation. With Webots, the user can design complex robotic setups, with one or several similar or different robots, in a shared environment. The key parameters such as mass, moment of inertia, shape, and even the color of the robots and the environment can be defined by users. Therefore, it can create 3D virtual worlds with user-defined physical properties.

The most important advantage of Webots is that it allows the user to define the bounding surface of each object. This is particularly suitable for bipedal robot locomotion because it allows the user to specify both the impact and friction properties.

Additionally, one could use any of the common programming languages such as C++, Java, Python and Matlab to program the controllers. In this research, we use the C language in most parts of the simulation, while Matlab is used to implement some of the optimal controllers. Fig.1.2 shows a typical user interface for Webots 5.8.

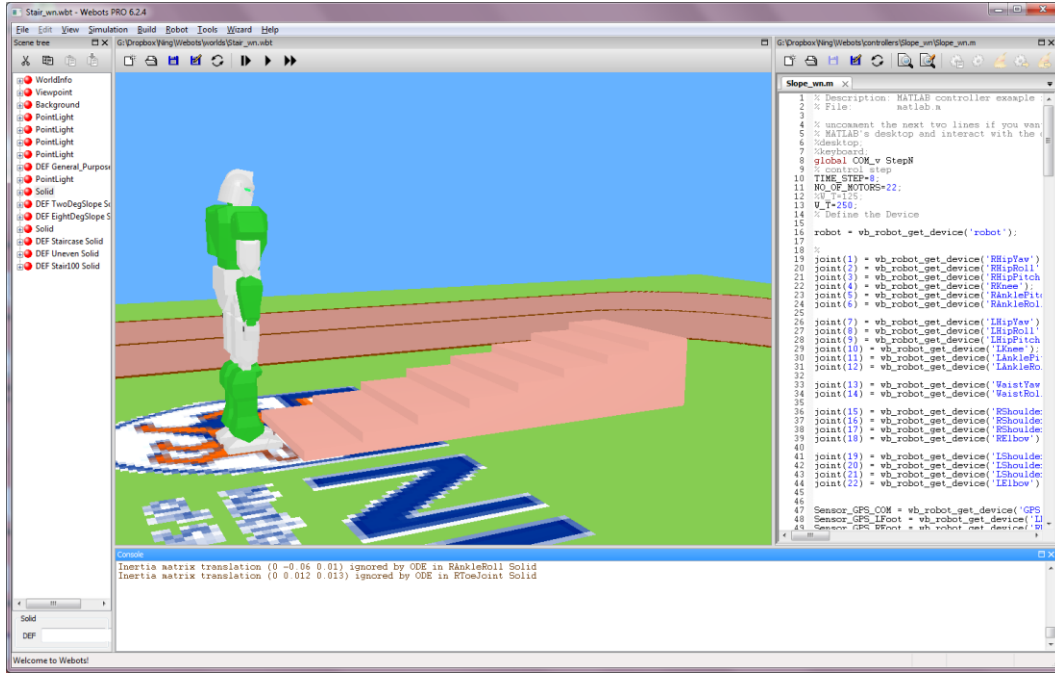


Figure 1.1 User interface of Webots [8]

1.4 Organization of the Thesis

The thesis is organized as follows:

Chapter 2 first looks at current biped walking research, which includes fully actuated, passive and semi-passive robots. The stability criteria for biped robots during walking are then reviewed. These methodologies involve the Poincare Map, ZMP, angular momentum, etc. Finally, a literature review for uneven terrain walking is presented.

Chapter 3 presents the concept of a proposed moving ground reference map, which allows for online adjustment of the ground reference points' locations, to achieve a more stable walking performance. In this chapter, the modeling of the bipedal robot is first discussed. A linear inverted pendulum model (LIPM) is adopted to generate the walking pattern. The properties of the LIPM are discussed to prepare for further illustrations. Secondly, ground reference points are introduced. Finally, the proposed moving ground reference map, which includes both the swing and the support phases, is discussed.

Chapter 4 presents the proposed control architecture for a bipedal robot walking on flat terrains with unknown disturbances. The original preview control and its practical problems are first discussed. Next, a walking pattern generated by a proposed modified preview control with moving ground reference map is presented. The results of the application of the proposed algorithm for a bipedal robot walking on flat terrains with some unknown disturbance are then presented.

Chapter 5 presents the control architecture of a bipedal robot walking on uneven terrains with unknown disturbances. The dynamics of the linear inverted pendulum model for uneven surfaces is discussed. This is followed by a presentation of a proposed modified preview control with moving ground reference map for bipedal walking on uneven terrains. The performance of the proposed moving ground reference map approach is then discussed using simulation results of a bipedal robot walking on terrains with slopes and staircases and with several unknown disturbances.

Chapter 6 concludes this study of bipedal robots walking on uneven terrains. The limitations of the proposed new approaches and areas for future research are then presented.

Chapter 2

Literature Review

The problem of bipedal robots walking on uneven terrains requires a comprehensive understanding of dynamic modeling, kinematics, control and walking pattern generation. In this chapter, a literature review of research on bipedal robots walking on uneven terrains is presented. The research gaps to achieving reliable robust stable bipedal walking on such uneven terrains are highlighted to provide the rationale for the motivation in the proposed research objectives in this thesis.

2.1 Overview of Bipedal Robot Walking

Generally, bipedal walking is the process of alternating the phase of the support leg and the swing leg while maintaining the displacement of the horizontal component of the robot's center of mass strictly monotonic.

In bipedal locomotion, we define the phase where only one leg is in contact with the ground as the single support or swing phase. Conversely, the phase where both feet are on the ground is called the double support phase. In the swing phase, the leg in contact with the ground is called the stance leg. The other leg is referred to as the swing leg, which is placed strictly on the ground in front of the stance leg end the end of the swing phase.

Many advanced robots such as Honda's ASIMO [11], HRP [12], HUBO [13] and BOSTON's PETMAN have all showed walking skills in the human environment as shown in Fig.2.1. Among all these existing bipeds, ASIMO and PETMAN show the best performance in terms of robustness and disturbance rejection ability [14]. Some researchers attempt to exploit the natural dynamics of the humanoid robot and use only simple control methods to achieve stable walking. A few others develop approaches which benefit

from the natural dynamics of the robot's mechanical and geometrical structure although none explicitly exploits this natural dynamics. In the following section, we will review passive dynamics in bipedal walking.

McGeer [15] firstly introduced passive dynamics in 1990. It was inspired by a bipedal toy that had the ability of walking down a slope without using any actuator system. A state-of-the-art passive bipedal robot is the “limit cycle walking” model introduced by Hobbelen and Wisse [16]. Passive walking has one interesting advantage in that it can achieve a gait requiring the minimum energy without active control [17]. However, it also has some disadvantages such as sensitivity to parameter variations, environment limitations, and poor ability for disturbance rejection, and difficulty to control. The following section mainly focuses on solving these problems.



Figure 2.1 Fully actuated biped robots: ASIMO, HRP, HUBO[11-13]

In the field of robotics, research into bipedal locomotion of humanoid robots has been very active in recent years. By virtue of their mechanical structure, one of the significant advantages of legged robots over other types of robots is their ability to navigate various terrains usually accessed by human beings. Walking on flat terrains has been well studied [11, 12, 18], but walking on rough terrains remains a challenge. In general, there are two main groups of approaches for achieving stable bipedal robot locomotion over uneven terrains.

In the first group, the focus is on developing, based on knowledge of the profile of the terrain, a motion plan which can achieve stable robot locomotion [1, 19]. If the robot's joint control systems can then ensure the accuracy of tracking of the predefined trajectories, stable walking will be achieved. In the other group, the assumption made is that there is insufficient knowledge of the terrain to develop a motion plan to achieve stable walking. The focus of this group is then on developing in the robot a strong disturbance rejecting capabilities so that the robot can maintain stable walking without falling even when faced with disturbances and unexpected unevenness in the terrain.

For model-based walking algorithm, many [20] use the pre-recorded joint trajectories generated during motion planning. The robot is primarily controlled by playing back these pre-recorded joint trajectories acquired from direct measurements of human subjects with these adjustments made online to these primary trajectories during locomotion. For example, in Honda's P2 robot, some additional controllers are used to modify the trajectory in order to maintain balance in light of disturbances, and terrain or modeling errors. A ground reaction force controller modifies the joint angle trajectories in order to reach the desired Zero Moment Point (ZMP) to allow the robot to adapt to the uneven terrain. A model ZMP controller shifts the desired ZMP by adjusting the ideal body trajectory when the robot is about to tip over. A foot landing position controller changes the stride length to compensate for changes in the body trajectory made by the model ZMP controller.

As it is difficult to achieve natural walking behaviors using the above pre-defined trajectory approaches, others use heuristic control approaches to generate better trajectories. Dunn and Howe [21] combined both preplanning and heuristic control. Walking speed was controlled by foot placement which changes the step length, based on a symmetry argument. The height of the robot's center of mass was controlled by leg length based on inverse kinematics. The pitch of the upper body was controlled using hip torque on the stance leg. The swing-leg was controlled to follow a cubic spline trajectory, ending with the desired step length. The height, step length and speed could be

changed by the user. The robot's top walking speed was approximately 0.3 meters per second with a step length of 20 centimeters. Because the robot had point feet, it appeared fairly natural, as the natural pendulum dynamics of the robot were exhibited. From previous works, we can see that fully-actuated bipeds show better robustness and adaptability than their under-actuated cousins.

2.2 Stability of Bipedal Robot Walking

The most crucial and difficult problem concerning bipedal robot walking on uneven terrains is their stability. As has been discussed above, the bipedal robot is a rather complex mechanism by itself not easily represented analyzed through a set of simple differential equation. Analyzing its walking dynamics is made more difficult because the locomotion is not continuous.

Bipedal robot walking can be categorized into three types: statically stable walking, quasi-static stable walking and dynamic stable walking. In statically stable walking, the vertical line through the center of mass (CoM) of the biped does not leave the robot's support polygon during the normally periodic locomotion. That is, at all times, the robot is statically stable. Quasi-static stable walking is a gait where the center of pressure (CoP) of the biped's stance foot always remains strictly within the interior of the support polygon, and does not even lie on the boundary. In dynamic stable walking the biped is not statically stable at all times. There will be time periods in each stride when the robot's center of gravity falls outside of its support polygon such that a moment will be created which will cause it to start to "fall". However, before it can fall too far, the swing foot would be placed in such a location as to generate a moment on it to cause it to "fall" in the opposite direction. The robot thus does not fall all the way to the ground but oscillate between "falling" in one direction and then the other as it walks along.

The bipedal robot is a very complex dynamic system which is nonlinear, under-actuated, combines both continuous and discrete dynamics, and with its

motion not necessarily periodic. Several questions thus arise: How do we define what a stable biped is? Can there be some mathematical characterization of this stability that can be constructed based on a detailed knowledge of the robot's structure and the approach used to control its locomotion? As we will see next, it is very difficult to use the traditional stability criterion. Most researchers define the stability for a bipedal robot in terms of whether or not the robot will fall down during locomotion[22]. The goal of this section is to present some tools which can serve for the stability analysis of bipedal models.

2.2.1 Poincaré Return Map

The Poincaré return map [23] is introduced here as a tool to analyse the stability. Generally, this approach takes into account two facts about bipedal locomotion. The first is that the motion is discontinuous because of the impact of the swing foot with the ground, and the second is that the dynamics is highly nonlinear and non-smooth and linearization about the vertical stance generally should be avoided. The periodic motions of a simple biped can be represented as closed orbits in the phase space, or

$$x_{n+1} = Kx_n \quad (2.1)$$

where x is the vector of deviations from the fixed point on its limit cycle trajectory and K is the return matrix. If the eigenvalues of K are all less than one, the system is stable. The Poincaré return map is commonly used for analyzing the passive dynamics of robots. This is done by determining the eigenvalues of the Poincaré return map [24-26]. However, it is not suitable for analyzing non-periodic motions, which are more general, since there is nothing about the bipedal walking problem that requires periodicity.

2.2.2 Gait Sensitive Norm

In the previous section, we discuss the Poincaré return map, which can be used to measure the local stability of periodic gaits. In 2007, Hobbelen and Wisse

[27, 28] provided a novel disturbance measurement of limit cycle walkers based on the Poincaré return map. This measurement is called the gait sensitivity norm and is a quantity of the effect of disturbance on a walking gait. The gait sensitivity norm is a H_2 norm, which uses a set of disturbances \mathbf{e} as the system input and the gait indicator \mathbf{g} as the system output. Disturbances \mathbf{e} can consist of those disturbances that are of interest to the designer, such as the terrain's irregularities, sensor noise or torque ripple. The gait indicator \mathbf{g} quantifies the characteristics of the walking gait that are directly related to the failure mode, such as step width and step time. The Gait Sensitive Norm is defined as follows:

$$\left\| \frac{\partial \mathbf{g}}{\partial \mathbf{e}} \right\|_2 = \frac{1}{|e_0|} \sqrt{\sum_{i=0}^q \sum_{k=0}^{\infty} (g_k(i) - g^*(i))^2} \quad (2.2)$$

in which $g_k(i)$ is the value of the i th gait indicator k steps after the disturbance has happened and q is the number of gait indicators.

2.2.3 Zero Moment Point (ZMP)

Beside the above stability criterion, there are various approximated disturbance rejection measures based on the assumption that a biped can only prevent itself from falling if and only if its stance foot is in contact with the ground. In this group, the most well-known approach makes use of the ZMP.

The Zero Moment Point [29, 30] is defined to be the point under the stance foot about which the sum of all moments of active forces is equal to zero. The ZMP stability margin is the distance from the ZMP to the nearest edge of the convex hull of the robot's support polygon. The actual ZMP is calculated using information of the CoM or measured from the force sensors in the foot. The deviations between the pre-computed and calculated actual locations of the ZMP can be used to modify the trajectory[31]. Although the ZMP is equivalent to the Center of Pressure (CoP), the ZMP is used to denote the computed point at the foot based on the position and the acceleration of the

robot whereas the CoP is commonly determined from measurements taken of the ground reaction forces at the foot.

2.2.4 Capturability

Another measure of stability, called Capturability [32, 33], has been proposed which focuses on the ability of a system to come to a stop without falling by taking N or fewer steps. This stability measurement is inspired by the Capture Point [22, 34, 35], which is a foot placement estimator considering the footstep location to be of primary importance. The capture point for the linear inverted pendulum model is obtained through the use of zero orbit energy.

Capturability is a useful robustness metric and is described as the initial distance between the contact reference point and the instantaneous capture point. It is shown that an increase in the freedom of the stabilizing mechanisms may lead to an increase in the size of the capture region. Additionally, a larger capture region indicates a more robust robot walking performance or, in other words, stronger disturbance rejection ability.

However, the use of capture points and Capturability does not make use of terrain information. They can only be used for a robot walking on rough terrains with relative little disturbance.

2.3 Bipedal Robot Walking on Uneven Terrains

Given its mechanical structure which mimics the human beings, there is a significant benefit in using a bipedal robot to negotiate uneven terrains much like humans do. This has thus been a very popular topic in the area of bipedal robot walking research. For robot walking on uneven terrains, there are two important issues. One is the information on the terrain directly in front of the robot. For stable walking without falling, it is very important to obtain the ground profile, especially when there is large unevenness such as large and deep holes or staircases in front of the robot. Human have eyes (vision), hands (haptic), and other sensors which can be used to acquire accurate terrain

information. This, however, cannot be easily achieved for robots due to current limitations in sensor technology. As such, it is necessary that robots have excellent disturbance rejection abilities to be able to achieve stable walking in terrains with significant unknown unevenness or disturbances.

2.3.1 Walking on Known Terrain

For the biped robot walking on an uneven terrain for which prior detailed knowledge of the unevenness is known, Kajita, et al. [36] first introduced in 2006 the “preview control of ZMP” approach to generate a stable gait which places the foot at the specified location. For uneven terrain walking, the most crucial constraint is the allowable location for placing the footstep. How the trajectory of Center of Mass (CoM) needs to be adjusted so as to generate foot placements within these constraints then becomes very important. However, we find that the ZMP will not be achieved given its present target value alone, but the CoM needs to start moving prior to the ZMP. Therefore, further information of ZMP is needed.



Figure 2.2 Biped robot walking on varied terrain[37]

A quasi-static walking algorithms for bipedal walking on the uneven terrains have been proposed by Hauser [37]. In his approach, in order to improve the motion quality, the algorithm first generates candidate foot falls based on the

terrain profile and then generates continuous motions that can reach these. However, the motion planner used is offline so that it is difficult to reject any significant disturbances which occur during motion in real-time.

2.3.2 Walking on Unknown Terrain

For the biped robot walking on the uneven terrain with unknown terrain information, one of the most important aspects is the way to adapt the regular terrain. Since there are several regular patterns, the robot can adapt the terrain by following these patterns. An intuitive approach for a bipedal robot walking on an uneven terrain blindly was proposed by Chew et. al. [38]. They demonstrated a successful application of Virtual Model Control (VMC) using a simulated seven-link planar biped for walking dynamically and steadily over sloped terrains with unknown slope gradients and transition locations. The biped used the natural compliance of the swing foot so that it could land flat onto an unknown slope. After completion of the touchdown of the swing foot, a global slope was computed and this was used to define a virtual surface. The algorithm was very simple and did not require the biped to have an extensive sensory system for blind walking over slopes. However, this method is limited because it is only suitable for regular uneven terrains without any unknown unevenness. The knowledge required for the implementation mainly consisted of intuition and geometric considerations.

To extend the terrain types of bipedal robot walking, Erez and Smart [39] used the manifold control to achieve stable walking on rough terrains. They proposed an algorithm using reinforcement learning for adapting to a periodic behavior by gradually shifting the task parameters. They parameterized the policy only along the limit cycle traversed by the gait and focused the computational effort on a closed one-dimensional manifold, embedded in the high-dimensional state space. Therefore, the combination of local learning and careful shaping holds a potential promise for periodic tasks.

However, unexpected perturbations with small unevenness always exist in the human environment. Obviously, a controller which could improve the robot's disturbance rejection ability is necessary. Therefore, Wieber et al. [2-5] used Model Predictive Control to generate stable walking motion without using predefined footsteps. This novel approach attempted to stabilize the motion of the CoM of the system by minimizing its jerk over a finite prediction horizon through keeping the contact forces in the middle of the feasible set. However, this approach required intensive computation, which can be a problem for real-time implementation.

In order to overcome this drawback, a provably-stable feedback control strategy was developed for efficient dynamic walking bipeds over uneven terrains by Manchester et al. [7]. This approach used transverse linearization about the desired motion. Since walking on an uneven terrain is a non-periodic motion, their approach can generate provably stabilized arbitrary non-period trajectories arriving in real-time from an online motion planner.

2.4 Summary

From the above review, it can be seen that it is a challenge to build a robot that can handle almost all kinds of different terrains. Even humans use different strategies in different situations. For a gentle terrain with some unevenness, we may walk blindly while for steep terrain walking, we will need to use our eyes and may even need the help of tools such as a walking stick. Therefore, these challenges highlight the importance of an approach which can generate an online adjustable walking pattern with capabilities of not only online adaption but which also take into account terrain information. For this reason, this thesis combines these two requirements and develops a more robust controller. This controller should not only be able to adapt in real-time to small unknown unevenness and disturbances but it should also consider known information on the terrain as well.

Chapter 3

Moving Ground Reference Map

3.1 Introduction

In this chapter, moving ground reference map will be introduced. The background knowledge and biped dynamic model will be investigated.

In this thesis, we use simple linear inverted pendulum model (LIPM) [40] in order to facilitate the development of novel walking trajectory generation.

In dynamic walking, it is important to identify the relationship between robot and ground support area. A ground reference point [41] is a reference point on the ground that describes the relationship between the robot state and the ground reaction force, such as zero moment point (ZMP), centroidal moment pivot (CMP) and foot rotation indicator (FRI). We define a moving ground reference map as a map containing a sequence of online updated ground reference points. The locations of these points are optimized to achieve a robust walking performance.

It is generated based on both the current state of the robot and terrain information to regulate Center of Mass (CoM) trajectory and to achieve desired step location. The above objectives are realized through both swing and support legs.

- for swing leg: To optimize the next foot placement point in order to balance the robot as well as to achieve a desired body motion and reach preplanned footstep location.
- for support leg: To adjust the zero moment point reference to regulate the state of center of mass.

This ground reference map is continuously adjusted in real time based on the robot's actual dynamic during locomotion to maintain stable walking in the presence of external disturbances. By implementing this moving ground reference map, optimized bipedal locomotion over uneven terrains can be achieved.

In Section 3.2 the dynamic of LIPM (Linear Inverted Pendulum Mode) is discussed. The section starts by introducing the dynamics of LIPM. Then the natural step time is obtained by assuming zero ankle torque at the stance leg. In Section 3.3, the ground reference point is introduced. The definition and dynamic analysis of ZMP are discussed. In Section 3.4, the novel moving ground reference map is proposed.

3.2 Dynamic Model of Biped Robot

In this section, we will discuss the dynamic model of biped robot. The dynamic of humanoid robot is very complex. It is challenging to generate stable motion for it. In general, there are two main approaches to achieve stable bipedal robot locomotion. In the first approach, the focus is on the accuracy of the model. It requires the precise information of robot dynamics including the location of each joint, mass, and inertia of each link. However, if there is any error in the dynamic model, the controller may not work well. Conversely, in the other approach, the assumption made is that there is insufficient knowledge about the robots' dynamics. For example, only the height and CoM position are known. The focus of this approach is to apply feedback control to generate a robust motion of biped locomotion. In the following sub-section, we will introduce a simple dynamic model: LIPM (Linear Inverted Pendulum Mode) for bipedal walking, which is based on the feedback approach.

3.2.1 Linear Inverted Pendulum Mode

Bipedal walking of a robot can be simply modeled as Linear Inverted Pendulum Mode [40]. It consists of a point mass and massless leg as shown in Fig. 3.1.

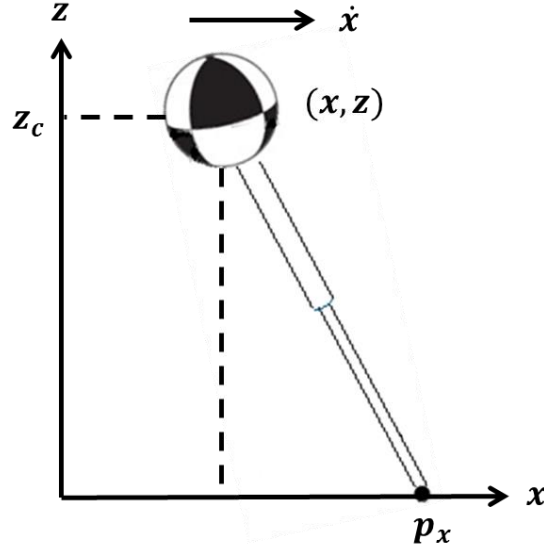


Figure 3.1 2D Linear Inverted Pendulum

Then the ground reaction force point (ground reference point) based on Linear Inverted Pendulum Mode (LIMP) can be solved as follows:

$$m\ddot{x}z_c = mg(x - p_x) \quad (3.1)$$

$$\ddot{x} = \frac{g}{z_c}(x - p_x) = w^2(x - p_x) \quad (3.2)$$

where x and \dot{x} are the horizontal position and velocity of CoM, $w = \sqrt{g/z_c}$, z_c is the height of CoM, m is the mass of the LIPM, g is gravity acceleration, and p_x is the position of ground reference point. The constraints are:

- There is no angular momentum and no change in angular momentum about the center of mass (CoM).

- The lumped CoM is at a constant height. $z = z_c$ and $\ddot{z} = 0$.

The dynamics in the lateral plane are same as the sagittal plane. They are decoupled [40].

Through the above equations, it is easy to obtain the final state based on the initial state of the linear inverted pendulum. Solving Eq.(3.2), we have the relationship between the initial state $x_0^{(n)}, \dot{x}_0^{(n)}$ and the final state $x_T^{(n)}, \dot{x}_T^{(n)}$ of the n^{th} step in a fixed coordinate system as shown in Fig 3.2 as follows.

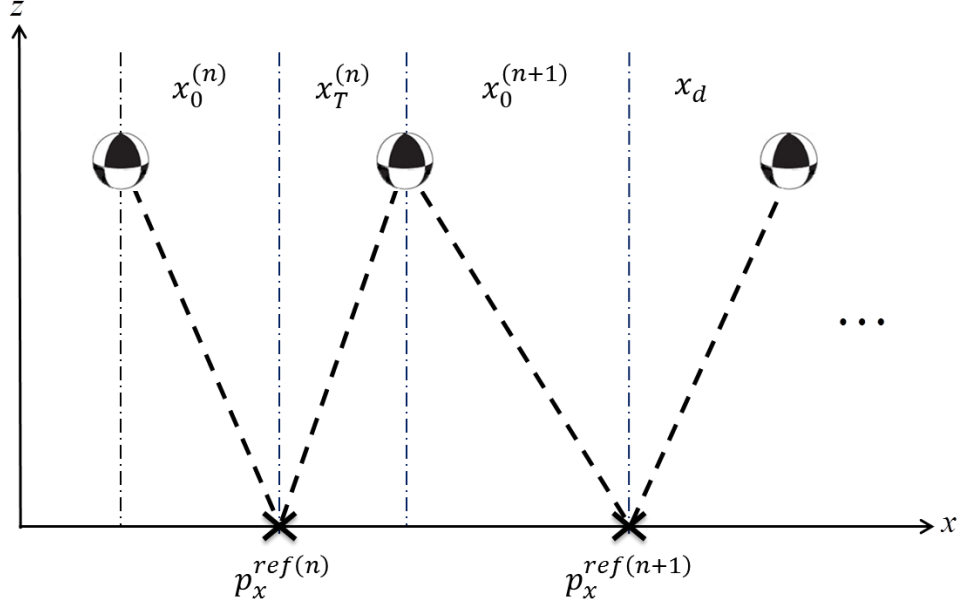


Figure 3.2 Transition of linear inverted pendulum

$$\begin{bmatrix} x_T^{(n)} \\ \dot{x}_T^{(n)} \end{bmatrix} = \begin{bmatrix} \cosh(wT) & \sinh(wT)/w \\ \sinh(wT)w & \cosh(wT) \end{bmatrix} \begin{bmatrix} x_0^{(n)} \\ \dot{x}_0^{(n)} \end{bmatrix} - \begin{bmatrix} \cosh(wT) - 1 \\ \sinh(wT)w \end{bmatrix} p_x^{ref} \quad (3.3)$$

where $\sinh(wT)$ and $\cosh(wT)$ are the hyperbolic functions as follows:

$$\cosh(wT) = \frac{1}{2}(e^{wT} + e^{-wT}); \sinh(wT) = \frac{1}{2}(e^{wT} - e^{-wT})$$

In this thesis, we define an absolute coordinate system whose origin is fixed at the starting point of walking. Its x-axis is pointing to the walking direction while its z-axis is point vertically up. Conversely, a relative coordinate system

is a frame that uses the foot placement reference in x-axis p_x^{ref} as the origin with the same orientation as the absolute coordinate system.

The relationship between the initial state $x_0^{(n)}, \dot{x}_0^{(n)}$ and the final state $x_T^{(n)}, \dot{x}_T^{(n)}$ of the n^{th} step in relative coordinate is

$$\begin{bmatrix} x_T^{(n)} \\ \dot{x}_T^{(n)} \end{bmatrix} = \begin{bmatrix} \cosh(wT) & \sinh(wT)/w \\ \sinh(wT)w & \cosh(wT) \end{bmatrix} \begin{bmatrix} x_0^{(n)} \\ \dot{x}_0^{(n)} \end{bmatrix} \quad (3.4)$$

3.2.2 The Natural Stepping Time for the LIPM

The natural stepping time for the LIPM can be obtained by the following equations based on Eq. (3.4).

$$x_T = \cosh(wT)x_0 + w\sinh(wT)\dot{x}_0 \quad (3.5)$$

$$\dot{x}_T = \frac{1}{2}(e^{wT} + e^{-wT})\dot{x}_0 + \frac{w}{2}(e^{wT} - e^{-wT})x_0 \quad (3.6)$$

$$2we^{wT}x_T = (wx_0 + \dot{x}_0)e^{2wT} + (wx_0 - \dot{x}_0) \quad (3.7)$$

$$e^{wT} = \frac{wx_T + \sqrt{\dot{x}_0^2 - w^2x_0^2 + w^2x_T^2}}{wx_0 + \dot{x}_0} \quad (3.8)$$

Since it is natural stepping time, there is no additional energy input or output.

$$\therefore E_0 = \frac{1}{2}(\dot{x}_0^2 - w^2x_0^2) = E_T = \frac{1}{2}(\dot{x}_T^2 - w^2x_T^2) \quad (3.9)$$

$$\therefore e^{wT} = \frac{wx_T + \dot{x}_T}{wx_0 + \dot{x}_0} \quad (3.10)$$

$$\therefore T = \frac{1}{w} \ln \left(\frac{wx_T + \sqrt{\dot{x}_0^2 - w^2x_0^2 + w^2x_T^2}}{wx_0 + \dot{x}_0} \right) = \frac{1}{w} \ln \left(\frac{wx_T + \dot{x}_T}{wx_0 + \dot{x}_0} \right) \quad (3.11)$$

From the stepping time function, it is easy to obtain the swing time based on the final state and the initial state of CoM.

3.3 Ground Reference Point in Different Models

Ground reference points are important for motion definition and control in legged robotics and biomechanics [41]. An important property is that they resolve the ground reaction force distribution to a single point.

There are several ground reference points used for motion identification and control in bipedal locomotion, such as zero moment point (ZMP) [42], centroidal moment pivot (CMP) [43] and foot rotation indicator (FRI) [44]. The location of these reference points provides important local and sometimes global characteristics of the whole robot body movement patterns [41]. In this, thesis we use ZMP as the ground reference point to illustrate the moving ground reference map.

3.3.1 Point Foot Biped

Borelli firstly discussed a biomechanical point, called support point [45], a ground reference location where the resulted ground reaction force acts in the case of static equilibrium. Following Borelli, Elftman et, al [46] introduced “point of the force” which is a more general ground reference point for both static and dynamic cases. In general, this ground reference point is the support base point for point foot robot.

In this thesis, the Linear Inverted Pendulum Mode (LIPM) [40] with point foot is used to explain the foot placement point position. The LIPM with a point contact is an integral part of overall dynamics of biped walking [47]. In this model, as shown in Fig. 3.3, the base of inverted pendulum can be seen as a foot placement point. When the robot walks, the support foot position changes as steps are taken. In LIPM, the point mass is constrained to move in a horizontal plane. Here, we assume no actuation between the foot and the ground.

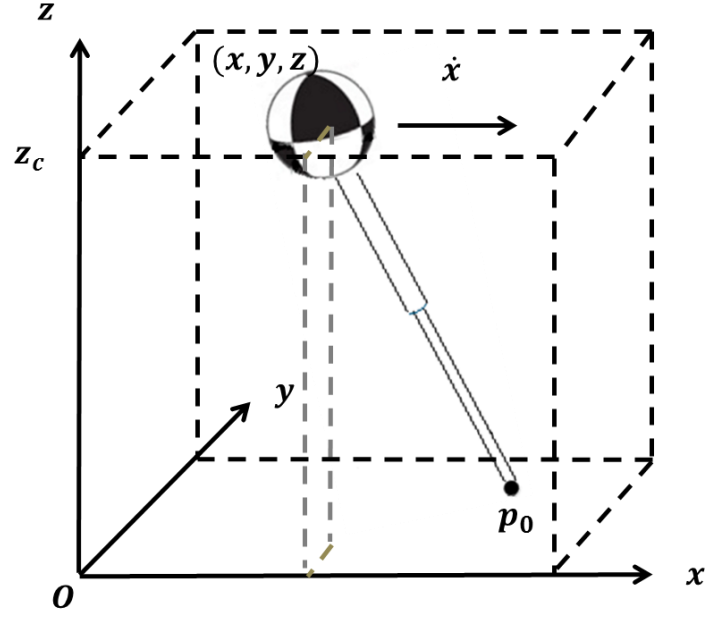


Figure 3.3 Foot placement point in the point foot LIPM

In addition, the following assumptions are made. Firstly, change of support foot occurs instantaneous. Secondly, there is no effect on the position and velocity of the center of mass when the foot lands. Thirdly, it is under-actuated at the point of contact between the stance leg and ground, that is, no slippage between the support foot and ground. Finally, there are two symmetric legs connected at hip joints and both leg ends are terminated in points. The foot placement point is one of the most crucial parameters of bipedal walking. The stable walking performance can be achieved by a suitable foot placement position choice. The methodology will be introduced in the section 3.4.

3.3.2 Finite-Size Foot Biped: Zero Moment Point

In the previous section, we have explained the ground reference point in point foot LIMP. In this section, we will introduce the best known ground reference point: zero moment point. Although it has been defined in the literature, here we define the zero moment point using consistent terminology and mathematical notation. Furthermore, to make the model more realistic, we use a finite size foot to derive the mathematic model in Fig. 3.4. Idealize a robot with one leg in contact with the ground as a linear inverted pendulum that is

attached to a base consisting of a finite-size foot with torque applied at the ankle. We assume that all other joints are independently actuated and there is no slippage between the contact foot and the ground.

In normal case, the foot does not rotate, if the zero moment point (ZMP) remains strictly within the interior of the support polygon. This can be used as the criterion to estimate the stability of biped walking. In this situation, the biped system is considered to be fully actuated (two degrees of freedom with two actuators). However, if the ZMP has moved on the toe of support foot, allowing the foot to rotate, the system becomes under-actuated (two degrees of freedom with only one actuator). In this situation, it is no realistic to control the biped stability by ZMP criterion anymore.

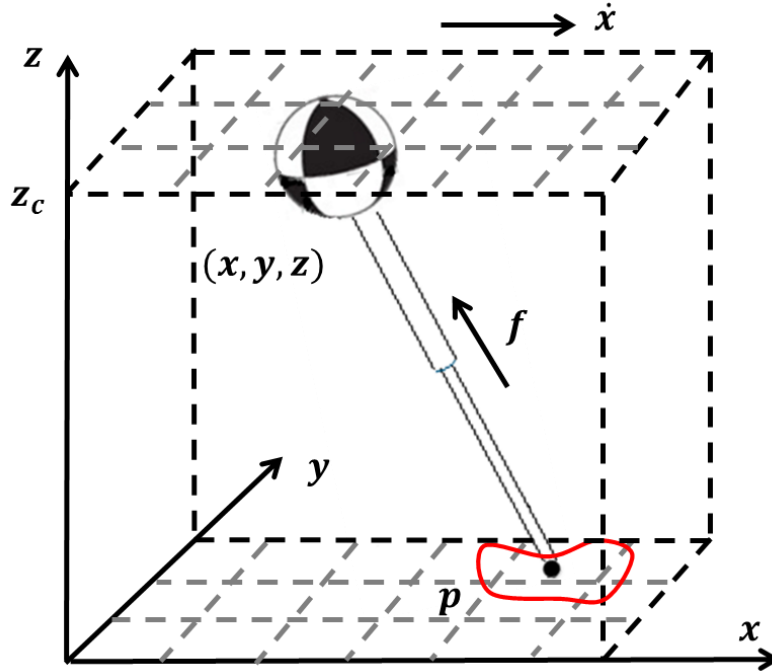


Figure 3.4 ZMP in finite-size foot based on 3D linear inverted pendulum mode

An amount of technology has been developed based on ZMP criterion [42, 48]. It is found that by using ZMP criterion, small deviations from the planned trajectory can be attenuated via feedback control, improving the stability of the walking motion. The position of the ZMP is approximately proportional to

ankle torque. Therefore, the control on the location of ZMP corresponds to torque control at the ankle joint. In this thesis, we use this property to generate the novel ground reference map.

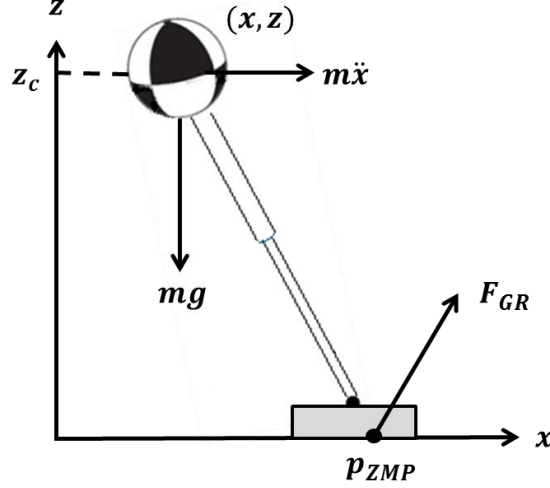


Figure 3.5 2D Dynamic analysis of linear inverted pendulum mode

In this thesis, we define ZMP as follows:

Definition (Zero Moment Point) *The Zero Moment Point is the point of resulting the ground reaction forces at contact surface, i.e., the point on the ground at which has no horizontal component of moment due to inertial and gravitation forces.[49]*

The location of the ZMP can be calculated based on the CoM position and ground reaction force, as shown in Fig. 3.5.

$$\mathbf{p} = \begin{bmatrix} p_x \\ p_y \\ p_z \end{bmatrix} = \begin{bmatrix} x - \frac{F_x}{F_z + mg} - \frac{\tau_y}{F_z + mg} \\ y - \frac{F_y}{F_z + mg} - \frac{\tau_x}{F_z + mg} \\ 0 \end{bmatrix} \quad (3.12)$$

where $[x, y, z]^T$ is the position of CoM, and $[p_x, p_y, p_z]^T$ is the ZMP position.

$F_{GF} = \begin{bmatrix} F_x \\ F_y \\ F_z \end{bmatrix}$ is the ground reaction force in x, y, z axes.

3.4 Moving Ground Reference Map

By virtue of their mechanical structure, one of the significant advantages of legged robots over other types of robots is their ability to navigate various terrains commonly accessed by human beings. Walking on flat terrains has been well studied [11, 12, 18], but walking on rough terrains remains a challenge.

In general, there are two main challenges for achieving stable bipedal robot locomotion over uneven terrains. For the first challenge, the focus is on developing a motion planner based on the knowledge of the terrain profile, which can achieve stable robot locomotion [1, 19]. If the robot's control systems can then ensure the accuracy of tracking of the predefined trajectories, stable walking will be achieved. For the other challenge, the assumption made is that there is insufficient knowledge of the terrain to develop a motion plan to achieve stable walking. The focus of this group is then on developing on strong disturbance rejecting capabilities so that the robot can maintain stable walking without falling even when faced with disturbances and unexpected unevenness in the terrain.

In previous studies, several robots have realized stable walking over uneven terrains by maintaining the ZMP within the support polygon [1, 19, 36]. However, robustness is poor and the approaches fail in the presence of significant unknown disturbances. Some researchers have attempted to improve the disturbance rejection ability by adjusting the ZMP reference online [2, 36, 50] and some improvements have resulted. However, there is still a need to develop an effective strategy capable of adapting to large disturbances. An effective strategy would be one which can adapt to unknown

disturbances such as unevenness in the terrain and include preview action to overcome large disturbances, such as stairs and steep slopes, when these can be known beforehand.

According to the analysis of human walking over uneven terrain, the intuitive strategies could be summarized as follows: an approximate terrain profile of the ground is obtained by the vision system. Then, based on the approximated terrain profile, the allowable step region is attained in advance. When the robot walks, the proper stepping location could be online calculated so that the robot can handle the unknown unevenness which is not captured by the vision system. One of the key issues for bipedal robot walking on the uneven terrain is generating a suitable stepping position of the swing foot [32, 33]. In order to land on the optimized position in the allowable step region, the future information of the terrain profile would be useful.

Therefore, we propose the moving ground reference map. The moving ground reference map is a map containing a sequence of ground reference points which is moving as the robot moves. Once the robot has started walking, and it has not reached the N^{th} step, it will continuously modify the moving ground reference map. After switching support foot, the next foot placement for the swing foot will be generated and updated. Then, after the foot has landed, the ZMP for the support foot will be continuously updated in each sampling time until swing foot becomes support foot.

3.4.1 Moving Ground Reference Map for Next Step

In this section, moving ground reference generation of next step foot placement will be presented. Stepping on the proper location is critical to biped walking, especially on uneven terrain. The objective of generating moving ground reference map for the swing foot is to generate a suitable next foot placement at the certain time T , considering the unknown unevenness on the terrain. In order to maintain stable walking and avoid falling in spite of unknown disturbances, an online adjustable foot placement is proposed. This

foot placement takes advantage of available information on both future desired stepping positions and the current robot state (CoM position, velocity and support foot position in the absolute coordinate system).

The foot placement point for $(n + 1)^{th}$ step is updated at n^{th} step by minimizing the errors in the position and the velocity of the robot's CoM, and the foot placement tracking error. This is done by treating it as a Quadratic Programming problem which tries to minimize a quadratic cost function with constraint. This constraint represents the allowable step region for the next step. This allowable step region is depending on the terrain profile and robot mechanical structure. For example, the robot needs to step on some specific locations, such as crossing a stream with stepping stones. In this situation, the size and location of the stone will determine the constraint of allowable step region. Moreover, the robot structure, such as the length of the legs, will affect the maximum distance that it can reach within one step. Therefore the Quadratic Programming can be expressed as follows:

$$\begin{aligned} \min \mathbf{R} \quad & \left\| \mathbf{x}_T^{ref(n+1)} - \mathbf{x}_T^{(n+1)} \right\|^2 + p \left\| \mathbf{p}_x^{ref(n+1)} - \mathbf{p}_x^{(n+1)} \right\|^2 \\ \text{s. t.} \quad & x_{0(min)} \leq x_0^{(n+1)} \leq x_{0(max)} \end{aligned} \quad (3.13)$$

where $x_{0(min)}$ and $x_{0(max)}$ are the constraint for the updated foot placement.

$\mathbf{x}_T^{ref(n+1)} = \begin{bmatrix} x_T^{ref(n+1)} \\ \dot{x}_T^{ref(n+1)} \end{bmatrix}$ is the desired CoM state at the end of $(n + 1)^{th}$ step,

$\mathbf{x}_T^{(n+1)} = \begin{bmatrix} x_T^{(n+1)} \\ \dot{x}_T^{(n+1)} \end{bmatrix}$ is the actual CoM state at the end of $(n + 1)^{th}$ step

(subscript T indicates values at the end of a step, and subscript 0 indicates values at the beginning of a step). $\mathbf{p}_x^{ref(n+1)}$ is the pre-defined ground reference (foot placement point) at $(n + 1)^{th}$ step.

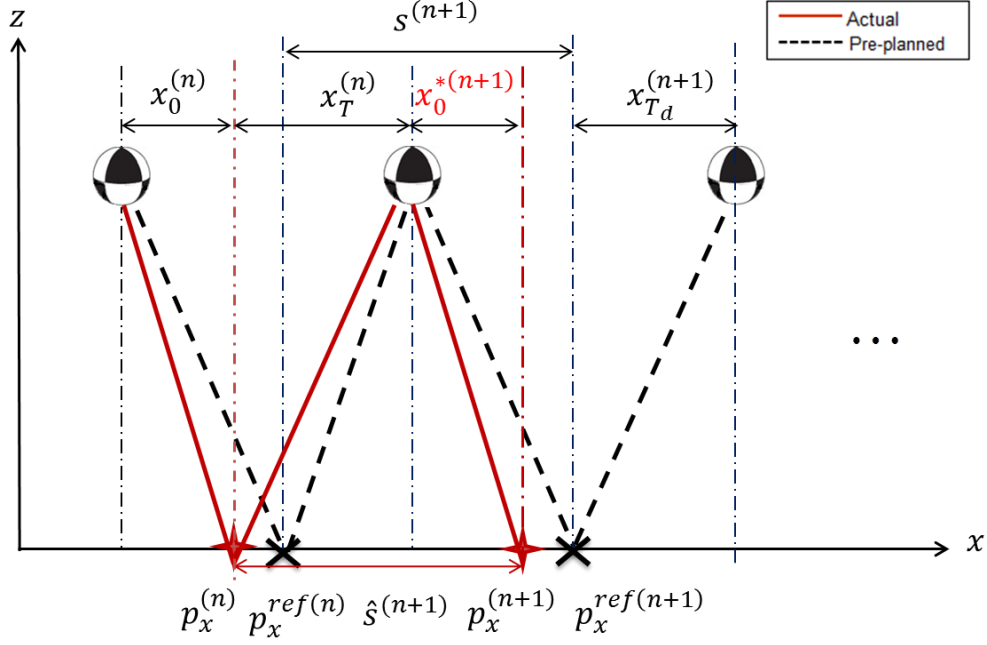


Figure 3.6 Comparison between pre-planned and actual walking process

From the Fig.3.6, we can see that $p_x^{ref(n+1)} = p_x^{ref(n)} + s^{(n+1)}$, ($s^{(n+1)}$ denotes the planned step length). $p_x^{(n+1)}$ is the actual foot placement position at $(n+1)^{th}$ step, $p_x^{ref(n+1)} = p_x^{ref(n)} + \hat{s}^{(n+1)} = p_x^{(n)} + x_T^{(n)} + x_0^{(n+1)}$ ($\hat{s}^{(n+1)}$ denotes the actual step length). r_1 and r_2 of $\mathbf{R} = \begin{bmatrix} r_1 & 0 \\ 0 & r_2 \end{bmatrix}$ and p , are non-negative weights of the cost function.

Assuming no energy loss during foot exchange, we have $\dot{x}_0^{(n+1)} = \dot{x}_T^{(n)}$ and $\dot{x}_T^{(n)}$ can be obtained from Eq.(3.4). Expanding Eq.(3.13), we can obtain the cost function as follows:

$$\begin{aligned}
J(x_0^{(n+1)}) &= R \left\| x_T^{ref(n+1)} - x_T^{(n+1)} \right\|^2 + p \left\| p_x^{ref(n+1)} - p_x^{(n+1)} \right\|^2 \\
&= r_1 \left(x_T^{ref} - \cosh(wT) x_0^{(n+1)} - \frac{\sinh(wT)}{w} \dot{x}_T^{(n)} \right)^2 \\
&\quad + r_2 \left(\dot{x}_T^{ref} - \sinh(wT) w x_0^{(n+1)} - \cosh(wT) \dot{x}_T^{(n)} \right)^2 \\
&\quad + p \left(p_x^{ref(n)} + 2x_T^{ref} - p_x^{(n)} - x_T^{(n)} - x_0^{(n+1)} \right)^2 \\
J'(x_0^{(n+1)}) &= -2r_1 \cosh(wT) \left(x_T^{ref} - \cosh(wT) x_0^{(n+1)} - \frac{\sinh(wT)}{w} \dot{x}_T^{(n)} \right) \\
&\quad - 2r_2 \sinh(wT) w \left(\dot{x}_T^{ref} - \sinh(wT) w x_0^{(n+1)} - \cosh(wT) \dot{x}_T^{(n)} \right) \\
&\quad - 2p \left(p_x^{ref(n)} + 2x_T^{ref} - p_x^{(n)} - x_T^{(n)} - x_0^{(n+1)} \right) \\
J''(x_0^{(n+1)}) &= 2(r_1 \cosh^2(wT) + r_2 w^2 \sinh^2(wT) + p) > 0
\end{aligned}$$

Since the second derivative of J with reference to $x_0^{(n+1)}$ is always positive, we can obtain the local minimum of the cost function J by setting $J'(x_0^{(n+1)}) = 0$.

Therefore, the optimized solution is:

$$x_0^{*(n+1)} = \frac{A - B\dot{x}_T^{(n)} - p(x_T^{(n)} + p_x^{(n)})}{D} \quad (3.14)$$

where

$$\begin{aligned}
A &= r_1 \cosh(wT) x_T^{ref} + r_2 \sinh(wT) w \dot{x}_T^{ref} + p(p_x^{ref(n)} + 2x_T^{ref}) \\
B &= r_1 \sinh(wT) \cosh(wT) \frac{1}{w}
\end{aligned}$$

$$D = \cosh^2(wT) + w^2 \sinh^2(wT) + p$$

Since $x_0^{*(n+1)}$ represents the next foot placement in the relative coordinate system with respect to the stance foot, the updated next foot placement $p_x^{*(n+1)}$ in the absolute frame can be represented as:

$$p_x^{*(n+1)} = x_0^{*(n+1)} + p_x^{(n)} + x_T^{(n)}$$

Therefore, we have the moving ground reference map as follows:

$$p_x^{ref} = \begin{bmatrix} \mathbf{v}_1 \\ \mathbf{v}_0 \\ \mathbf{v}_0 \\ \vdots \\ \mathbf{v}_0 \end{bmatrix} p_x^{ref(n)} + \begin{bmatrix} \mathbf{v}_0 \\ \mathbf{v}_1 \\ \mathbf{v}_0 \\ \vdots \\ \mathbf{v}_0 \end{bmatrix} p_x^{*(n+1)} + \dots + \begin{bmatrix} \mathbf{v}_0 \\ \vdots \\ \mathbf{v}_0 \\ \mathbf{v}_1 \\ \mathbf{v}_0 \end{bmatrix} p_x^{ref(n+N_L-1)} + \begin{bmatrix} \mathbf{v}_0 \\ \vdots \\ \mathbf{v}_0 \\ \mathbf{v}_0 \\ \mathbf{v}_1 \end{bmatrix} p_x^{ref(n+N_L)} \quad (3.15)$$

where $p_x^{*(n+1)}$ is the optimal foot placement for the $(n+1)^{th}$ step at step n . Each term on the right hand side of Eq. (3.15) represents one foot position. N_L is the number of future foot placement locations, which will be introduced in the next chapter. The column vectors \mathbf{v}_1 and \mathbf{v}_0 containing m number of 1's or 0's respectively with m being the number of sampling periods required to complete one foot step. The rows of Eq. (3.15) represent the sampling instances. The column vector of Eq. (3.15) comprises values of the foot placement positions for the sampling periods required to move from the start of the n^{th} step to the end of the $(n+N_L)^{th}$ step.

The moving ground reference map for next step is a reference map composed by the most suitable foot placement point based on current state of the robot and the allowable stepping location. Since the location of the stance foot does not change within one step, it only needs to be updated once every step. The update frequency of the moving ground reference map for the swing foot is equal to the stride frequency.

3.4.1.1 Selection of the Weighting Factors

There are two weighting factors in the cost function:

The weighting factors \mathbf{R} and p express the relative importance of keeping $e_x = \mathbf{x}^{ref} - \mathbf{x}_T^{(n+1)}$ and $e_f = p_x^{ref(n+1)} - x_f^{(n+1)}$ close to zero. If we place

more importance on e_x , then we select \mathbf{R} to be larger relative to p , and vice versa. Although we are interested in minimizing J , the actual value of J that results is usually not of interest. This also means that we can set either \mathbf{R} or p to unity for convenience because it is their relative weight that is important.

- \mathbf{R} is the weight of converging CoM to its desired state. This may help the robot to balance the unexpected disturbance. Therefore, if it is required to be more robust, the weighted in \mathbf{r} will be heavier.
- p is the weight of converging footstep position to the preplanned ground reference point. It is used to avoid the positions that are not suitable for the robot to step on. Therefore, if it is more important to track the preplanned reference (accurate), the weighted in p will be heavier.

From the above analysis, these two weighting factors are used in different situations. For the small landing constraint, such as level ground with small steps, slope with small gradient, it is better to use larger \mathbf{R} and smaller p so that the robot can recover faster from disturbances. Therefore, in this situation, it is acceptable to set both of them to unity for convenience. The details and implementations will be shown in Chapter 4. On the other hand, for environments with strict constraints, such as narrow staircase, stone in the river, etc., it should use larger p so that stepping on improper location can be better avoided. The implementation of this situation will be demonstrated in Chapter 5.

3.4.1.2 Optimization Tools

In order to improve the walking performance based on the moving ground reference map, we use genetic algorithm (GA) to choose the optimal weighting factors. The objective of this GA is finding the optimal \mathbf{R} and p in cost function to adapt to the different environments. The value of weighting factors would be related with environments and how the robot adapts to the

environment. According to GA learning, the meaning of trend of weighting factors could be verified.

A Genetic algorithm (GA) is a global optimization technique which used in computing to find the solutions to search problems. It can avoid the shortcomings exhibited by local searching techniques on different search space. Genetic algorithms are considered as a type of evolutionary algorithms that use techniques inspired by evolutionary biology [51]. Genetic algorithms have been shown to be effective in solving different problems through the genetic operators, such as mutation, crossover, and selection operations applied to individuals in the population [51]. There are several elements of genetic algorithms: initial population size, chromosome representation, evaluation function, selection functions, genetic operators including crossover and mutation and the termination criteria.

The GA must be provided an initial population as indicated at beginning. This population size is important. For the small population, the GA may work poor since the information is insufficient. However, if it is very large, the evaluation process may take a long time to converge. Randomization is commonly used to initialize the starting population parameters. However, the beginning population can be offered with potentially good solutions, with the remainder of the population being randomly generated solutions, since GAs can iteratively improve existing solutions. Choosing initial population with good solution is better than randomly choosing. Therefore, in this thesis, we use 100 as the population size and the initialization is based on the terrain profile. If the terrain profiles contained the strict constraints, such as narrow staircase, stone in the river, etc., the initial values of weighting factors may within the range of [0,1]. If there are few narrow constraints on the environment, the initial value of weighting factors could be chosen larger than one.

In genetic algorithm, a chromosome representation is traditionally used the binary representation. However, its performance may poor when it apply to

the problem with high-precision and multi-dimensional problem. In addition, the chromosome representation can be integer, matrices, symbols, and floating point (FP) as well. It can be proven that the GA with FP chromosome representation is an order of magnitude more efficient in terms of CPU time. In addition, a FP representation moves the problem closer to the problem representation which offers higher precision with more consistent results across replications [51]. Therefore, in this thesis, the more efficient FP representation is chosen.

The fitness function is the goal for optimization process. It is one of the most important elements in GA. In order to find optimal weighting factors of moving ground reference map to adapt to the different terrains, an objective function is formulated as

$$f_T = -w_1 f_1 - w_2 f_2 \quad (3.16)$$

f_1 is the standard deviation of the CoM velocity from the resulting average velocity over a walking cycle:

$$f_1 = \sqrt{\frac{(v_1 - \bar{v})^2 + (v_2 - \bar{v})^2 + \dots + (v_m - \bar{v})^2}{m}} \quad (3.17)$$

where v_i , $i = 1, 2, \dots, m$, is the velocity of CoM at the i^{th} sampling instant and \bar{v} is the resulting average CoM velocity over a walking cycle. m is the number of sampling instants within one step. Smaller standard deviation of CoM velocity indicates smaller fluctuation around the average velocity. Hence, less oscillation will occur while robot walking.

$$f_2 = \text{swing foot ground reaction velocity}$$

which prevents any instability from larger ground impacts on landing[52].

Smaller impact force will introduce fewer disturbances. The walking performance will be better.

Therefore, f_1 and f_2 will be minimized to address to a suitable weighting factors of moving ground reference map to adapt to the different terrain profiles.

To distinguish between different solutions, the selection function plays an important role of an environment. At each generation, the “good” solution has higher probability to reproduce while “bad” solution has a lower probability to reproduce. The selection operator is also called reproduction operator. A probabilistic selection is worked based on the fitness such that the better individual in the population can be selected more than once with all individuals in the population having a chance of being selected to reproduce into the next generation [51]. There are also several other schemes for the selection process: roulette wheel selection and its extensions, scaling techniques, tournament, elitist models, and ranking methods [53]. In this thesis, we use the probabilistic selection as the selection function.

During the alteration section of GA, two classical genetic operators are used: crossover and mutation. They provide the basic search mechanism of the GA. The operators are used to create new chromosome based on existing genes in the population. Crossover takes two chromosomes and produces two new chromosomes at the crossover point. Mutation alters one or more genes from a chromosome to produce a single new solution. The application of these two basic types of operation and their derivatives depends on the chromosome representation that is used. In this thesis, the following operators have been used: uniform mutation, non-uniform mutation, multi-non-uniform mutation, boundary mutation, simple crossover, arithmetic crossover, and heuristic crossover [51].

A termination criterion is applied to stop the process of GA. This criterion should guarantee the convergence of the results. A specific maximum number of generations is commonly used as the stopping criterion. In this thesis, the termination condition is simply based on a specific maximum number of generations $T = 200$.

Therefore, the structure of GA implementation is as follows:

```
t ← 0;
initialize  $P(t)$ ;
evaluate  $P(t)$ ;
while (termination condition not satisfied) do
begin
    t ← t + 1;
    selected  $P(t)$ ;
    genetic operator  $P(t)$ ;
    evaluate  $P(t)$ ;
end;
```

The optimal weighting factors can be obtained by applying the above iterative procedure. $P(t)$ is the the population at time t . The initial population $P(0)$ can be chosen based on the terrain profiles. The new population can be generated by applying reproduction operator. Based on the selection function, there are higher probabilities to select the ones have better fitness values. Then, apply the genetic operator: crossover and mutation by randomly choosing the mating gene pair. Repeat the above step until the termination condition is satisfied.

3.4.2 Moving Ground Reference Map for Current Step

In the previous subsection, we presented the optimized next step location to achieve walking stability. It mainly focuses on the foot placement of the next step. However, due to the unknown unevenness, the robot may not step onto the foot placement point; the real ZMP will deviate from the desired trajectory. Therefore, the ground reference points: ZMP are adjusted in the current step. Although this error could be reduced at the next step by generating a new foot placement point based on the robot state, the additional adjustment in the current step will reduce or even eliminate the ZMP error.

We derived the moving ground reference map generation for current step on the Linear Inverted Pendulum Mode with finite-size foot. In this model, the ZMP position can be represented by the foot placement point and the foot size, i.e. $p_x = p_0 + \delta^\pm$, where δ^+ and δ^- are the distance from the front and back

edge of the support region to the foot placement point, respectively. The ZMP reference for the support foot will be modified to increase the stability region. The modified ZMP is utilized to stabilize in the presence of unknown disturbances when the foot lands on the floor. The difference between the real ZMP and the desired ZMP planned in the last step will create an additional torque at the ankle to compensate for the ZMP error.

Since the ZMP is approximately proportional to ankle torque, we decided to use this feature to change the ZMP reference. As long as the foot placement point remains inside the contact region, the motion can be realized by controlling the ZMP at that point.

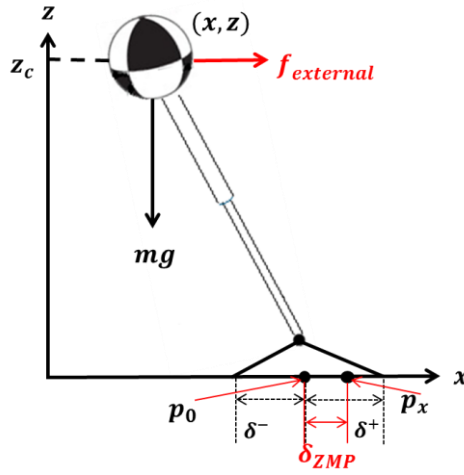


Figure 3.7 Stability Region of the Finite-Size Foot

We assume all the unexpected disturbance can be expressed as an external force. Then, the objective of ground reference adjustment in the current step is to compensate for this external force f_{external} . Based on the dynamics of LIPM in Fig 3.7,

$$(f_{\text{external}} - m\ddot{x})z_c = (p_x - p_0)mg = \delta_{\text{zmp}}mg \quad (3.18)$$

the external force can be written as

$$f_{external} = m\ddot{x} + m \cdot \delta\ddot{x}, \quad (3.19)$$

We can obtain the relationship between the changes of acceleration with the additional modification on ZMP reference:

$$\delta_{zmp} = \frac{mz_c \cdot \delta\ddot{x}}{mg} = \delta\ddot{x}/w^2 \quad (3.20)$$

where $w = \sqrt{g/z_c}$.

Therefore, the ground reference map can be presented as

$$p_x^{ref} = \begin{bmatrix} \mathbf{v}_1 \\ \mathbf{v}_0 \\ \mathbf{v}_0 \\ \vdots \\ \mathbf{v}_0 \end{bmatrix} p_x^{ref(n)} + \begin{bmatrix} \delta_{zmp} \\ 0 \\ 0 \\ \vdots \\ 0 \end{bmatrix} + \begin{bmatrix} \mathbf{v}_0 \\ \mathbf{v}_1 \\ \mathbf{v}_0 \\ \vdots \\ \mathbf{v}_0 \end{bmatrix} p_x^{*(n+1)} + \dots + \begin{bmatrix} \mathbf{v}_0 \\ \mathbf{v}_0 \\ \mathbf{v}_0 \\ \vdots \\ \mathbf{v}_1 \end{bmatrix} p_x^{ref(n+N_L)} \quad (3.21)$$

In more detail, the equation can be expressed as following.

$$p_x^{ref} = \begin{bmatrix} 1 \\ \vdots \\ 1 \\ 0 \\ \vdots \\ 0 \\ \vdots \\ 0 \\ \vdots \\ 0 \\ \vdots \\ 0 \end{bmatrix} p_x^{ref(n)} + \begin{bmatrix} \delta_{zmp}^1 \\ \vdots \\ \delta_{zmp}^m \\ 0 \\ \vdots \\ 0 \\ \vdots \\ 0 \\ \vdots \\ 0 \end{bmatrix} + \begin{bmatrix} 0 \\ \vdots \\ 0 \\ 1 \\ \vdots \\ 1 \\ 0 \\ \vdots \\ 0 \\ \vdots \\ 0 \\ \vdots \\ 0 \end{bmatrix} p_x^{*(n+1)} + \dots + \begin{bmatrix} 0 \\ \vdots \\ 0 \\ 0 \\ \vdots \\ 0 \\ \vdots \\ 0 \\ \vdots \\ 0 \\ \vdots \\ 1 \\ \vdots \\ 1 \end{bmatrix} p_x^{ref(n+N_L)} \quad (3.22)$$

where $\delta_{zmp} = [\delta_{zmp}^1 \quad \delta_{zmp}^2 \quad \dots \quad \delta_{zmp}^m]^T$ is the ZMP reference modification in each sampling time, and there are m sampling instants in each step.

Ground reference points make use of the next step landing position to recover from disturbances, such as push or large unevenness, while the additional ZMP reference modification in the current step make use of additional ankle torque to compensate for disturbance within a step. Either modification could reduce or eliminate ZMP errors due to disturbances if there is no constraint on

the robot motion, such as speed and motion range. However, in practice, motor speed is limited and robot step length is constrained by its size. Thus, the moving ground reference map contains both to generate robust walking patterns.

The functions of this current foot step adjustment in moving ground reference map are as follows:

- Handle unexpected disturbances (ground unevenness) on support foot during foot landing. This usually happens when there are some small rocks and sands on the area of support foot landing.
- Recover from small push.
- Compensate for large body acceleration when body is inclined.
- Maintain the walking direction to avoid vibration.

From the analysis, we can see that foot placement point is the base of ZMP adjustment and it is also one point of ZMP reference in a step. The moving ground reference map contains the reference of ZMP in the current step and the foot placement point reference for the future steps. Therefore, in the following chapters, we use the ZMP reference to represent the moving ground reference at each moment.

3.5 Discussion

3.5.1 Comparison with Capture Point

Capture point [22, 34] is a well-known concept to determine the footstep position. In general, the "capture point" concept is used to estimate the next foot placement. Our proposed approach is also a motion planner. In this case, we will compare the moving ground reference map with capture point.

3.5.1.1 Orbit Energy

Before we talk about the relationship with capture point, the orbit energy is introduced first.

The energy for linear inverted pendulum moving from time 0 to t is:

$$E_0 = \frac{1}{2} m \dot{x}_0^2 - \frac{mg}{2z_c} x_0^2$$

$$E_t = \frac{1}{2} m \dot{x}_t^2 - \frac{mg}{2z_c} x_t^2$$

We represent it as a mass-spring system with unit mass and a negative-rate spring with a stiffness of $-g/z_c$. Substituting Eq. (3.4) into E_t ,

$$\begin{aligned} E_t &= \frac{1}{2} m \dot{x}_t^2 - \frac{mg}{2z_c} x_t^2 \\ &= \frac{1}{2} m (w^2 S_t^2 x_0^2 + C_t^2 \dot{x}_0^2 + 2w S_t C_t x_0 \dot{x}_0) - \frac{1}{2} m w^2 x_t^2 \\ &= \frac{1}{2} m (w^2 S_t^2 x_0^2 + C_t^2 \dot{x}_0^2 + 2w S_t C_t x_0 \dot{x}_0) - \frac{1}{2} m (w^2 C_t^2 x_0^2 + S_t^2 \dot{x}_0^2 + 2w S_t C_t x_0 \dot{x}_0) \\ &= \frac{1}{2} m w^2 x_0^2 - \frac{1}{2} m \dot{x}_0^2 \\ &= \frac{1}{2} m \dot{x}_0^2 - \frac{mg}{2z_c} x_0^2 = E_0 \end{aligned}$$

Therefore, we obtain the conserved Orbit Energy as:

$$E = \frac{1}{2} \dot{x}^2 - \frac{g}{2z_c} x^2 \quad (3.23)$$

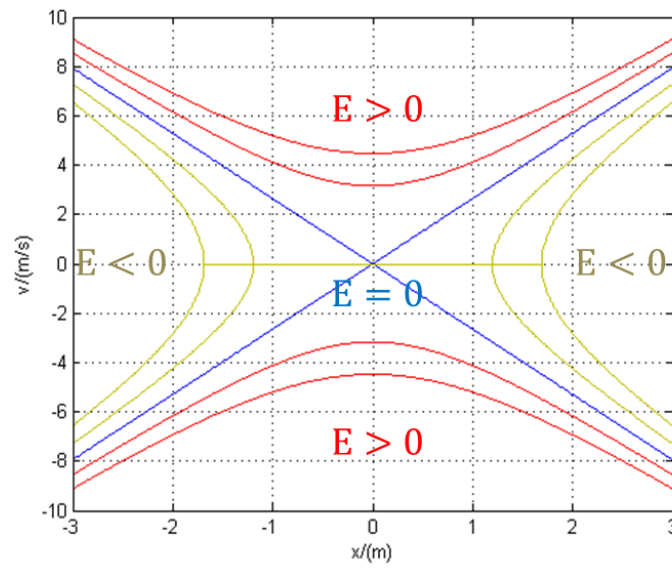


Figure 3.8 2D Orbit Energy

Fig 3.8 shows the Orbit Energy in the different situations in 2D. It shows that when the CoM is moving toward the foot, if the orbit energy is positive, then there is enough energy for the CoM to go over the foot and continue on its way. If the orbit energy is negative, then the CoM will stop and reverse directions before getting over the foot. If the orbit energy is zero, then the CoM will come to rest over the foot.

Fig. 3.9 shows the Orbit Energy in 3D view, where the three axes are: CoM position, CoM velocity and Orbit Energy. The saddle shape graph shows that at a given position x , larger velocity means higher Orbit Energy. For example, the CoM pass the centre point ($x = 0$) with larger velocity corresponds to a higher Orbit Energy. In the next section, we will compare the capture point and the moving ground reference map.

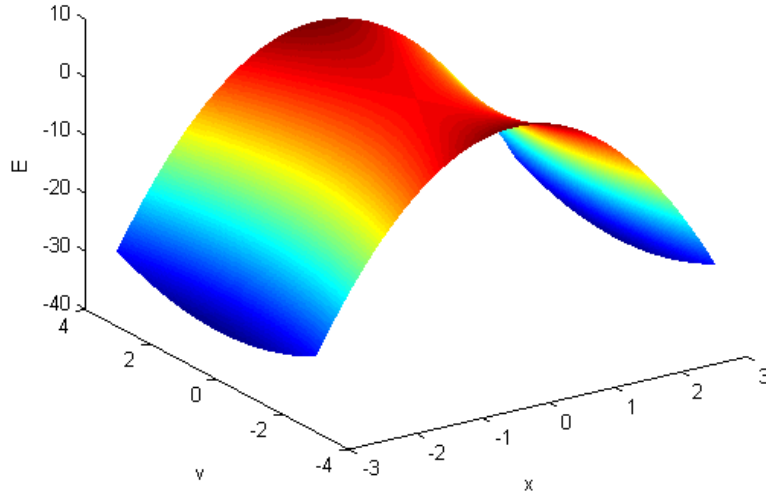


Figure 3.9 3D Orbit Energy

3.5.1.2 Relationship with Capture Point

A Capture Point is a point on the ground where the robot can achieve a complete stop by step to that point. A Capture Region is the collection of all Capture Points [34]. If the ZMP is placed inside this region, then the biped can stop by taking several steps. If one assumes a lossless transfer of support in each step, one can then determine where to place the foot to achieve a new orbit energy, and hence the initial velocity of the next step. Then, the capture point can be represented by letting orbit energy equals to zero:

$$E = \frac{1}{2} \dot{x}^2 - \frac{g}{2z_c} p^2 = 0 \quad (3.24)$$

$$p = \dot{x} / w \quad (3.25)$$

where \dot{x} is the CoM velocity in x direction, p is the capture point, $w = \sqrt{g/z_c}$.

During each step, the orbit energy remains constant until the swing leg has landed. Assuming no energy is lost during landing and landing happens instantaneously, the capture point can be obtained.

The formal definition of capture point and capture state are as follows [22]:

Capture State: State in which the kinetic energy of the biped is zero and can remain zero with suitable joint torques. The CoM must lie above the CoP in the Capture state, such as the vertical upright.

Capture Point: For a biped, in state x , a Capture Point P , either with its stance foot or by stepping to P in a single step, then there exists a NOT FALL trajectories leading to a Capture State.

Following is the proof of the relationship between the moving ground reference map and Capture point:

Condition: When the stepping time T_n , and the weight $\mathbf{R}=\mathbf{I}$, $p=0$ and the moving ground reference is equivalent with Capture Point.

Proof:

$$\because \sinh(wT_n) + \cosh(wT_n) = e^{wT_n}$$

The moving ground reference point calculated based on:

$$x_0^{*(n+1)} = \frac{A - B\dot{x}_T^{(n)} - p(x_T^{(n)} + x_f^{(n)})}{D} \quad (3.26)$$

where

$$A = r_1 \cosh(wT) x_d + r_2 \sinh(wT) w\dot{x}_d + p(p_{x_d}^{(n)} + 2x_d)$$

$$B = r_1 \sinh(wT) \cosh(wT) \frac{1}{w}$$

$$D = \cosh^2(wT) + w^2 \sinh^2(wT) + p$$

By applying the weighting factors $r_1 = r_2 = 1$ and $p = 0$, the next foot placement will be:

$$x_0^{(n+1)} = \frac{\cosh(wT_n) \left(x_d - \frac{\sinh(wT_n)}{w} \dot{x}_T^{(n)} \right) + \sinh(wT_n) w \left(\dot{x}_d - \cosh(wT_n) \dot{x}_T^{(n)} \right)}{\cosh^2(wT_n) + w^2 \sinh^2(wT_n)}$$

Then we find that if we choose the stepping time to be

$$T_n^* = \frac{1}{w} \ln \left(\frac{wx_d}{\sinh(wT_n) w x_0^{(n)} - \cosh(wT_n) \dot{x}_0^{(n)}} \right)$$

i.e, $x_d = \frac{e^{wT_n^*}}{w} \dot{x}_T^{(n)}$ and $\dot{x}_d = e^{wT_n^*} \dot{x}_T^{(n)}$. Therefore,

$$\begin{aligned} x_0^{(n+1)} &= \frac{\cosh(wT_n^*) \left(\frac{e^{wT_n^*}}{w} \dot{x}_T^{(n)} - \frac{\sinh(wT_n^*)}{w} \dot{x}_T^{(n)} \right) + \sinh(wT_n^*) w \left(e^{wT_n^*} \dot{x}_T^{(n)} - \cosh(wT_n^*) \dot{x}_T^{(n)} \right)}{\cosh^2(wT_n^*) + w^2 \sinh^2(wT_n^*)} \\ &= \frac{\cosh^2(wT_n^*) \frac{\dot{x}_T^{(n)}}{w} + \sinh^2(wT_n^*) w \dot{x}_T^{(n)}}{\cosh^2(wT_n^*) + w^2 \sinh^2(wT_n^*)} \\ &= \frac{\dot{x}_T^{(n)}}{w} \frac{\cosh^2(wT_n^*) + w^2 \sinh^2(wT_n^*)}{\cosh^2(wT_n^*) + w^2 \sinh^2(wT_n^*)} = \frac{\dot{x}_T^{(n)}}{w} \end{aligned}$$

The result of capture point will be the same as the foot placement generated for next step of moving ground reference map by the above conditions.

Therefore, it can be proven that the moving ground reference map is a more general motion plan algorithm and capture point is a subset of it under the above condition. Capture Point is more suitable for fast walking while the moving ground map can be implemented to robots with limited driving power and limited walking speed, since it considers the constraint on the step length and speed of the joint.

3.6 Summary

In this chapter, a novel moving ground reference map has been proposed for motion planning of bipedal robot locomotion subject to unknown disturbance. The foot placement point reference is generated for the next step. It optimizes

the swing foot landing position in order to balance the robot as well as achieve desired body motion and reach preplanned footstep location. The ZMP reference is modified in the current step to regulate the height and orientation of the body. The weights for optimization have been discussed. We also compared the moving ground reference map with the capture point and proofed that the capture point is a part of the moving ground reference map.

In the next chapter, the control architecture of bipedal robot walking will be discussed. The implementation of moving ground reference map will be presented as well.

Chapter 4

Biped Robot Walking Algorithm Based on Proposed Moving Ground Reference Map

4.1 Introduction

In this chapter, we will present the control of bipedal robot walking on the flat ground with unknown evenness by applying the moving ground reference map based on preview control. In order to increase the disturbance rejection ability of the robot, an online optimized controller based on preview control is proposed. By applying the moving ground reference map, robust locomotion trajectories can be generated.

In this chapter, the bipedal robot walking will be discussed as follows. In Section 4.2 the background and motivation of bipedal robot walking on uneven terrain will be introduced. The basic technology and problem of preview control will be discussed. In Section 4.3, we will introduce the bipedal robot walking on flat terrain. The whole control architecture will be proposed. A dynamic model on flat terrain will be presented based on 3D Linear Inverted Pendulum Model (3D - LIPM). In Section 4.4, we will introduce the bipedal robot walking on flat terrain with unknown unevenness. We will summarise the work presented in Section 4.5.

4.2 Motivation

One of the most attractive properties of a bipedal robot is the capacity to move in the human environment. This environment may contain a lot of obstacles, such as staircase, ladders and rocks and so on, which are very challenging for the other types based robot. In order to achieve a better walking performance, there are three important conditions in Fig 4.1: an accurate perception system,

an adaptive path planner that generates suitable step location, and a robust walking controller. The accurate perception may provide the more information to plan the locomotion. The adaptive path planner would suggest suitable footstep locations in real time. The robust controller can online control the robot to follow the above footstep locations to achieve a better walking performance.

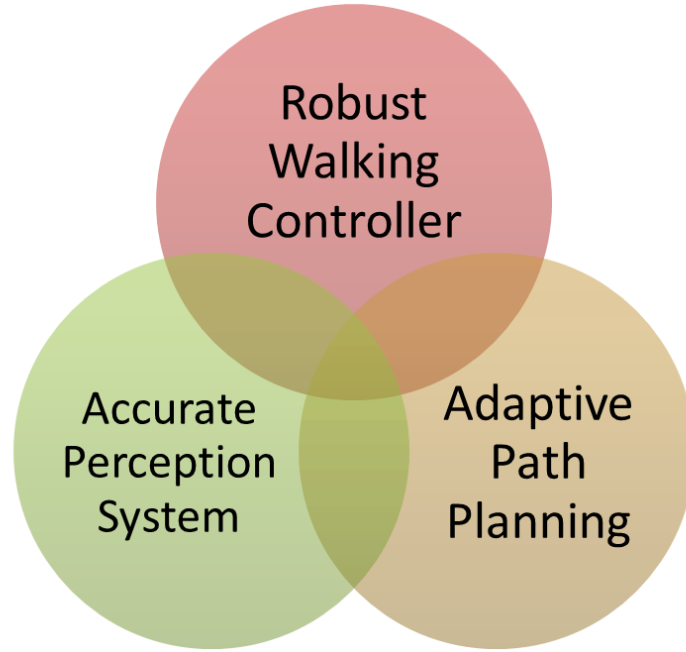


Figure 4.1 Requirements of stable walking on uneven terrain

In the previous chapter, we proposed an optimal ground reference planning, called moving ground reference map, which can provide an online suitable ZMP reference. It can overcome the problem due to inaccurate information of surrounding environment. Since accurate terrain profiles are very difficult to obtain based on the current sensor technology, it is not reliable to adopt pre-defined trajectory based on the detected terrain profiles to generate stable walking pattern in the real world environments.

We have developed a walking controller based on preview control which meets the above requirement. In previous studies, several robots have realized stable walking over uneven terrains by generating CoM trajectory based on the pre-defined the ZMP trajectory [1, 19]. Using fixed ZMP reference may lead

to poor disturbance rejection ability. Some researchers have attempted to improve the disturbance rejection ability by adjusting the ZMP reference online [2, 36, 50] and some improvements have resulted. However, there is still a need to develop an effective strategy which can adapt to large disturbances. An effective strategy would be one which can adapt to unknown and unexpected disturbances such as unevenness on the terrain. It includes preview action to take the known unevenness into consideration, such as stairs and steep slopes, when these can be known beforehand.

The approach proposed in this thesis, which is modified based on the preview controller first proposed by Kajita, et. al. [1], is shown to significantly improve the robot's ability to reject disturbances. In this approach, the moving ground reference map is utilized instead of the fixed pre-planned reference. An appropriate CoM trajectory is generated by tracking the moving ground reference map based on an optimized preview control. The trajectories of all the joints are then generated through inverse kinematics.

4.3 Bipedal Robot Walking Based on Preview control

In this section, we will introduce the basic algorithm of preview control. In the practical control system design, it is very important to make the output track the desire signal without steady-state error. Tomozuka and Rosenthal (1979) [54] developed a digital controller with state feedback, integral and preview actions. It is shown that the preview of future information is very effective in improving the tracking quality. Kajita et.al [1] was the first to apply preview control to humanoid walking.

4.3.1 Background

In preview control [1], a cart-table model (as shown in Fig 4.2) is used, in which the mass of robot is lumped in the CoM, and the height of CoM is assumed to be constant when the robot moves forward. Since the dynamics equations of the sagittal and lateral planes are linear independent and same on

the flat terrain, we use the x-axis as an example and the following algorithm can be applied to y-axis as well.

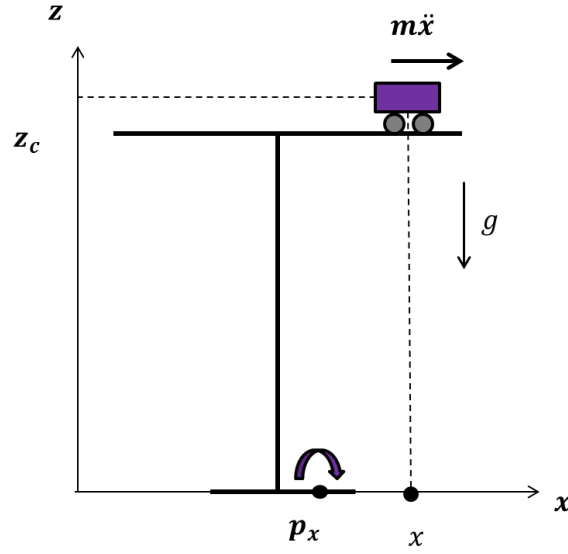


Figure 4.2 2D Cart-Table Model[1]

The overall torque τ_x in x-axis at ZMP p_{zmp} is:

$$\tau_x = m\ddot{x}z_c + mg(p_x - x) = 0 \quad (4.1)$$

where $x(k)$, $\dot{x}(k)$, $\ddot{x}(k)$ are the position, velocity and accelerator of CoM, respectively. m is the mass of cart and z_c is the constant height of table. Therefore, the position of ZMP p_x can be obtained as

$$p_x = x - \frac{z_c}{g} \ddot{x} \quad (4.2)$$

Let $w = \sqrt{z_c/g}$, and then the above equation can be rewritten as

$$p_x = x - w^2 \ddot{x} \quad (4.3)$$

Rewrite the Eq. (4.3) into state space form with \ddot{x} equal to input $u_x(t)$:

$$\frac{d}{dt} \begin{bmatrix} x(t) \\ \dot{x}(t) \\ \ddot{x}(t) \end{bmatrix} = \begin{bmatrix} 1 & 0 & 0 \\ 0 & 1 & 0 \\ 0 & 0 & 0 \end{bmatrix} \begin{bmatrix} x(t) \\ \dot{x}(t) \\ \ddot{x}(t) \end{bmatrix} + \begin{bmatrix} 0 \\ 0 \\ 1 \end{bmatrix} u_x(t) \quad (4.4)$$

$$p_x(t) = \begin{bmatrix} 1 & 0 & -w^2 \end{bmatrix} \begin{bmatrix} x(t) \\ \dot{x}(t) \\ \ddot{x}(t) \end{bmatrix}$$

Discretizing Eq. (4.4), the dynamic system equation is as follows:

$$\begin{aligned} \mathbf{x}(k+1) &= A\mathbf{x}(k) + Bu_x(k) \\ p_x(k) &= C\mathbf{x}(k) \end{aligned} \quad (4.5)$$

where $\mathbf{x}(k) = [x(k) \quad \dot{x}(k) \quad \ddot{x}(k)]^T$ is the state vector. $u_x(k)$ is the control vector.

In order to minimize tracking error, a cost function is used as follows:

$$J = \sum_{i=k}^{\infty} [Q_e e^2(i) + \Delta \mathbf{x}^T(i) Q_x \Delta \mathbf{x}(i) + R \Delta u^2(i)] \quad (4.6)$$

where $e(i) = p_x(i) - p_x^{ref}(i)$ is the error of ZMP with respect to its reference, $\Delta \mathbf{x}(i)$ and $\Delta u(i)$ are the incremental state vector and input, respectively. Q_e, R are positive weights and Q_x is a non-negative definite weight.

The optimal solution of minimizing Eq. (4.6) with the N_l preview steps is:

$$u_x(k) = -K_i \sum_{i=0}^k e(i) - K_x \mathbf{x}(k) - \sum_{j=1}^{N_l} K_d(j) p_x^{ref}(k+j) \quad (4.7)$$

where K_i, K_x, K_d are the gain [1]. The basic structure of preview control is in Fig. 4.3.

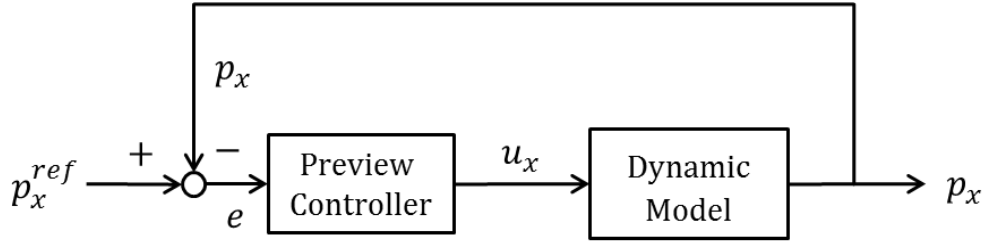


Figure 4.3 Block Diagram of Preview Control

In preview control, the use of future information is very effective in improving the tracking quality in preview control. In order to create the ZMP reference needed to generate a suitable and stable walking pattern, accurate information on the terrain is required. However, except for a specially controlled environment, accurate information on the terrain is usually not available. Some disturbances will always be presented, for example, undulation or unevenness in the terrain which can prevent the foot from reaching the expected location. Such disturbances will create errors between the support foot position and the ZMP reference as shown in simulation example in Fig. 4.4. In the simulation, trajectories generated based on flat ground was given to the robot, but the robot unexpectedly stepped onto a flat plate, of height 10mm, placed in its path when it is about 3s into its locomotion. It is shown that the disturbance caused a significant error between the foot position and the ZMP reference. And the error grew bigger with each step taken by the robot.

In order to avoid falling in the presence of unknown disturbances, an online adjustable moving ground reference map is proposed in the previous chapter. This map takes advantage of available information on both future desired stepping positions and the current robot state (CoM position, velocity and foot position). In the next section, we will present how to use the moving ground reference map in preview control to generate a robust bipedal robot walking.

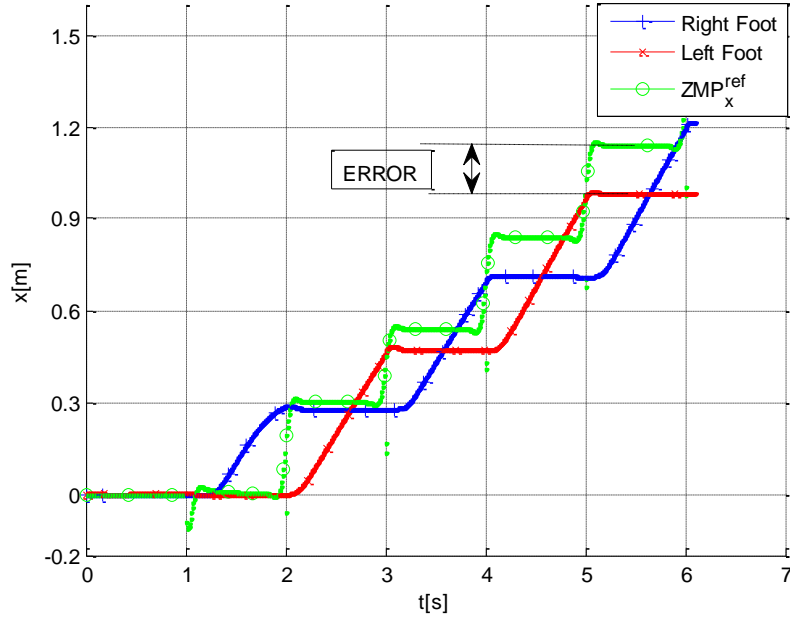


Figure 4.4 The Error of Support Foot Position and ZMP Reference

4.3.2 Control Architecture of Bipedal Robot Walking

The moving ground reference map has been proposed in the previous chapter. It can online generate the optimized next footstep location and adjust the current ZMP position to stabilize the robot walking. In this section, we will present the robust controller which enables a bipedal robot to walk on a previously unknown uneven terrain based on preview control. We propose a systematic control design for stable biped robot walking motion on uneven terrain. The terrain perception is assumed to be realized by online measurement of terrain information in relative coordinate with an accuracy of a few centimeters.

As shown in Fig. 4.5, terrain map perception provides the robot with the knowledge of the terrain with some measurement errors. Based on this, pre-planned step locations (p_x^{ref}) for the next few steps can be obtained. For the first step, the robot walks to follow the pre-defined trajectories (p_x^{ref}). Starting

from the second step, the ZMP reference will be modified and the CoM trajectory error will be compensated by modifying the ZMP reference ($p_x^{*(n+1)}$) in Eq. (4.8). By following the moving ground reference map (\hat{p}_x^{ref}), as can be seen in Eq.(4.9), continuously adjustment according to the robot's actual dynamics during locomotion can be achieved.

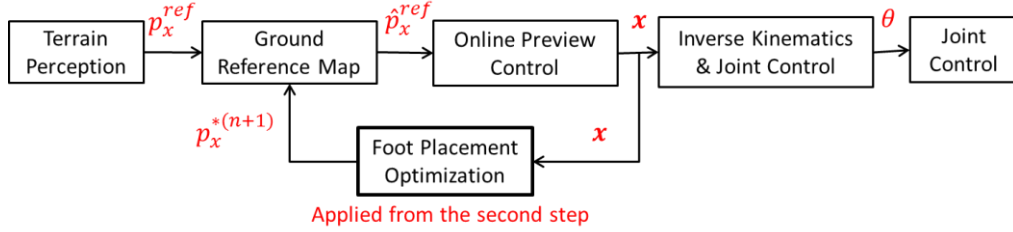


Figure 4.5 Structure of Bipedal Robot Walking on Uneven Terrain

As we discussed in 3.4.1, the optimized foot placement is calculated as follows:

$$x_0^{*(n+1)} = \frac{A - B\dot{x}_T^{(n)} - p(x_T^{(n)} + p_x^{(n)})}{D}$$

Since $x_0^{*(n+1)}$ represents the next foot placement in the relative coordinate system with respect to the stance foot, the updated next foot placement $p_x^{*(n+1)}$ in the absolute frame can be represented as:

$$p_x^{*(n+1)} = x_0^{*(n+1)} + p_x^{(n)} + x_T^{(n)} \quad (4.8)$$

Therefore, we have the moving ground reference map as follows:

$$\hat{p}_x^{ref} = \begin{bmatrix} v_1 \\ v_0 \\ v_0 \\ \vdots \\ v_0 \end{bmatrix} p_x^{ref(n)} + \begin{bmatrix} v_1 \\ v_0 \\ v_0 \\ \vdots \\ v_0 \end{bmatrix} p_x^{*(n+1)} + \dots + \begin{bmatrix} v_0 \\ v_0 \\ v_1 \\ \vdots \\ v_0 \end{bmatrix} p_x^{ref(n+N_L-1)} + \begin{bmatrix} v_0 \\ \vdots \\ v_0 \\ v_0 \\ v_1 \end{bmatrix} p_x^{ref(n+N_L)} \quad (4.9)$$

The CoM trajectories of the robot will be adjusted by online preview control in order to follow the moving ground reference map. Finally, all the CoM trajectories in Cartesian space can be converted into joint space (θ) by inverse kinematics.

4.3.3 Online Preview Control

In this section, we explain the online preview control to generate the CoM trajectories from the moving ground reference map. We consider our robot model as a linear time-invariant discrete system with sampling time as T . Hence, the system model can be described as:

$$\begin{aligned} \mathbf{x}(k+1) &= \begin{bmatrix} 1 & T & T^2/2 \\ 0 & 1 & T \\ 0 & 0 & 1 \end{bmatrix} \mathbf{x}(k) + \begin{bmatrix} T^3/6 \\ T^2/2 \\ T \end{bmatrix} u(k) \\ p_x(k) &= [1 \quad 0 \quad -w^2] \mathbf{x}(k) \end{aligned} \quad (4.10)$$

where $\mathbf{x}(k)$ is a 3×1 state vector

$$\mathbf{x}(k) = [x(k) \quad \dot{x}(k) \quad \ddot{x}(k)]^T$$

Let $p_x^{ref}(k)$ be the ZMP reference and this reference is previewable at each time k , N_l future values $p_x^{ref}(k+1), \dots, p_x^{ref}(k+N_l)$ as well as the present and past values of the demand are available. In order to make the real ZMP track the reference well, it is required to introduce the integrators to eliminate the tracking error $e(i) = p_x(i) - p_x^{ref}(i)$, $i = k, k+1, \dots, k+N_l-1$. It is known that the integral action of controller can be introduced by including the incremental control in the performance index [55]. Then we can set the performance index as follows to obtain the optimal controller $u(k)$:

$$J = \sum_{i=k}^{k+N_l-1} [Q_e e^2(i) + \Delta \mathbf{x}^T(i) Q_x \Delta \mathbf{x}(i) + R \Delta u^2(i)] \quad (4.11)$$

where $\Delta \mathbf{x}(k) = \mathbf{x}(k) - \mathbf{x}(k-1)$, $\Delta u(k) = u(k) - u(k-1)$, Q_e and R are positive scalar weights and Q_x is 3×3 symmetric positive semi-definite matrix. This performance index minimizes the tracking error, the incremental state and control vectors respectively. It can asymptotic regulation without excessive rate of change in the state and control vectors [55].

In order to make the cost function as the standard forms, an augmented state-space equation is derived. This description includes tracking error $e(i)$, incremental state vector $\Delta \mathbf{x}(k)$, the incremental control vector $\Delta u(k)$ and the incremental future ZMP reference $\Delta p_x^{ref}(i)$.

From Eq.(4.5) and (4.8), the incremental state can be presented as:

$$\Delta \mathbf{x}(k+1) = A\Delta \mathbf{x}(k) + B\Delta u(k)$$

For tracking error, it can be obtained from Eq. (4.8) and (4.9) as follows:

$$\begin{aligned} e(i+1) &= p(i+1) - p_x^{ref}(i+1) \\ &= CA\mathbf{x}(i) + CBu(i) - p_x^{ref}(i+1) - p_x^{ref}(i) \\ &\quad + p_x^{ref}(i) \\ &= CA\mathbf{x}(i) + CBu(i) - p_x^{ref}(i) - \Delta p_x^{ref}(i+1) \\ &= CA\Delta \mathbf{x}(i) + CB\Delta u(i) + e(i) - \Delta p_x^{ref}(i+1) \end{aligned} \quad (4.12)$$

where $\Delta p_x^{ref}(i) = p_x^{ref}(i) - p_x^{ref}(i-1)$.

Based on the above equation, the argument system can be built as:

$$\begin{aligned} \begin{bmatrix} e(i+1) \\ \Delta \mathbf{x}(i+1) \end{bmatrix} &= \begin{bmatrix} 1 & CA \\ 0 & A \end{bmatrix} \begin{bmatrix} e(i) \\ \Delta \mathbf{x}(i) \end{bmatrix} + \begin{bmatrix} CB \\ B \end{bmatrix} \Delta u(i) \\ &\quad - \begin{bmatrix} 1 \\ 0 \end{bmatrix} \Delta p_x^{ref}(i+1) \end{aligned} \quad (4.13)$$

Since the terrain profile information is assumed to be known, the reference for the future N_l steps $p_x^{ref}(i)$, $i = k, k+1, \dots, k+N_l$, in preview control is available at time k .

We define the incremental ZMP reference as a vector:

$$\mathbf{x}_d(k) = [\Delta p_x^{ref}(k+1), \dots, \Delta p_x^{ref}(k+N_l)]^T$$

It can be converted into a state space equation as:

$$\mathbf{x}_d(i+1) = A_d \mathbf{x}_d(k)$$

$$\text{where } A_d = \begin{bmatrix} 0 & 1 & 0 & 0 & 0 \\ 0 & 0 & 1 & 0 & \vdots \\ 0 & 0 & 0 & \ddots & 0 \\ \vdots & & & \ddots & 1 \\ 0 & & & \dots & 0 \end{bmatrix}_{N_l \times N_l}.$$

Then the new augmented state vector is defined as:

$$\tilde{\mathbf{x}}(i) = [e(i) \quad \Delta \mathbf{x}^T(i) \quad \mathbf{x}_d^T(i)]^T$$

$$\tilde{\mathbf{x}}(i+1) = \begin{bmatrix} 1 & CA & -1 & 0 & \dots & 0 \\ \mathbf{0} & A & 0 & 0 & \dots & 0 \\ 0 & & & A_d & & \end{bmatrix} \tilde{\mathbf{x}}(i) + \begin{bmatrix} CB \\ B \\ \dots \\ 0 \end{bmatrix} \Delta u(i), i = k, k+1, \dots$$

Let the performance index of the augmented system to be:

$$J = \sum_{i=k}^{k+N_l-1} \left[\tilde{\mathbf{x}}^T(i) \begin{bmatrix} Q_e & 0 & 0 \\ 0 & Q_x & 0 \\ 0 & 0 & 0 \end{bmatrix} \tilde{\mathbf{x}}(i) + R \Delta u^2(i) \right] \quad (4.14)$$

Therefore, the optimal controller $u(k)$ is given by minimizing Eq.(4.14) as:

$$u_x(k) = -G_e \sum_{i=0}^k \mathbf{e}(k) - G_x \Delta \mathbf{x}(k) + \sum_{l=1}^{N_l} G_d(l) \Delta p_x^{ref}(k+l) \quad (4.15)$$

where G_e, G_x and G_d are the gain matrix generated by Eq.(4.15).

Applying the ground reference map, the optimal controller can be calculated as follows:

$$\hat{u}_x(k) = -G_i \sum_{i=0}^k e(i) - G_x \Delta \mathbf{x}(k) - \sum_{j=1}^{N_L} G_d(j) \Delta \hat{p}_x^{ref}(k+j) \quad (4.16)$$

Noted that the optimal controller $\hat{u}_x(k)$ consists of three terms: the first term represents the integral action on the tracking error, the second term is the feedback of the CoM state and the third term is the preview action based on the moving ground reference map. Robust locomotion can be generated since the moving ground reference map is used instead of the pre-defined reference.

4.3.4 Simulation Environment

In order to evaluate the proposed approach, simulations in Webots have been conducted. The dynamic software Webots can create 3D virtual worlds with physical properties, which was introduced in Chapter 1.

Table 4.1 Simulated humanoid robot parameters

Simulated Robot Parameters	
Total Mass	86.59 Kg
Pelvis + Torso + Head Mass	42.53 Kg
Each Arm Mass	3.44 Kg
Each Leg Mass	18.59 Kg
Leg Length	0.95 m
Standing Center of Mass Height	0.8464 m
Foot Length	0.34 m
Foot Width	0.144 m

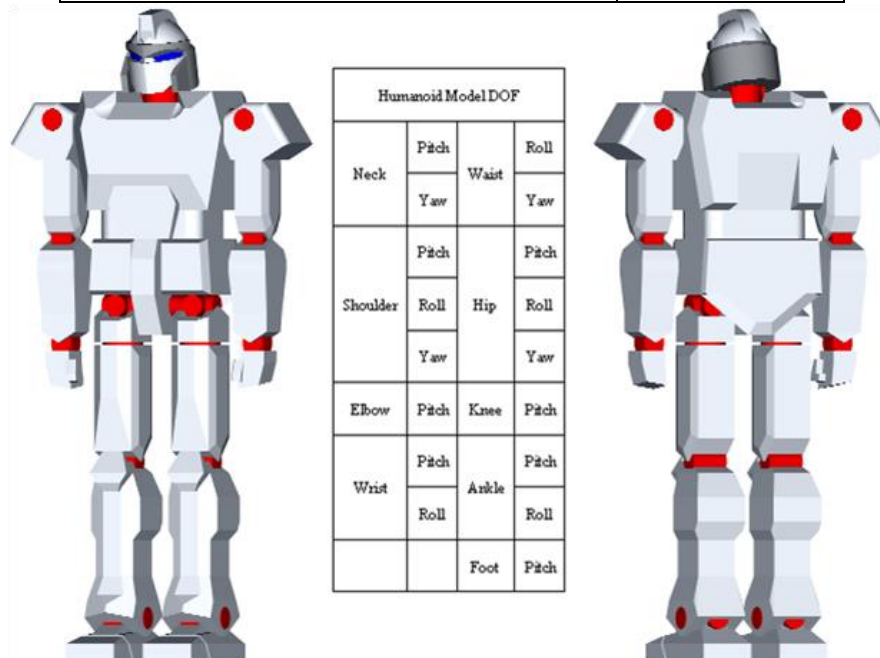


Figure 4.6 Degrees of freedom for simulated humanoid robot

A humanoid robot model is developed as the simulation subject as shown in Fig. 4.6. The robot stands 1.7 m, weighs 86.59 kg (distributed mass), and has 6 degrees of freedom in each of its two limbs. In the simulation, it is equipped with GPS, gyro, accelerometer in the pelvis (CoM). Table 4.1 details the major parameters.

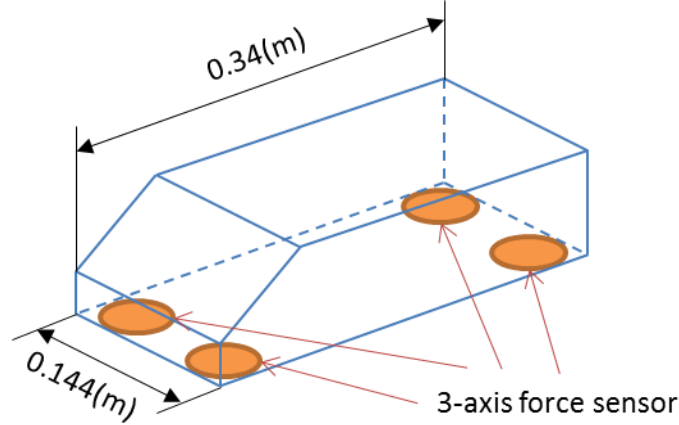


Figure 4.7 Foot structure with force sensors

In order to obtain ZMP, there are four 3-axis force sensors mounted at the corner of foot to measure contact force, which can be seen in Fig. 4.7. Then, ZMP can be calculated based this information [56].

4.3.5 Simulation Results

In this section, we applied the proposed approach to evaluate the walking performance of the above robot. We applied moving ground reference map to preview control without the presence of disturbance. The results are very close, indicating that there is little difference in these two methods for the situations without any disturbance. However, in real environment, disturbances will always exist. Therefore, further experiment is conducted to evaluate the performance when there is disturbance.

First of all, the preview gain is chosen for the following experiment. Fig.4.8 shows that the preview action gain decreases as time goes by. The magnitude

of preview gain is almost zero after 2s. Therefore, our controller takes into account only a finite number of steps.

Fig. 4.9 and 4.10 show the normal flat ground walking trajectory in x and y axis. Results show that without any disturbance, the ZMP reference was very close to the real ZMP trajectory. And the smooth CoM trajectory can be generated. The resulted ZMP can track with the ZMP reference as well. The walking step length is 0.3m through the entire walking process.

They show that the generated foot trajectories are smooth and continuous. Since the walking step length is 0.3m through the entire walking process, the second step landed at 0.6m away from the starting point, as marked in Fig. 4.9. Fig 4.11 and 4.12 shows the joints trajectories in both legs. They clearly show that the generated trajectories are smooth and continuous.

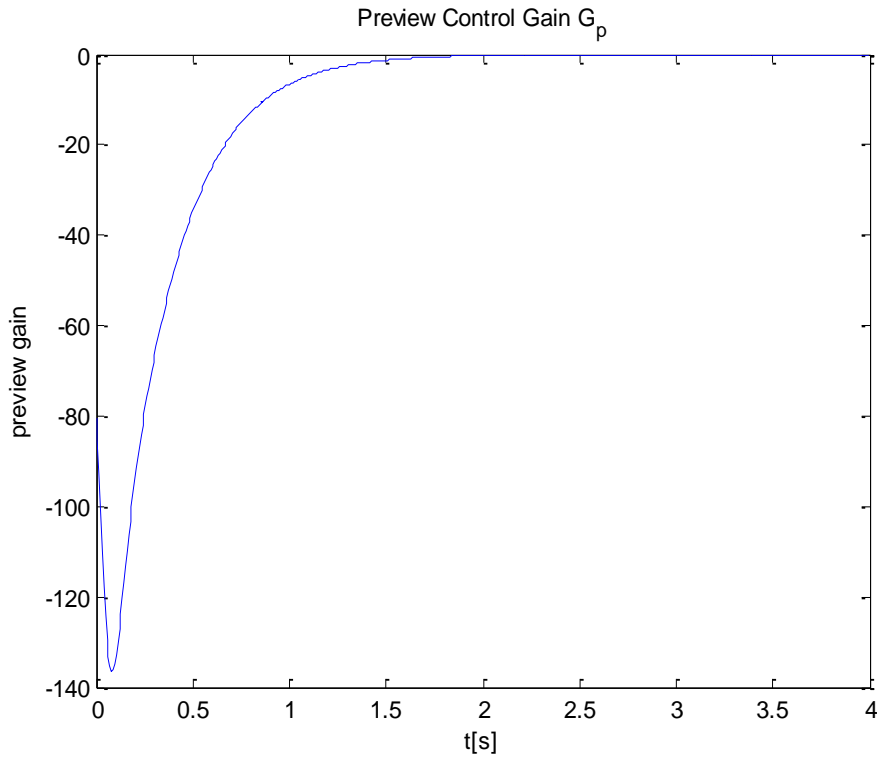


Figure 4.8 Gain of Preview Action

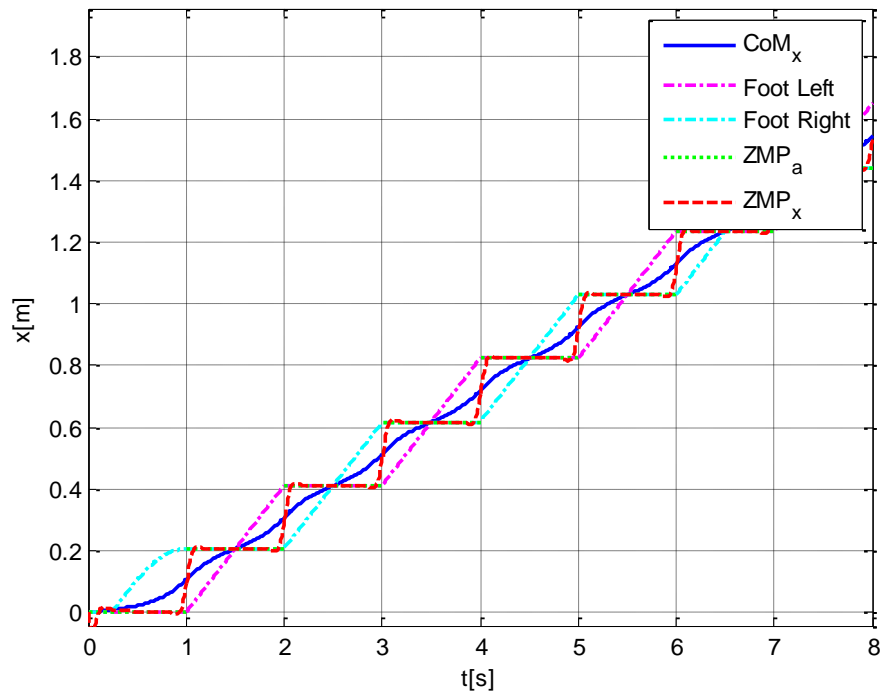


Figure 4.9 The walking on flat terrain trajectories of CoM, ZMP and foot in x direction

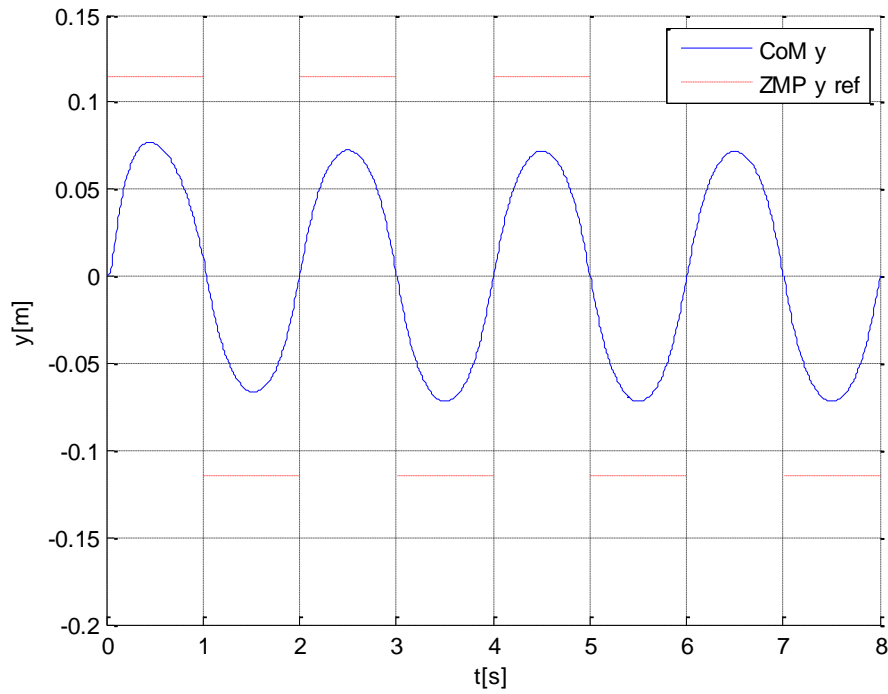


Figure 4.10 The walking on flat terrain trajectories of CoM, ZMP in y direction

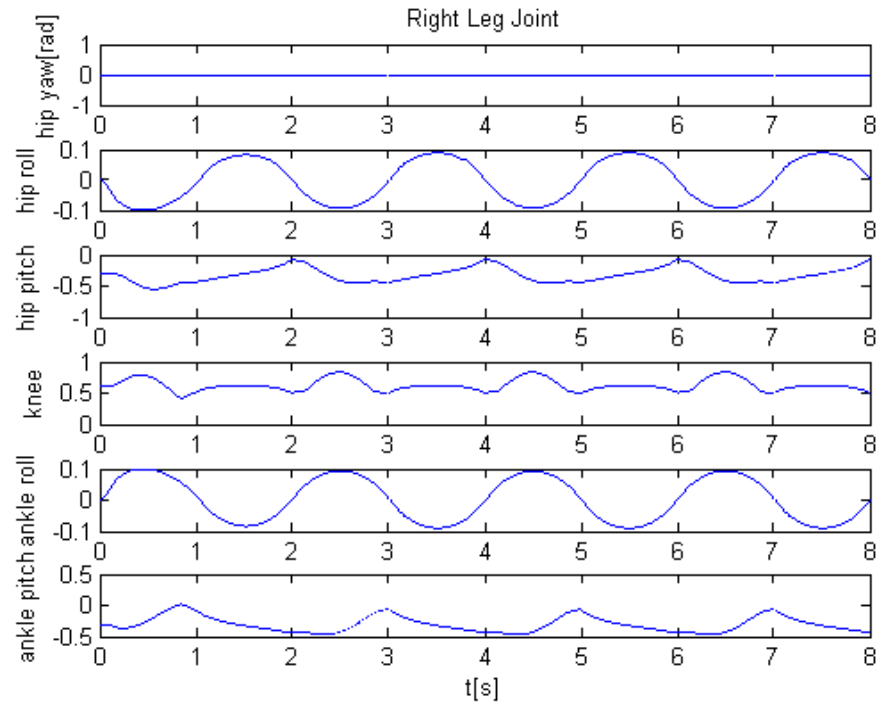


Figure 4.11 Joints trajectories of walking on flat terrain in right leg

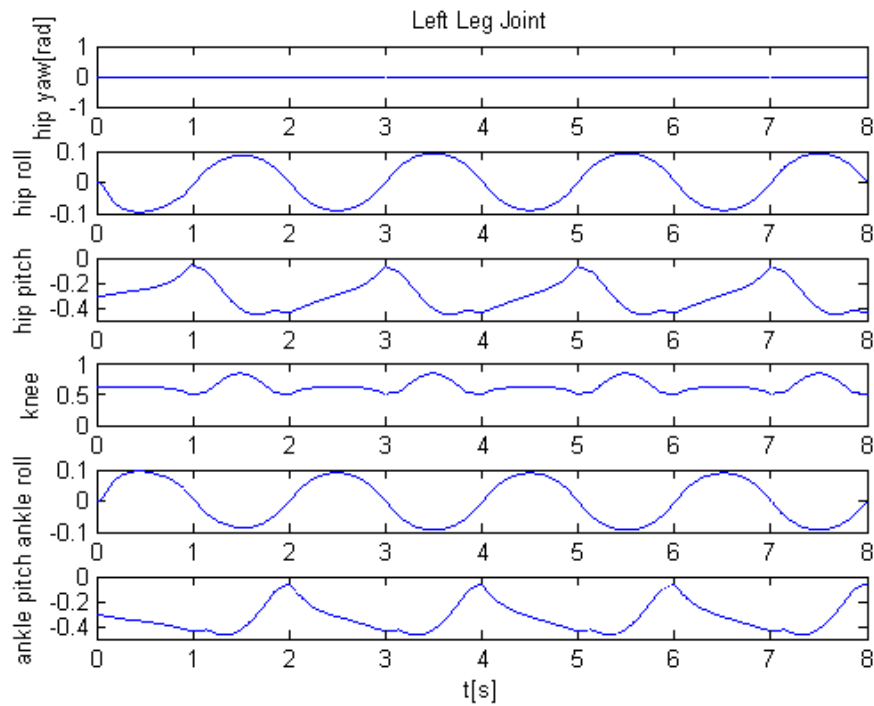


Figure 4.12 Joints trajectories of walking on flat terrain in left leg

4.4 Walking on Uneven Terrain with Unknown Disturbance

In the previous section, we have found that the walking performances in the normal flat ground are similar for the walking generation methods with and without moving ground reference map. To examine the improvement of disturbance rejection ability in the proposed approach, several experiments have been conducted by adding unevenness on the ground.

- Walking on the terrain with unknown stairs with small height.
- Walking on the terrain with several unknown stairs and slope

4.4.1 Example 1: with Unknown Staircase

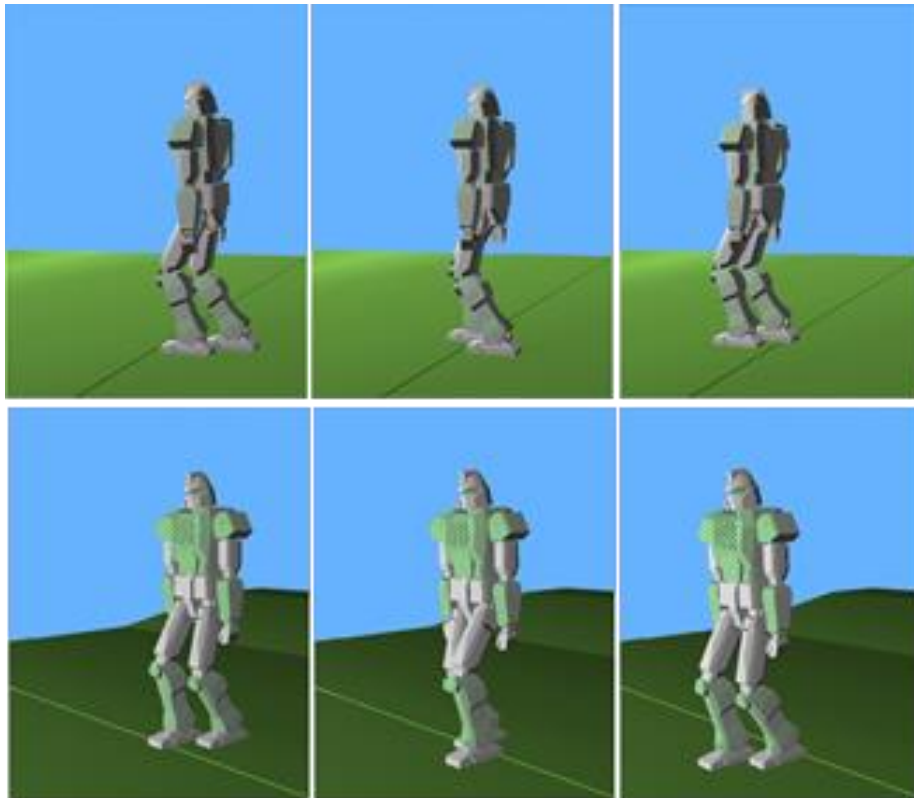


Figure 4.13 Walking on the flat terrain with unknown staircase with the proposed approach

As shown in Fig.4.13, we used a flat ground, on top of which a small plate with height 10 mm is randomly placed. In this simulation, the normal step length is 0.3m. When it is at about 3s, the robot unexpectedly stepped onto a flat plate of height 10mm.

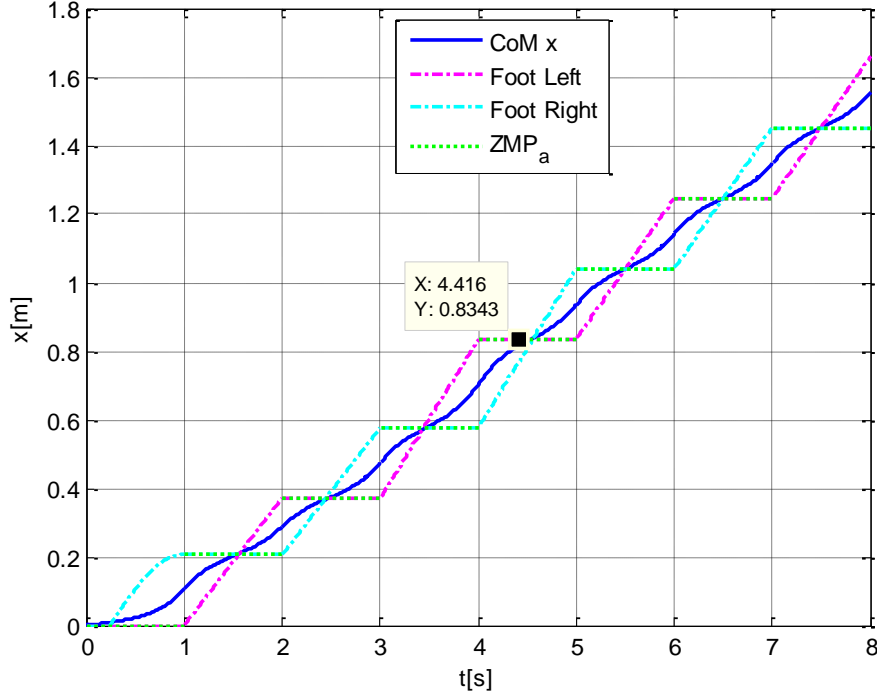


Figure 4.14 Walking on terrain containing step trajectories in x direction

Fig. 4.14 shows the walking trajectories in x direction (horizontal). The CoM trajectories (blue line) of the robot were generated based on the controller with moving ground reference map. The footstep location was changed from $0.6m$ to $0.54m$, which meant the step length is decreased to $0.24m$ in the second step. When the error in the step location was detected, the controller changed the future ZMP reference accordingly. After two steps, the foot trajectory was recovered to the original ZMP trajectory. Similarly, at 7 second, the robot walked down from the small step. The robot was able to recover to the original trajectory in the next step. The result shows the real ZMP follows the ZMP reference in the moving ground reference map closely. Moreover, the swing foot stepped on the ZMP reference every step so that stability is ensured.

However, results in Fig. 4.4 in section 4.2.3 showed that without using the proposed controller, the traditional preview control could not handle such disturbance.

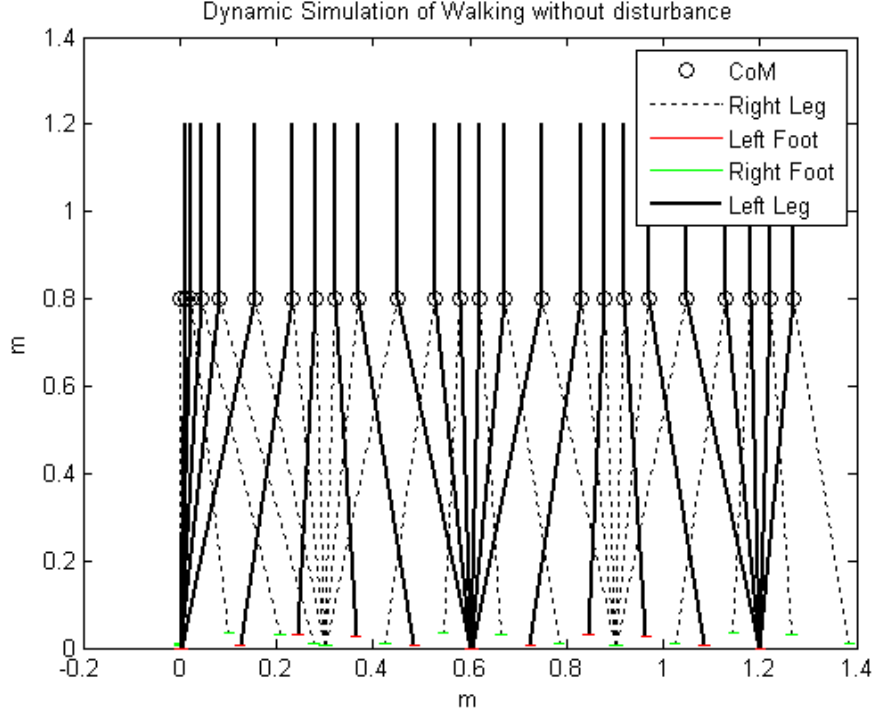


Figure 4.15 Walking without disturbance

Fig 4.15 shows the normal walking gait without any disturbance. Fig 4.15 and 4.16 show the successful robot walking over uneven terrain with unknown disturbances. Comparing with Fig 4.15, it can be seen that walking up to a step may decrease the step length while walking down from a step may increase the step length. By adopting the proposed algorithm, a more feasible next step ZMP reference is generated according to both the current state of the robot and footstep location. Since the moving ground reference map minimized the error between the pre-defined ZMP reference and the current foot step position, it could eventually recover to the pre-defined ZMP reference. This process takes one or a few steps, depending on the magnitude of the disturbance.

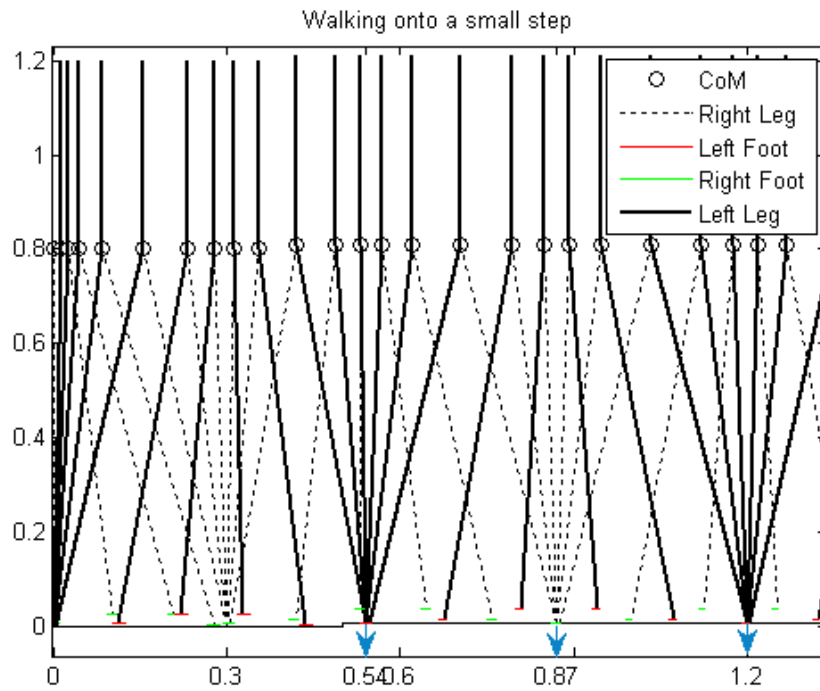


Figure 4.16 Walking on the step

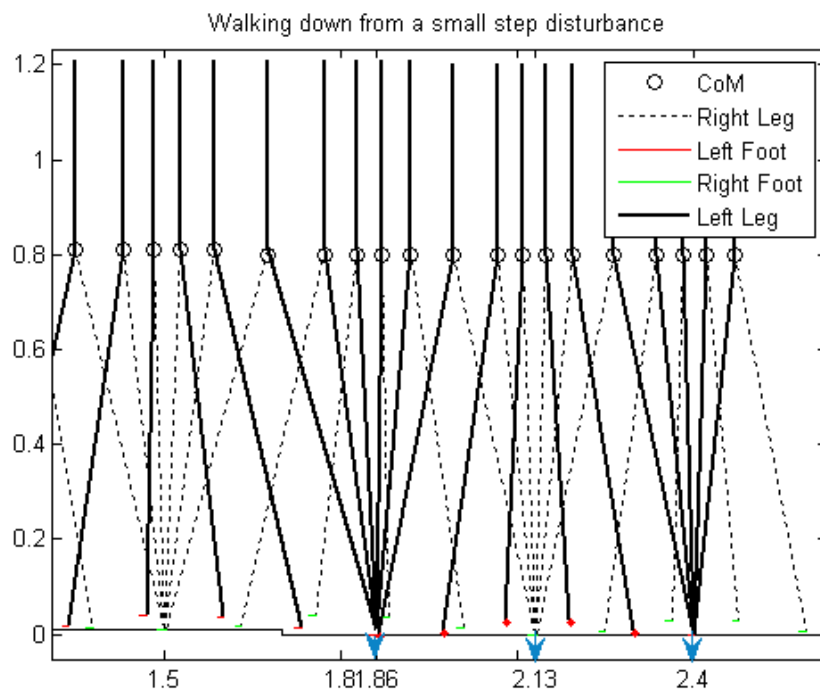


Figure 4.17 Walking down from the step

4.4.2 Example 2: with Unknown Staircase and Slope

Result in section 4.2.3 has shown that applying the traditional preview controller failed to handle the disturbance. The proposed controller needs to be employed in such situation, as shown by the results in section 4.4.1.

In order to test the limit of our approach, we increase the difficulty of experiment. In this experiment, the robot is walking based on the flat terrain. However, the actual terrain includes unknown disturbance such as a 10mm staircase and a 2° slope as shown in Fig.4.18.

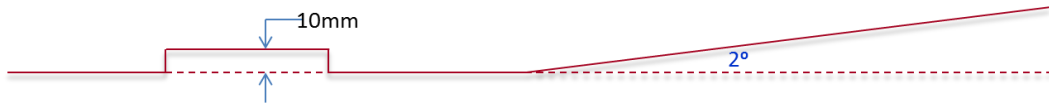


Figure 4.18 Terrain profiles in horizontal plane

Experiment shown in Fig. 4.19 has successfully demonstrated that the robot can adapt to the different unevenness by applying the proposed approach. However, Fig. 4.20 shows the walking performance with preview control. It is easy to see that, without moving ground reference map, the robot cannot walk on that terrain with disturbances.

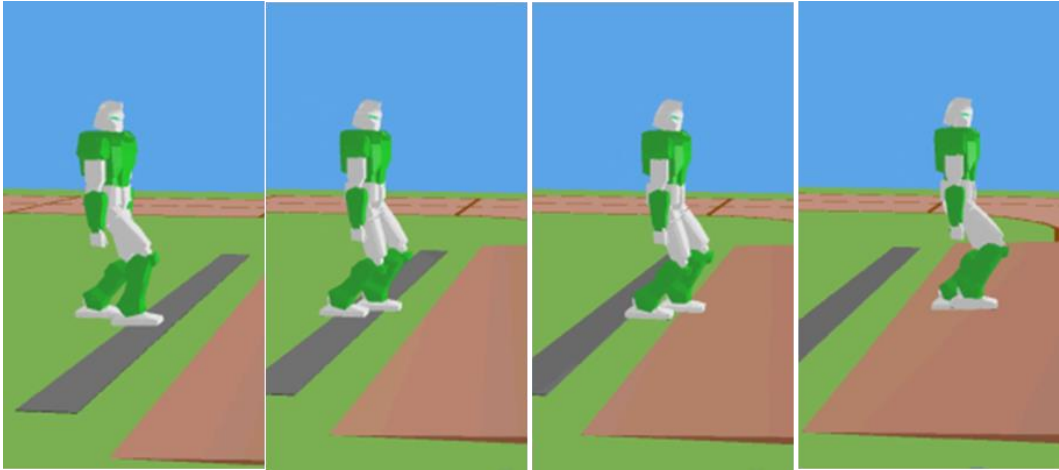


Figure 4.19 Walking performance with the proposed approach

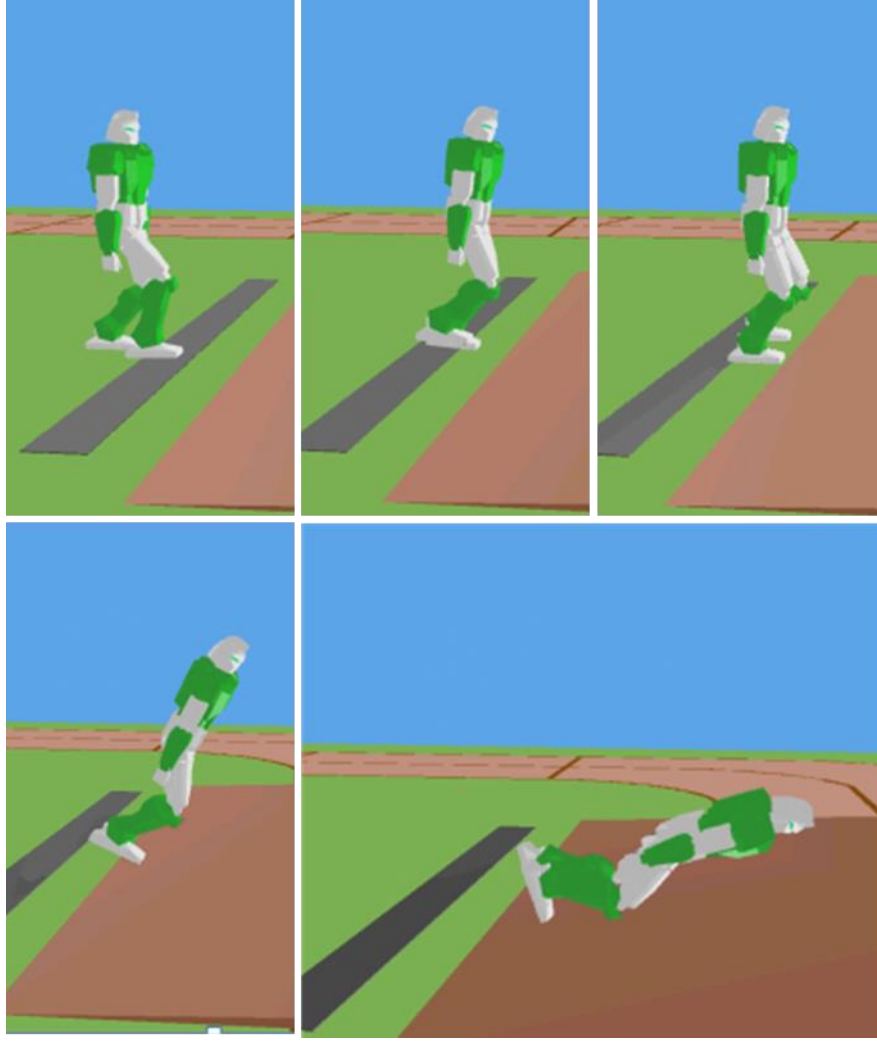


Figure 4.20 Walking performance without the proposed approach

In this experiment, the resulting ZMP and CoM trajectories in the x direction are shown in Fig. 4.21. In the figure, ZMP_d , shown by the pink dash line, is the pre-planned “desired” ZMP trajectory based on the flat ground. ZMP_a is the online adjusted trajectory using the moving ground reference map. ZMP_{real} is the trajectory of the ZMP of the robot calculated based on the state of the CoM..

In the first step, the robot encountered the 10mm height staircase without knowing it beforehand. The pre-planned ZMP does not react to the disturbance. However, the ZMP reference was adjusted such that it fitted better to the disturbance. It then, slowly adjusted itself and the difference was eventually eliminated such that the robot could adapt to the disturbance.

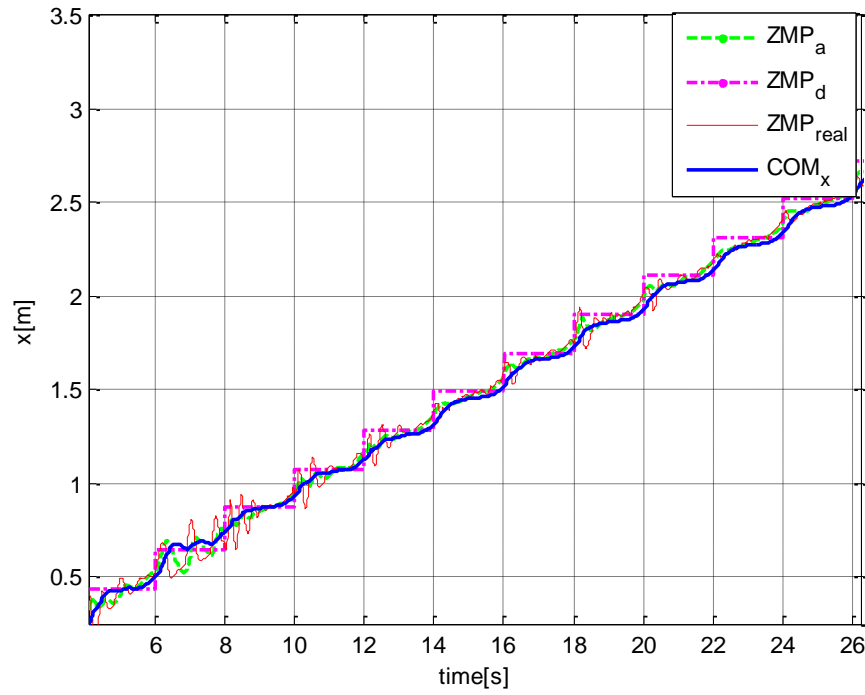


Figure 4.21 CoM and ZMP trajectories of biped walking on step and 2 degree slope in x direction

Fig. 4.22 indicates that using the proposed method, the generated ZMP_g had adapted quickly to the actual terrain profile. The real ZMP_{real} (green solid line) calculated based on the real CoM (blue solid line) is close to the generated ZMP_g . This simulation results also shows that with preview control, the generated ZMP has been tracked accurately and a smooth CoM trajectory can be generated.

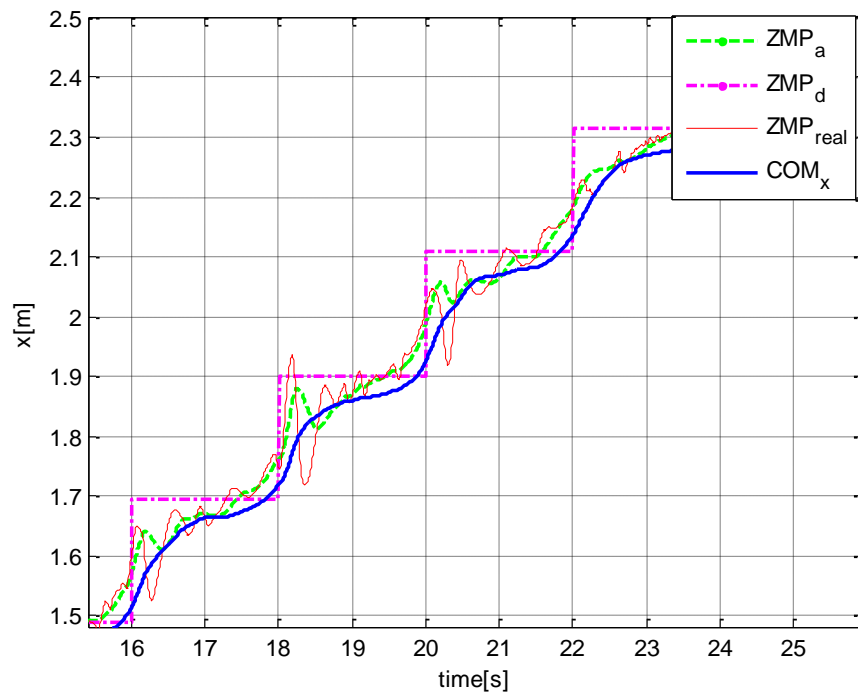


Figure 4.22 Zoomed in of CoM and ZMP trajectories of biped walking on step and 2 degree slope in x direction

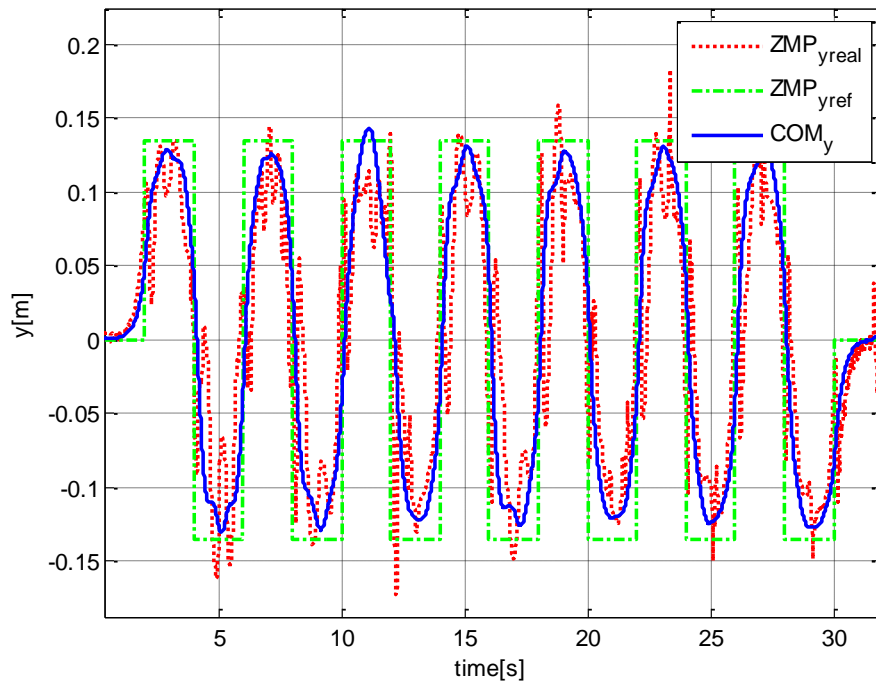


Figure 4.23 CoM and ZMP trajectories of biped walking on step and 2 degree slope in y direction

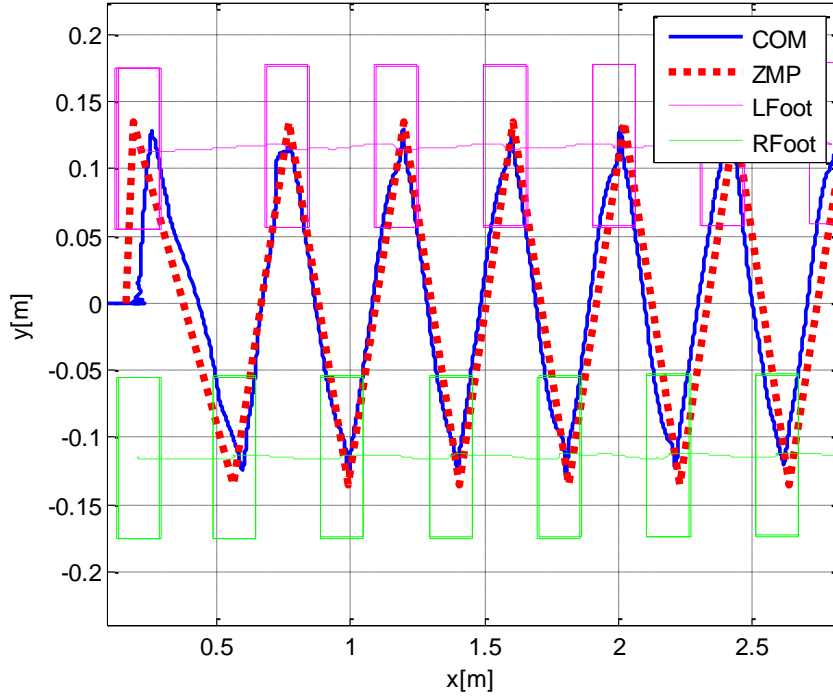


Figure 4.24 The ground projection of the real CoM and the real ZMP trajectories on the uneven terrain.

The corresponding trajectories in the y-direction are shown in Fig. 4.23. And Fig. 4.24 shows the ground projection of the real CoM and the real ZMP trajectories on the uneven terrain. It can be seen that the generated ZMP is always in the support polygon. As the robot moves, it can be observed that the real ZMP and CoM had shifted closer to the front edge of the support foot which indicated that there is an additional momentum to facilitate walking up the slope. Hence, by using the proposed moving ground reference map, the CoM trajectory will be modified to cater to external disturbances, such as inaccurate terrain information, and stable locomotion is achieved.

4.5 Summary

This chapter presents the overall control architecture of bipedal locomotion on the flat terrain with unknown disturbance. The moving ground reference scheme based on preview control is presented to realize the bipedal robot locomotion on not precisely known terrain. This preview control can be incorporated to achieve better ground reference points tracking. Simulation results show the effectiveness of the proposed approach with the robot achieving stable and smooth locomotion in spite of external disturbances and inaccurate information of the terrain.

Chapter 5

Biped Robot Walking Algorithm Based on Proposed Moving Ground Reference Map with Genetic Algorithm Adjustment

5.1 Introduction

In this chapter, we will present the simulation results for bipedal robot walking on an uneven terrain with unknown disturbance. The Moving Ground Reference Map with GA adjustment is applied to the walking algorithm. Simulation results with and without using the proposed approach will be compared and discussed.

The humanoid robot walking pattern generation will be shown in uneven environments such as slopes and stairs. In order to test the disturbance rejection ability of the robot, terrains with certain measurement errors are employed. The performances of using different weights for moving ground reference map will be presented as well. Simulation results will be used to demonstrate the effectiveness of the proposed approach.

In this chapter, bipedal robot walking experiments will be as follows: in Section 5.2, the 3D Linear Inverted Pendulum Model (3D - LIPM) on uneven terrain will be presented. The overall strategy of bipedal robot walking on uneven terrain with unknown disturbance will be discussed. In Section 5.3, bipedal robot walking on slope with and without unknown disturbance will be presented. In Section 5.4, bipedal robot walking on stairs with different weighting factors will be presented.

5.2 Walking Pattern Generation on Uneven Terrain

In the previous chapter, we have discussed the walking pattern generation of bipedal robot on the flat ground with small unevenness. Usually, this unevenness cannot be easily captured by sensors. This small unevenness includes the unevenness such as steps with less than 10mm height, slopes of less than 5° gradients, and their combination. In real human environment, there are many stairs with different heights, slopes with large inclination angles. An algorithm solely based on the flat model may not be able to handle these environmental variations. Therefore, a dynamic model of the bipedal robot based on slopes and stairs is required.

5.2.1 Dynamics of Bipedal Robot Walking on Uneven Terrain

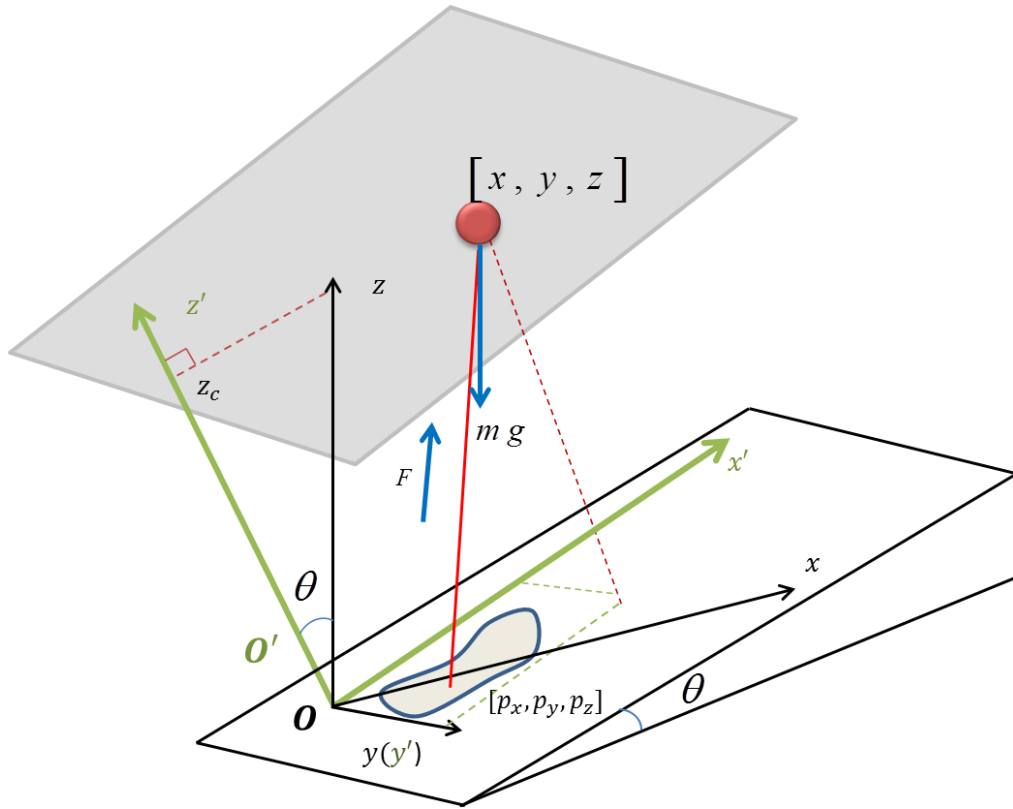


Figure 5.1 3D Dynamic Model of Bipedal Robot Walking on Uneven Terrain

Fig. 5.1 shows 3D - LIPM model [40] on a slope. The ankle joint position of the support foot is modified to adapt to the slope. 3D - LIPM model on stairs will be similar except there is no need for ankle joint modification. Therefore, this model shown in Fig. 5.1 can be used to represent both scenarios.

The mass of the robot is assumed to be lumped at the CoM and the height of the CoM with respect to the slope is assumed to maintain constant as the robot moves forward along the slope. The inclination of the slope is θ as shown in Fig. 5.1. In this figure, $X'Y'Z'$ (O') is the reference frame attached to the slope with its X' axis pointing up along the walking direction, the Y' axis is horizontal, and the Z' axis orthogonal to both the X' and the Y' axes.

From the dynamic analysis, we find that the gravity affects the COM trajectories in both x' and z' direction. The dynamic equations of LIPM with respect to the support foot location can be expressed as follows:

$$m\ddot{x}' = F'_x = \frac{x'}{r}F' - mg\sin\theta \quad (5.1)$$

$$m\ddot{y}' = F'_y = \frac{y'}{r}F' \quad (5.2)$$

$$m\ddot{z}' = F'_z = \frac{z_c}{r}F' - mg\cos\theta \quad (5.3)$$

where Eq. 5.1- 5.3 are the dynamics of the system in X' , Y' and Z' direction,

respectively. Since $\ddot{z}' = 0$, we obtain $F' = mg \cos \theta \frac{r}{z_c}$. Substituting it into

Eq.(5.1) and (5.2), we have

$$\ddot{x}' = \frac{g}{z_c} \cos\theta x' - g\sin\theta \quad (5.4)$$

$$\ddot{y}' = \frac{g}{z_c} y' \cos\theta \quad (5.5)$$

For the model with finite size foot, the dynamics of LIMP on slope with respect to the origin in a global frame is:

$$\ddot{x}' = \frac{g}{z_c} \cos\theta (x' - p'_x) - g \sin\theta \quad (5.6)$$

$$\ddot{y}' = \frac{g}{z_c} (y' - p'_y) \cos\theta \quad (5.7)$$

Then the ZMP on the slope can be expressed from Eqs.(5.6) and (5.7):

$$p'_x = x' - \ddot{x}' \cdot \frac{z_c}{g \cos\theta} + z_c \cdot \tan\theta \quad (5.8)$$

$$p'_y = y' - \ddot{y}' \cdot \frac{z_c}{g \cos\theta} \quad (5.9)$$

where x' and y' are the displacements of the CoM in the respective directions. p'_x and p'_y are the position of the ZMP along the X' - and the Y' -axis, respectively. \hat{u}'_x and \hat{u}'_y are the control inputs in X' - and Y' - directions. z_c is a constant representing the height of CoM in the same frame.

In X' direction, the dynamics of model is as follows,

$$\begin{aligned} \frac{d}{dt} \begin{bmatrix} x'(t) \\ \dot{x}'(t) \\ \ddot{x}'(t) \end{bmatrix} &= \begin{bmatrix} 0 & 1 & 0 \\ 0 & 0 & 1 \\ 0 & 0 & 0 \end{bmatrix} \begin{bmatrix} x'(t) \\ \dot{x}'(t) \\ \ddot{x}'(t) \end{bmatrix} + \begin{bmatrix} 0 \\ 0 \\ 1 \end{bmatrix} \hat{u}'_x(t) \\ p'_x(t) &= \begin{bmatrix} 1 & 0 & -\frac{w^2}{\cos\theta} \end{bmatrix} \begin{bmatrix} x'(t) \\ \dot{x}'(t) \\ \ddot{x}'(t) \end{bmatrix} - z_c \tan\theta \end{aligned} \quad (5.10)$$

In Y' direction,

$$\frac{d}{dt} \begin{bmatrix} y'(t) \\ \dot{y}'(t) \\ \ddot{y}'(t) \end{bmatrix} = \begin{bmatrix} 0 & 1 & 0 \\ 0 & 0 & 1 \\ 0 & 0 & 0 \end{bmatrix} \begin{bmatrix} y'(t) \\ \dot{y}'(t) \\ \ddot{y}'(t) \end{bmatrix} + \begin{bmatrix} 0 \\ 0 \\ 1 \end{bmatrix} \hat{u}'_y(t) \quad (5.11)$$

$$p_y(t) = \begin{bmatrix} 1 & 0 & -\frac{w^2}{\cos\theta} \end{bmatrix} \begin{bmatrix} y'(t) \\ \dot{y}'(t) \\ \ddot{y}'(t) \end{bmatrix}$$

The controller applied is the same as in Chapter 4,

$$\hat{u}'_x(k) = -G_i \sum_{i=0}^k e^{(i)} - G_x \Delta \mathbf{x}'(k) - \sum_{j=1}^{N_L} G_d(j) \hat{\mathbf{p}}_x'^{\text{ref}}(k+j) \quad (5.12)$$

Therefore, the CoM trajectory in the slope frame (O' frame) can be obtained. Then the desired CoM trajectory can be generated by transforming the CoM trajectory in the slope frame into the original flat frame (O frame). The same strategy can also be used in stair walking as it can be considered as a special case of slope walking where the swing foot lands on a flat plane instead of a slope. By applying this coordinate transformation method, walking on the inclined surface become possible.

5.2.2 Overall Strategy of Bipedal Robot Walking on Uneven Terrain

We propose a systematic control design for stable biped robot walking motion on uneven terrain. As shown in Fig. 5.2, terrain map perception provides the robot with the knowledge of the terrain with some measurement errors. The CoM trajectory on the uneven terrain can be obtained by coordinate transformation as shown section 5.2.1. Therefore, an online adjusted CoM trajectory is obtained by following the moving ground reference map. Finally, the joint trajectories are obtained by applying inverse kinematics.

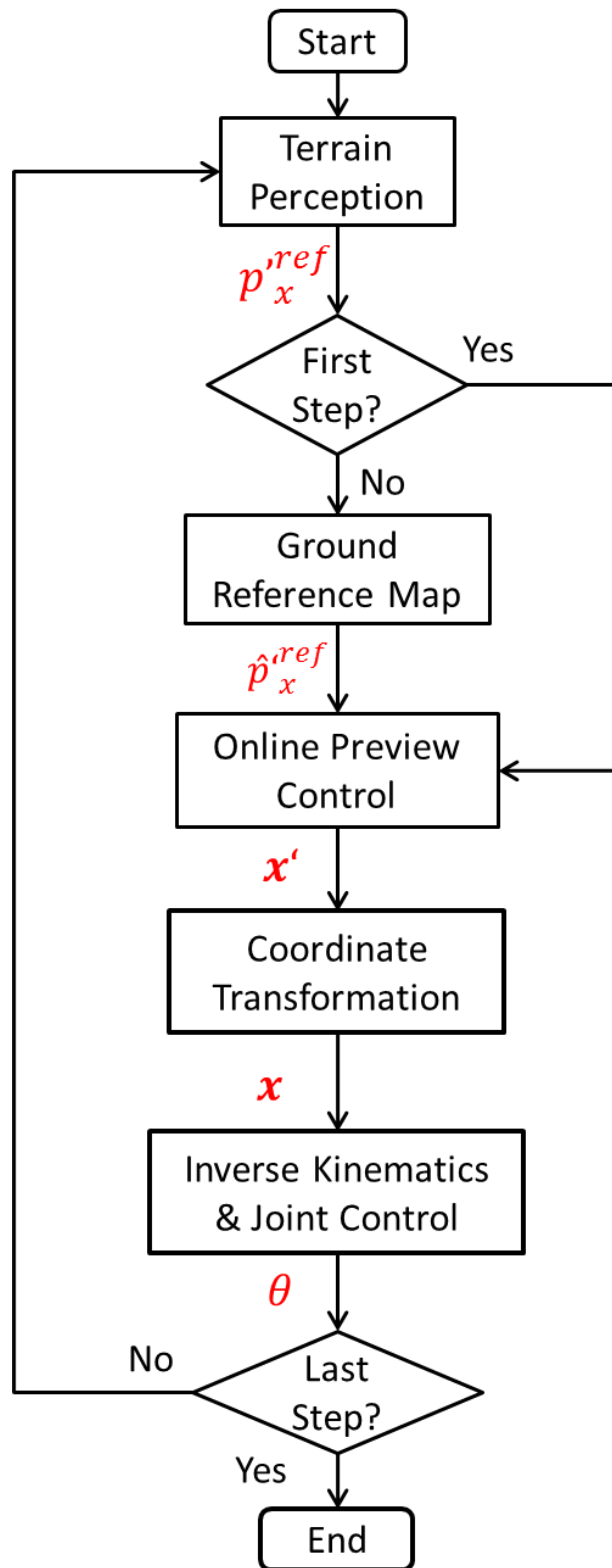


Figure 5.2 Structure of bipedal robot walking on uneven terrain

5.3 Bipedal Locomotion on Slope Terrain

In order to verify the proposed method, an experiment was conducted. We assume the terrain perception is not accurate. The robot is made to walk along a horizontal terrain and then up onto a slope. The slope is inclined at 8 degrees but the information provided to the robot for this slope is 5 degrees to simulate inaccurate terrain information obtained from the sensors. Since the robot step length is 0.3m, every step the robot walk, an error of 15.7mm will be induced in the Z direction. A sensor error was used to evaluate the efficiency of the proposed walking algorithm.

Fig 5.3 shows that without any adaption of the pre-planned ZMP trajectory, the robot is not able to achieve stable locomotion on the slope without falling. However, with the application of the moving ground reference map, stable walking up the slope was achieved in Fig 5.4.

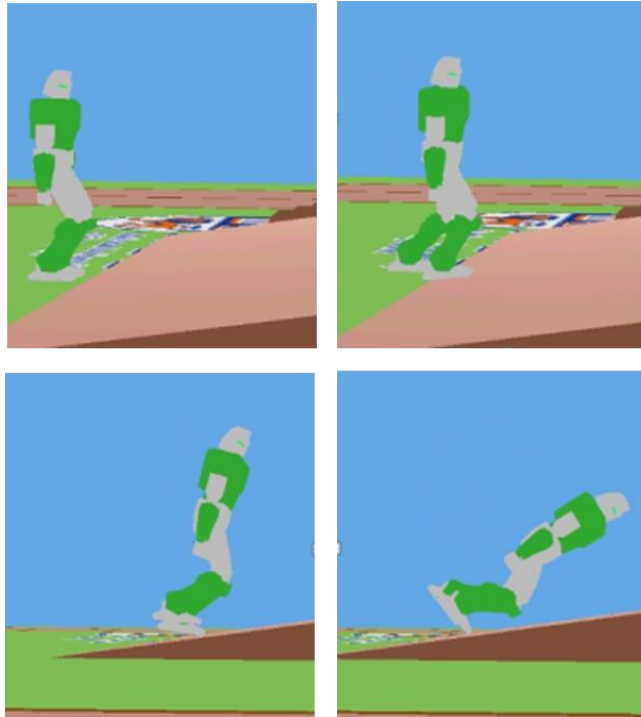


Figure 5.3 Biped walking on the slope without online ZMP reference adjustment

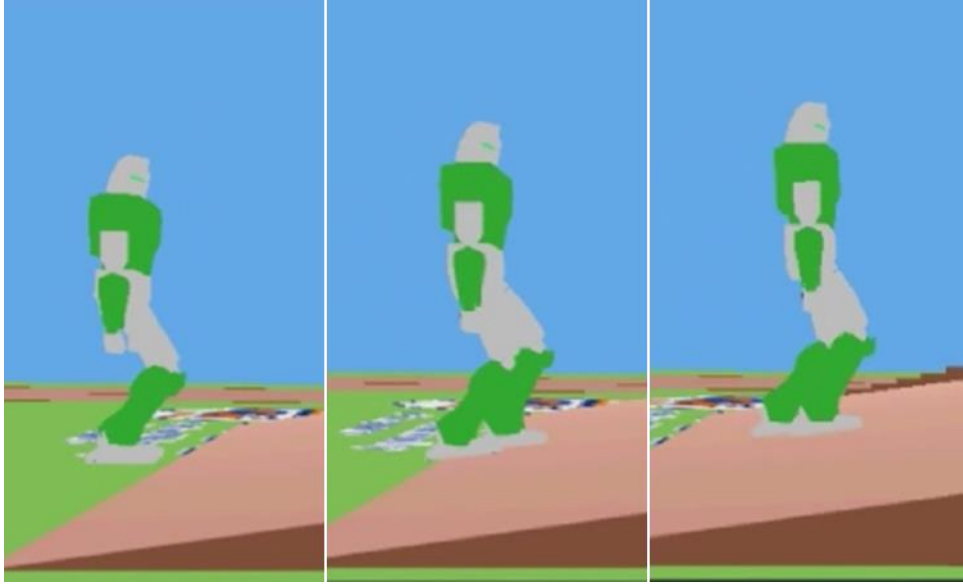


Figure 5.4 Biped walking on the slope with Moving Ground Reference Map

In Chapter 3.4.1, we discussed that, for the moving ground reference map, there are two weighting factors, \mathbf{R} and p . \mathbf{R} is the weight of converging CoM to its desired state, and p is the weight of converging footstep position to the preplanned ground reference point. In this thesis, we assume that the position and velocity have equivalent importance to the biped walking generation, which means that $\mathbf{R} = \begin{bmatrix} r_1 & 0 \\ 0 & r_2 \end{bmatrix}$. Genetic Algorithm is applied to optimize the weighting factors r_1, r_2 and p .

In this unknown slope environment, based on the fitness function and the other parameters referring to the previous section 3.4.1, the optimized weighting factors can be obtained. Table 5.1 gives the set-up of the GA for the generation of optimization of weighting factors.

The weights in fitness function are chosen to balance the scale of both fitness functions. The best results after the GA procedure are as follows: $[r_1 \ r_2 \ p] = [0.823 \ 0.942 \ 0.0433]$. In this situation, the value of the fitness function is largest, indicating a good optimization performance.

Table 5.1 GA Set-up for the generation of optimization of weighting factors

Description	Remark
Fitness Function	f_1, f_2
Chromosome Representation	Real-valued (floating point)
Initial population	100
Generation number	200
Crossover	simple crossover arithmetic crossover heuristic crossover
Mutation operation	uniform mutation multi-non-uniform mutation boundary mutation
Weights for fitness function	$w_i = [200 \ 1]$

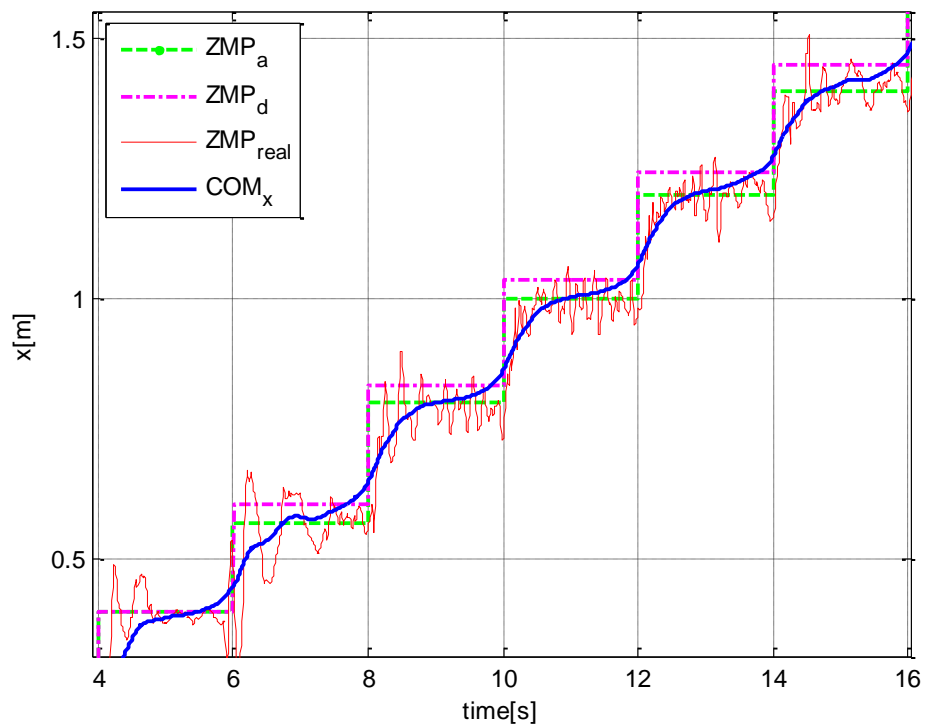


Figure 5.5 CoM and ZMP trajectories walking on the slope in x direction with the GA optimal weighting factors

The resulting ZMP and CoM trajectories obtained are shown in Fig. 5.6 for the x-direction with GA optimized weighing factors. In the figure, ZMP_d , shown by the pink dash line, is the pre-planned “desired” ZMP trajectory based on the 5-degree slope. ZMP_a is the re-computed trajectory adjusted online using the moving ground reference map. ZMP_{real} is the trajectory of the ZMP of the robot. It can be seen from Fig. 5.6, in which the adjusted ZMP_a (green dash line) deviates from the pre-defined ZMP_d from the second step after the robot has walked onto the slope. Then, the difference between the ZMP_a and ZMP_d gradually reduces to a constant. This indicates that using the proposed method, the adjusted ZMP_a had adapted quite quickly to the actual terrain profile. The real ZMP_{real} (red solid line) follows the generated ZMP with good accuracy. This simulation results also show that with preview control, a smooth CoM trajectory can be generated. The real ZMP tracked accurately with the adjusted ZMP reference provided by the moving ground reference map.

In order to check the effect of the weighting factors, another two experiments with extreme conditions were conducted. The first experiment was performed by letting $r_1 = r_2 = 0$ ($\mathbf{R} = \mathbf{0}$) and $p = 1$ while the second one was performed by letting $r_1 = r_2 = 1$ ($\mathbf{R} = \mathbf{I}$) and $p = 0$. The first experiment has shown that the robot cannot successfully walk on that slope with unknown disturbance. It indicated that following the pre-planned trajectory blindly without considering the stability will eventually lead to failure. For the second situation, the value of the fitness function is much smaller than the GA optimal one.

Fig. 5.8 shows the x-direction ZMP and CoM trajectories in the second simulation. Results showed the adjusted ZMP_a (green dash line) deviates from the pre-defined ZMP_d (pink dash line) from the second step after it walked onto the slope. In Fig. 5.8, the difference between the ZMP_a and ZMP_d increases as time went on. This indicates that using only weighting factor R , the adjusted ZMP_a only takes care of the stability of robot walking. It does not

take the constraints of allowable step location into consideration. This can be dangerous if only small regions are allowed to step on along a given path, for example, crossing a river by stepping on stones which are randomly placed across the river.

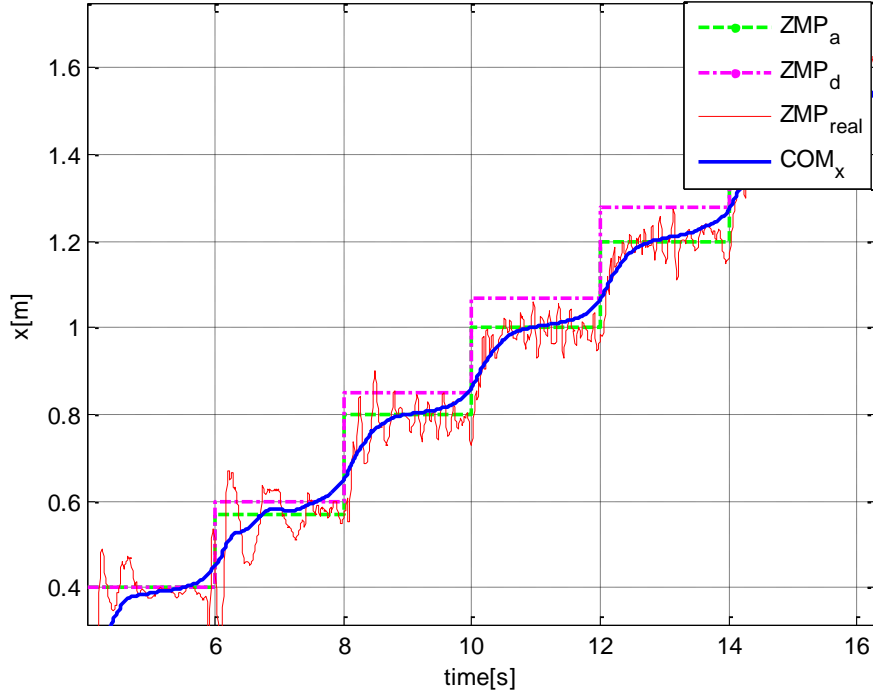


Figure 5.6 CoM and ZMP trajectories in x direction with not optimal weighting factors

In this experiment, the actual inclination angle is larger than the angle given by the sensors. Therefore, the resulting velocity of CoM is smaller than the pre-planned CoM velocity. Larger weighting factor \mathbf{R} will results in a smaller next step ZMP position. However, the weighting factor p will have counter effect on this change. The corresponding trajectories in the y-direction are shown in Fig. 5.9.

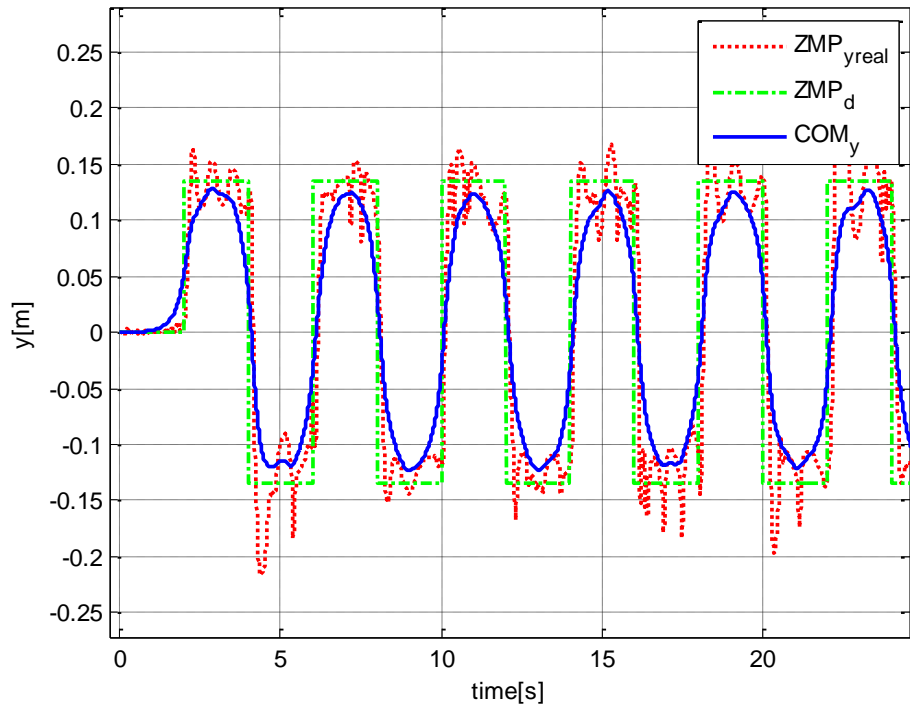


Figure 5.7 CoM and ZMP trajectories walking on the slope in y direction with the GA optimal weighting factors

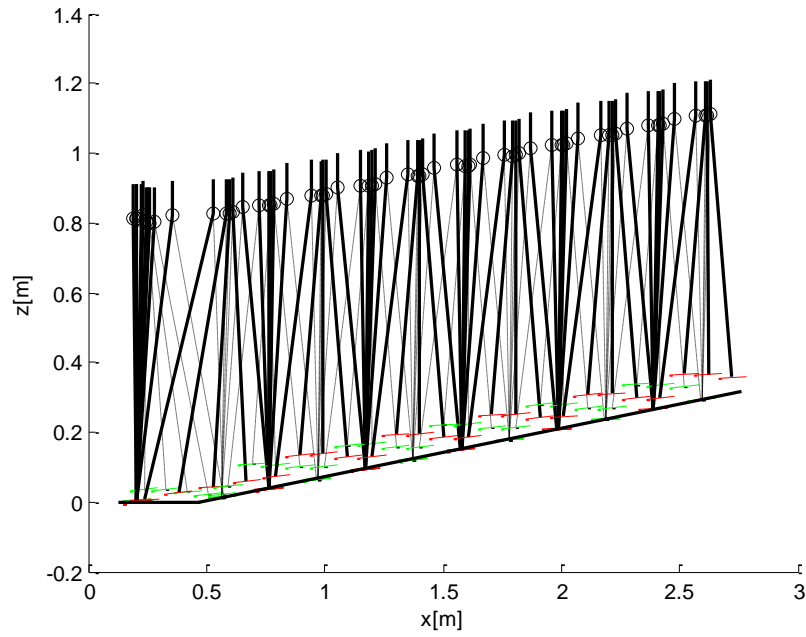


Figure 5.8 The stick diagram of the biped walking on the slope.

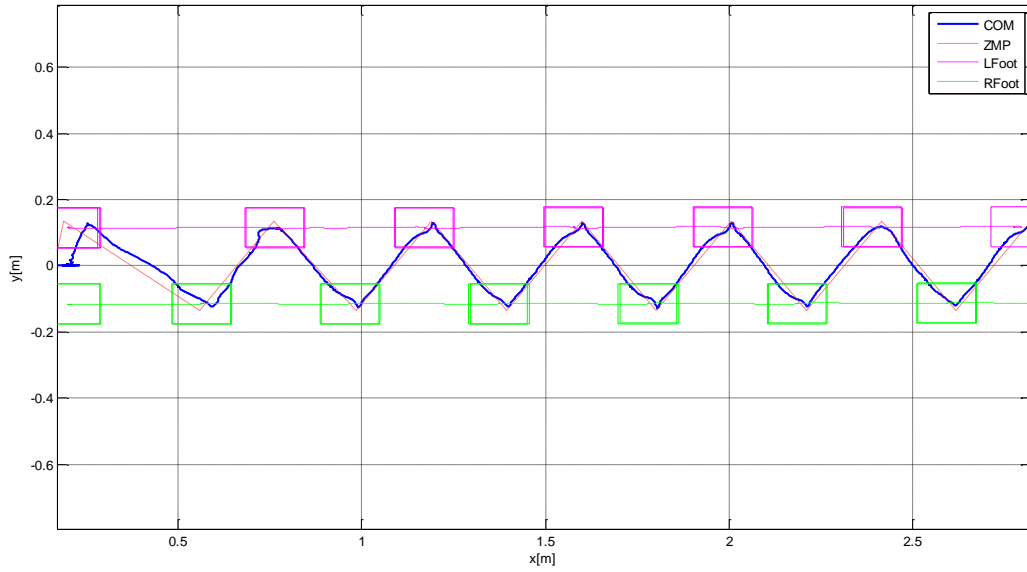


Figure 5.9 The ground projection of the real CoM and the real ZMP trajectories on the 8 degree slope.

The stick diagram of the biped walking on the slope is shown in Fig. 5.10. It shows that the proposed approach enables the biped walking on the unknown slope properly. Fig. 5.11 shows the ground projection of the real CoM and the real ZMP trajectories on the uneven terrain. As the robot moves, it can be observed that the generated ZMP is followed closely by the real ZMP. It moved beyond the CoM, creating an additional momentum to facilitate the extra torque required to walk up onto the slope. Hence, by using the proposed moving ground reference map, the CoM trajectory has been modified to cater to external disturbances, such as inaccurate terrain information. The results shows that stable locomotion on uneven terrain with disturbance can be achieved.

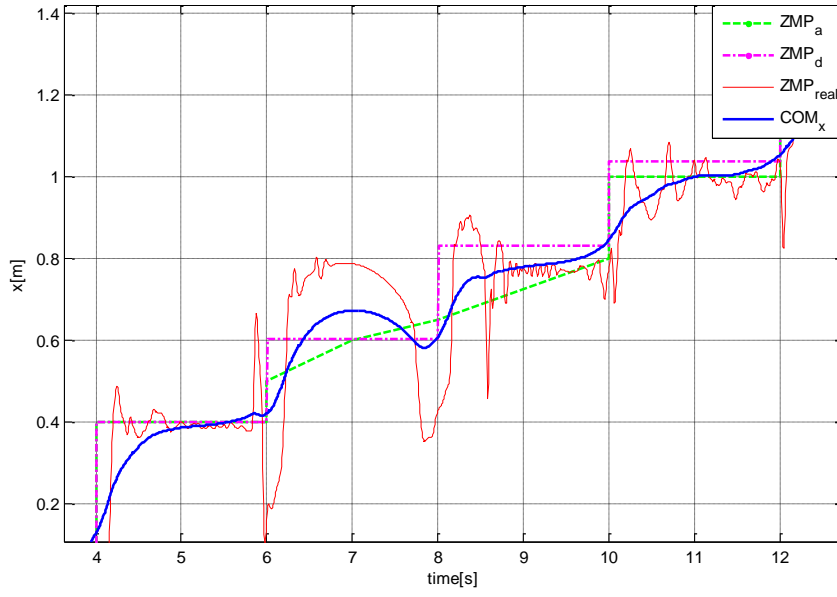


Figure 5.10 CoM and ZMP trajectories in x direction with sudden change due to the external force when 6s.

The above simulations results showed the biped robot walking performance in presence of constant disturbance with moving ground reference map on the unknown uneven terrain. In some other situations, sudden disturbances may happen between each step. In this case, the additional adjustment of ZMP reference in the current step can be used to generate a compensation torque to correct the CoM motion error due to the disturbances.

Fig.5.12 shows the resulted CoM and ZMP trajectories in x direction with sudden disturbance due to unexpected impact during walking with the same weighting factors. The sudden change of CoM occurred at $time = 6s$. To adapt to this disturbance, the additional adjustment of ZMP reference of the current step was generated as shown in Fig. 5.12. By applying this additional ZMP adjustment, the sudden change in the CoM and ZMP trajectories was eventually eliminated. This additional adjustment in the single support phase further increased the robustness of the walking algorithm.

5.4 Bipedal Locomotion on Stair Terrain

For stair walking, the strategy is similar to slope walking. However, it is more challenging. In build-up environment, stairs is very commonly. In order to examine the effect of the proposed approach walking on stairs, the robot walking was tested on a specifically designed stairs. For this design, the height of each step is randomly selected from a predetermined range. These stairs with variable step heights are more challenging for a humanoid to walk up or down.

We define two stairs:

1. Normal stair with the same height in each step. (65mm)
2. Stair with different height.

(65mm with random error $\delta \in [-2,2]$ mm)

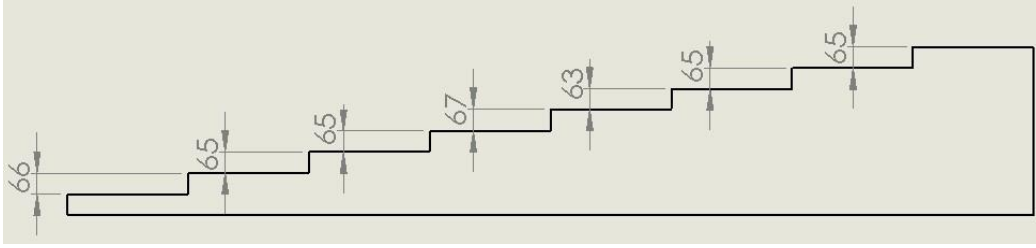


Figure 5.11 Terrain Profile in Side View

This random selected error δ is used to simulate the sensor measurement errors. In this section, we would like to find the trend of the weighing effect of moving ground reference map. Therefore, the disturbance may satisfy with all the weighting condition, ± 2 mm is chosen to represent this error. Furthermore, we assume there is no push or other disturbance during the walking. Only next step locations will be adjusted in the moving ground reference map. The pre-defined reference for preview action is generated by assuming same height (65mm) in each step. However, the real stairs is shown in Fig. 5.13.

Without any adaption to the pre-planned ZMP trajectory, simulations showed that the robot was not able to achieve stable locomotion onto the stairs without

falling. However, with the application of the moving ground reference map, stable walking up the stairs was achieved as can be seen in Fig.5.14.

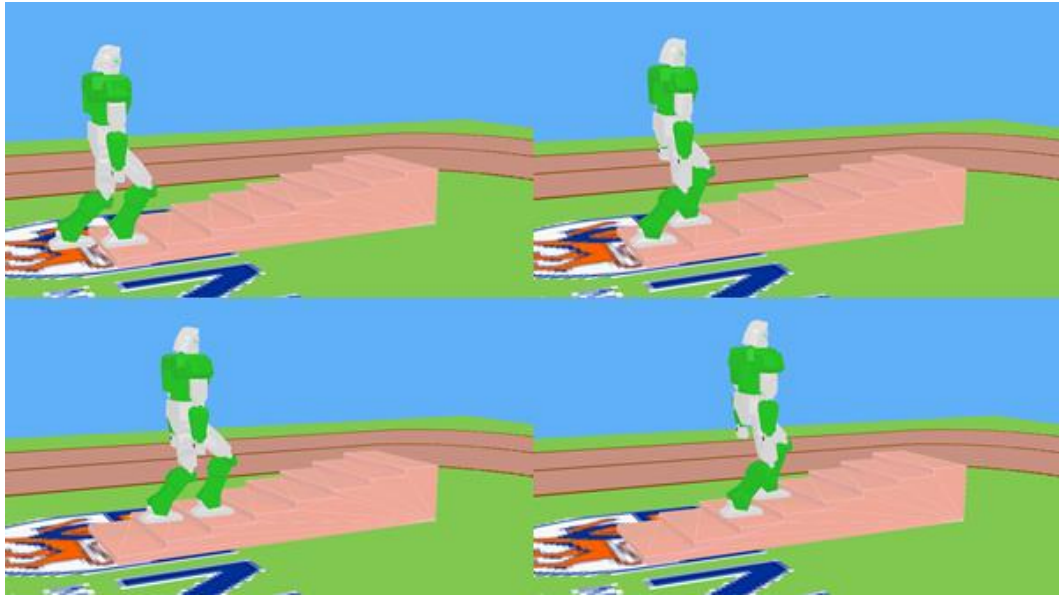


Figure 5.12 Stable Walking on Stair with unknown variations heights

Table 5.2 GA Set-up for the generation of optimization of weighting factors

Description	Remark
Fitness Function	f_1, f_2
Chromosome Representation	Real-valued (floating point)
Initial population	100
Generation number	200
Crossover	simple crossover arithmetic crossover heuristic crossover
Mutation operation	uniform mutation multi-non-uniform mutation boundary mutation
Weights for fitness function	$w_i = [100 \ 1]$

For this unknown stairs walking, the optimized weighting factors are $[r_1 \ r_2 \ p] = [0.533 \ 0.627 \ 0.973]$. Table 5.2 gives the set-up of the GA for the generation of optimization of weighting factors on the stairs.

The weights in fitness function are chosen to balance the both objectives to make them almost equally important. In this situation, the value of the fitness function is largest, indicating a good optimization performance.

The resulting ZMP and CoM trajectories obtained are shown in Fig. 5.16 for the x-direction. In the figure, ZMP_d , shown by the pink dash line, is the pre-planned “desired” ZMP trajectory based on the 65mm height stair. ZMP_a is the re-computed ZMP trajectory generated online using the moving ground reference map. ZMP_{real} is the trajectory of the ZMP of the robot obtained based on its actual CoM state. It can be seen that the adjusted ZMP_a (green dash line) deviates from the pre-defined ZMP_d from time = 4s . This indicates that using the proposed method, the adjusted ZMP_a had adapted quite quickly to the actual terrain profile. The real ZMP_{real} (red solid line) calculated based on the real CoM state is close to the adjusted ZMP.

Although the value of the fitness functions with GA is larger than the other situations. To exam how the weighting factors affect the performance of the moving ground reference map, we compare the adjusted ZMP reference with the pre-planned ZMP trajectory in another two experiments with extreme conditions. The first experiment was performed by letting $r_1 = r_2 = 0$ ($\mathbf{R} = \mathbf{0}$) and $p = 1$ while the second one was performed by letting $r_1 = r_2 = 1$ ($\mathbf{R} = \mathbf{I}$) and $p = 0$. Fig.5.16 shows the CoM and ZMP trajectories in x direction with the GA optimization. Fig 5.17 shows the CoM and ZMP trajectories with $\mathbf{R}=\mathbf{0}$, $p=1$, and Fig.5.18 shows the CoM and ZMP trajectories with. $\mathbf{R}=\mathbf{I}$; $p=0$

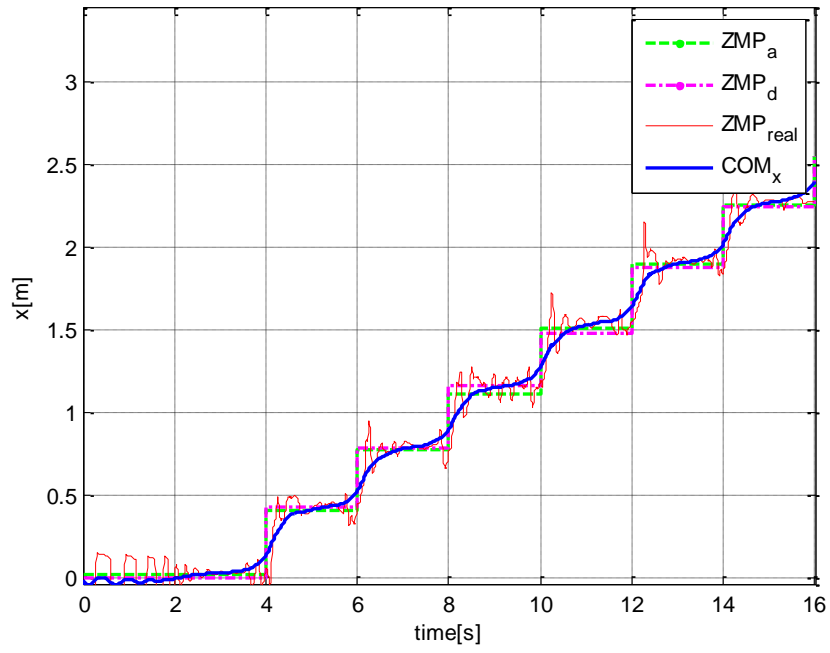


Figure 5.13 CoM and ZMP trajectories of biped walking on various heights stairs in x direction with the GA optimized weighting

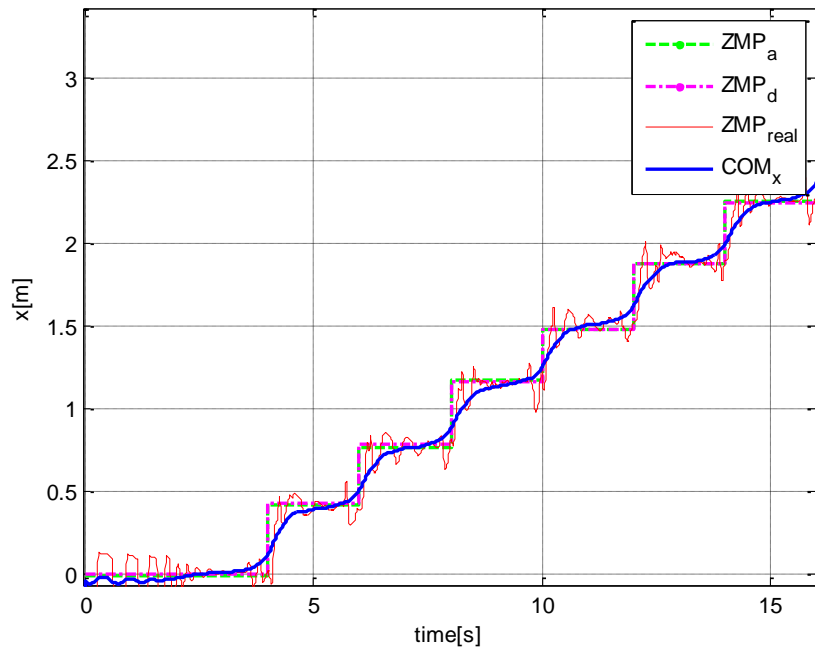


Figure 5.14 CoM and ZMP trajectories of biped walking on various heights stairs in x direction with $R=0$, $p=1$

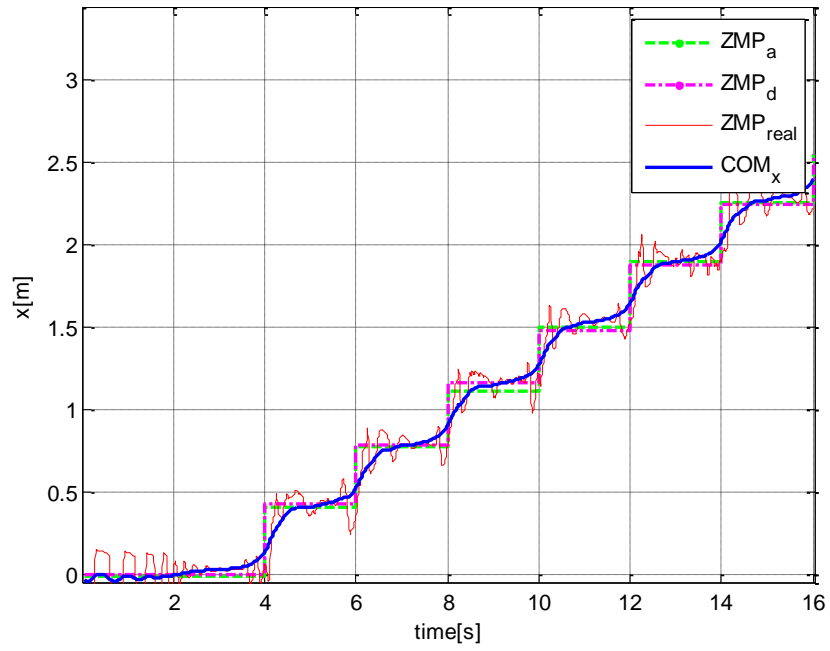


Figure 5.15 CoM and ZMP trajectories of biped walking on various heights stairs in x direction with $R=I$; $p=0$

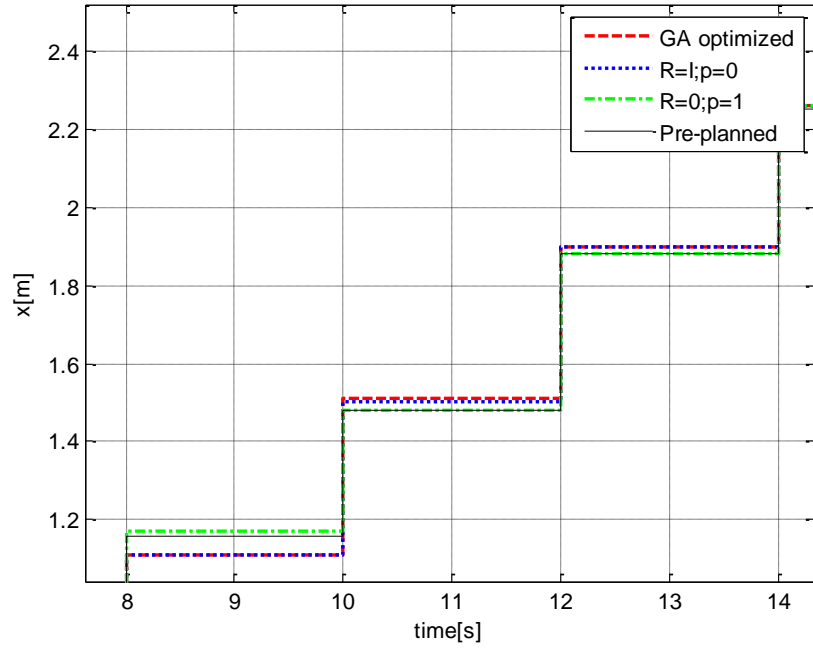


Figure 5.16 Comparison of difference adjusted ZMP reference of biped walking on various heights stairs in x direction

For the stairs with difference step heights, all of these three simulations can achieve the stable bipedal walking based on moving ground reference map with different weighting factors. The reference trajectories are shown in Fig 5.19. In the figure, the adjusted ZMP with $\mathbf{R}=\mathbf{0}$, $p=1$ was very closely to the pre-planned ZMP. It indicated that with larger weight on p , the moving ground reference will follow the pre-defined trajectory more closely.

In this simulations, at $time = 8s$, the robot started to walk onto the stair with height of $67mm$, which is higher than the normal $65mm$ height. The resulted foot placement location with GA optimized weighting factors and $\mathbf{R}=\mathbf{I}$; $p=0$ were smaller than the pre-planned, since the higher heights disturbance will reduce the velocity of CoM. Furthermore, when the robot walked onto the step with height of $63mm$ at $time = 10s$. The resulted step length with $\mathbf{R}=\mathbf{I}$ were higher than the one with $\mathbf{R}=\mathbf{0}$. It is because that the lower step height will result in higher CoM velocity when switching support foot. In order to balance the disturbance, the step length was increased as well.

From the comparison of the above situations, we can find that the optimized weighing factor in moving ground reference is affected by the terrain profiles. When the robot walks on gentle terrain, the weighting factor \mathbf{R} can be chosen larger to put more focus on disturbance rejection ability. When the robot walks on rough terrain, foot placement becomes more importance since landing locations are constrained to limited areas. Hence, the weighting factor p should be chosen smaller. In these cases, it may put more focus on the footstep location.

The corresponding trajectories in the y-direction are shown in Fig. 5.20. The stick diagram of the biped walking on the stairs is shown in Fig. 5.21. It can be seen that, with the proposed approach, the biped can walk on stairs with unknown step heights variation.

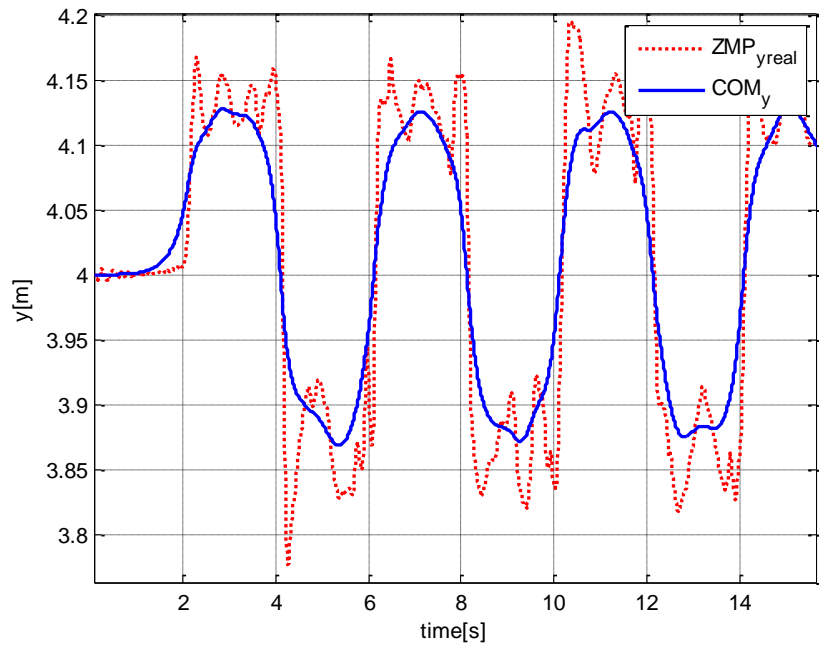


Figure 5.17 CoM and ZMP trajectories of biped walking on various heights stairs in y direction

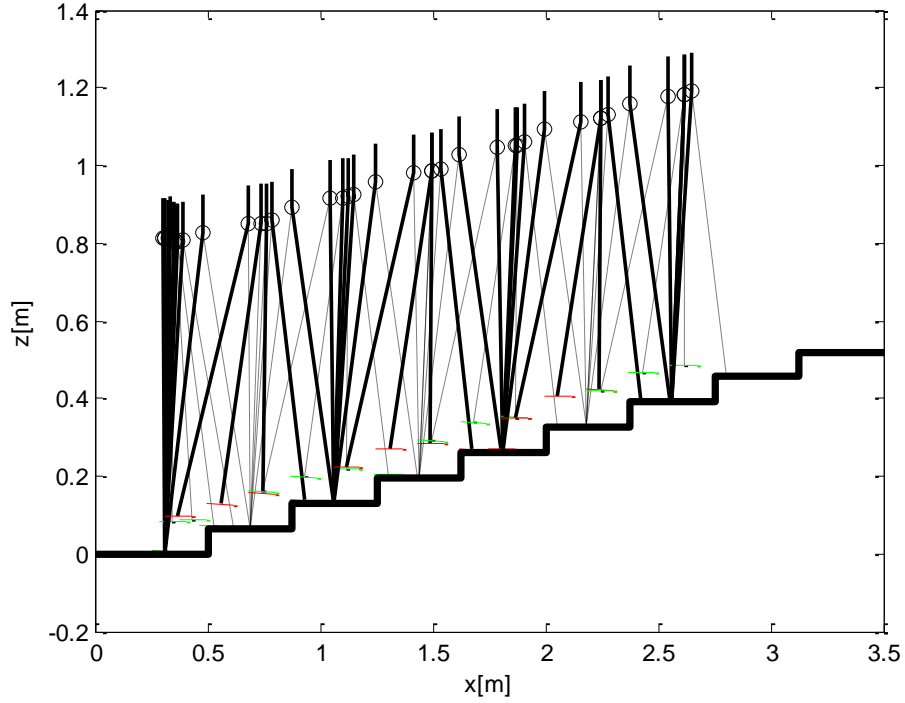


Figure 5.18 The stick diagram of the biped walking on the stairs

5.5 Summary

In this chapter, the control architecture for bipedal walking on uneven terrain is presented. The preview control with moving ground reference map is used to realize the bipedal robot locomotion on terrains with inaccurate information. Although the terrain information may not be accurate, stable walking could still be achieved. In the simulations, the preview control was incorporated to achieve better ground reference point tracking. For slope and stair terrain, the coordinate transformation matrix is derived. Simulation results have shown the effectiveness of the proposed approach with the robot achieving stable and smooth locomotion in spite of external disturbances and inaccurate information of the terrain.

Chapter 6

Conclusions

The main objective of this thesis is to analyze the dynamic control of bipedal robot walking, especially over uneven terrains. In particular, we analyzed the characteristics of uneven terrain walking for bipedal robot. Walking on flat terrains has been well studied and achieved, while the control of bipeds for stable walking on uneven terrains is still a challenge. In this thesis, therefore, the focus is on studying and developing suitable strategies which can be used to control a robot to achieve stable walking on uneven terrains in the presence of unexpected and unknown disturbances. An online adjustable walking pattern has been designed to realize more adaptive and stable walking motion on uneven terrains and also to handle the disturbance in real time.

6.1 Summary of Results

A systematic study on dynamics of bipedal locomotion has been conducted. This has led to a clearer understanding of the dynamics of a bipedal robot walking on uneven terrains. There are two main concerns in achieving stable bipedal robot walking on uneven terrains. One of these is disturbance rejection and the other is the accuracy of step location.

A moving ground reference map approach was proposed which, through online step adjustments and preview control, was shown to be capable of improving bipedal locomotion on uneven terrains with unexpected and unknown disturbances. In this approach, in order to improve the disturbance rejection ability, the next foot step location should be optimally adjusted to overcome the unknown disturbances. However, in certain situations, the robot needs to step on some specific locations, for example when it is required to cross a stream with stepping stones. Therefore, weighting factors are chosen in

the proposed moving ground reference map to balance the above two requirements depending on the situation. Robust walking trajectories can then be generated by applying the modified preview control, which can track the proposed moving ground reference map closely.

A simulation system has been developed to realize the algorithms walking over uneven terrain, which can optimize the CoM trajectory based on present and future information. According to the sensor readings, an allowable step region can be obtained and the moving ground reference map can be online generated. In addition, a preview control based on the modified linear inverted pendulum model was proposed and presented. Using our approach, given an uneven terrain, the robot can walk by following a pre-defined map and automatically modify its motion to achieve a more stable walking. Finally, a comparison using simulation of this new control algorithm and the preview control proved the effectiveness of this new proposed control algorithm.

6.2 Discussion of Practical Implementation

There are several requirements need to be considered before the proposed algorithm can be successfully implemented onto a real robot.

- Kinematics requirements:

The most important constraint is the ratio between the robot leg height and the unevenness of the terrain. It is intuitive that robot will not be able to walk on terrains filled with rocks or stairs similar to its own height. In this thesis, only achievable unevenness was present in the simulation environment. Large unevenness may require motion that is beyond the reach of the robot to balance itself. For example, velocity error due to large unevenness would require a robot to take a large step, which may be limited by the length of the legs.

Therefore, in this thesis, we emphasize on dealing with small unevenness that will result in taking steps within the reach of the robot.

- Dynamic requirements:

The other type of constraint one need to consider is the dynamic constraints. In order to quickly compensate for errors due to the unevenness, robot usually needs to respond fast. This would impose a high requirement on the power (velocity and torque) of the motor used on the robot. We tested the dynamic parameters in the flat terrain with some unknown unevenness. From the simulation studies, as shown in Table 6.1, the Root-Mean-Square (RMS) power consumption in the hip joints are higher than those of other joints. The peak power of each joint is in Table 6.2.

Table 6.1 Root-Mean-Square (RMS) power consumption in both legs

Joint	Hip Roll	Hip Pitch	Knee	Ankle Roll	Ankle Pitch
Left leg (W)	19.31	21.614	12.35	5.315	11.25
Right leg (W)	18.93	16.88	11.85	4.766	12.76

Table 6.2 Peak power (Max) in both legs

Joint	Hip Roll	Hip Pitch	Knee	Ankle Roll	Ankle Pitch
Left leg (W)	173.95	255.45	213.46	44.63	86.53
Right leg (W)	180.35	192.79	205.35	36.58	78.61

Therefore, in order to apply the proposed method on a robot with the same specification (height and weight, and joint length), the maximum power output at each joint needs to be larger than the Peak power shown in Table 6.2. Furthermore, the maximum torque and velocity should be considered as well. The velocity and torque consumption of each joint are shown in Fig. 6.1-6.4.

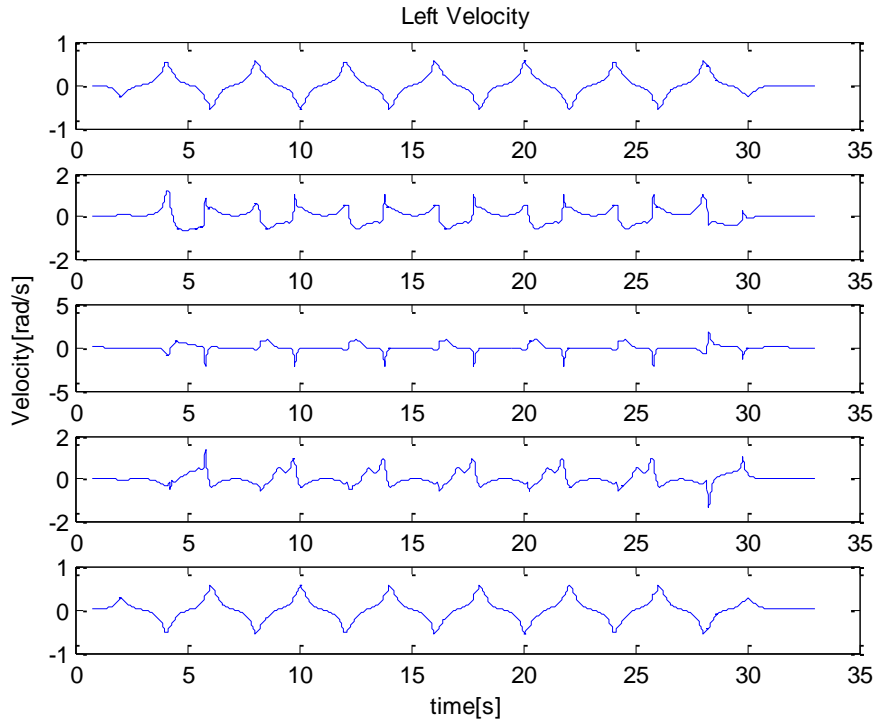


Figure 6.1 Left leg joints velocity, the sub-plots represent the joint velocity of: Hip Roll, Hip Pitch, Knee, Ankle Pitch, and Ankle Roll, respectively.

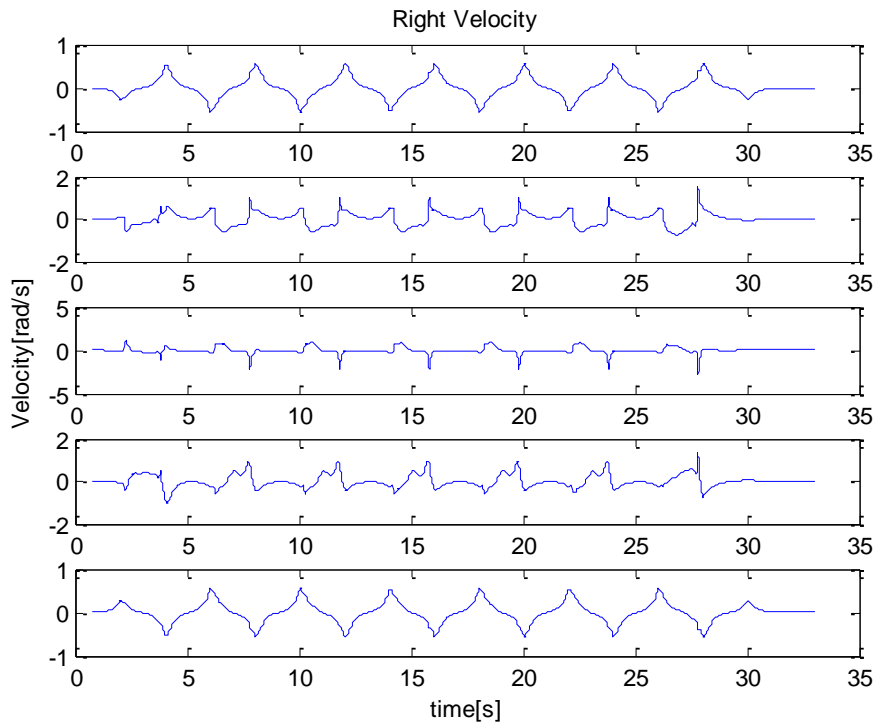


Figure 6.2 Right leg joints velocity, the sub-plots represent the joint velocity of: Hip Roll, Hip Pitch, Knee, Ankle Pitch, and Ankle Roll, respectively.

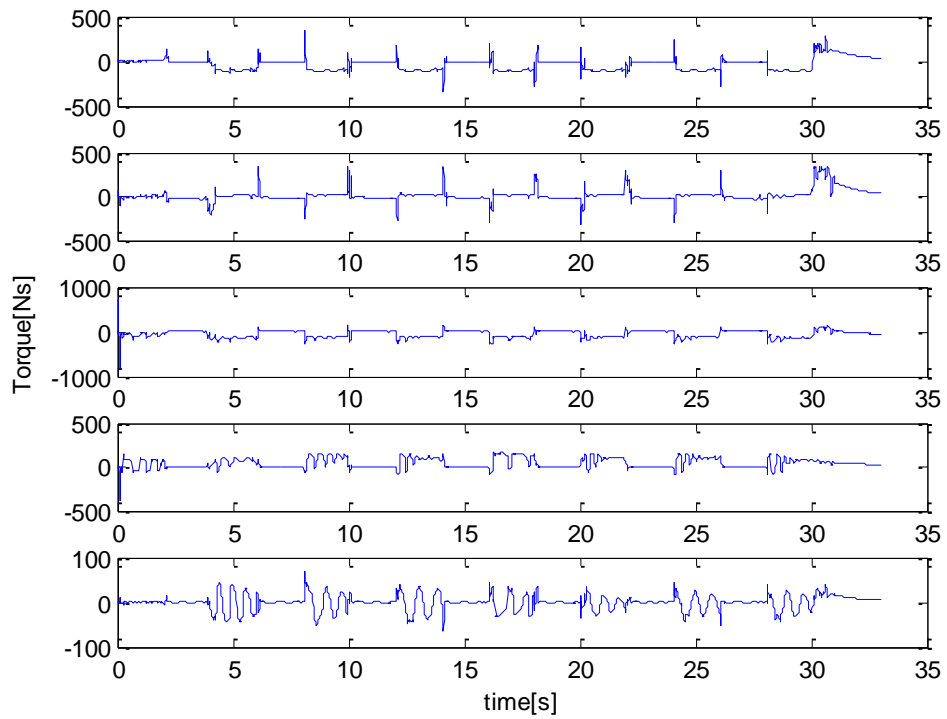


Figure 6.3 Right leg joints torque, the sub-plots represent the joint torque of: Hip Roll, Hip Pitch, Knee, Ankle Pitch, and Ankle Roll, respectively.

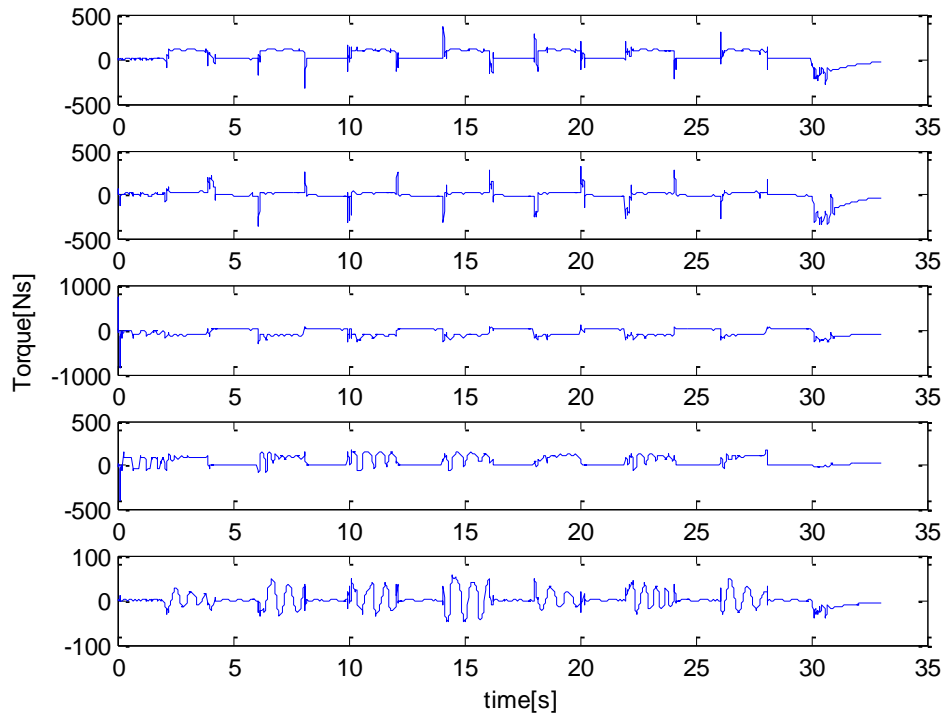


Figure 6.4 Left leg joints torque, the sub-plots represent the joint torque of: Hip Roll, Hip Pitch, Knee, Ankle Pitch, and Ankle Roll, respectively.

- Sensors requirements:

For the actual experiment, it is different with the simulation (Webots). GPS is not so accurate to satisfy our requirements. Gyro, accelerometer can be used to calculate the pelvis (Center of Mass) position, velocity and acceleration. Also, the 6-axis force torque sensors on the feet can be used to measure ZMP [56].

6.3 Contribution of the Research

The main contribution of this thesis is the development of a proposed approach which can adjust the footsteps to improve the stability of bipedal walking on uneven terrains with unknown features.

The simulation and experimental results confirmed that the proposed method is efficient in walking based on an optimal walking pattern. It not only takes into consideration the known terrain profiles but can also adapt to different unexpected and unknown disturbances.

Several previous approaches realized bipedal robot walking over uneven terrains by generating off-line pre-planned trajectories which maintain, at all times, the ZMP within the support polygon [1-3]. The main control strategy in these approaches is then to control the robot to follow the pre-computed trajectories accurately. Therefore for these approaches, the most important objective is the control of the robot to achieve maximum trajectory-tracking accuracy. Some researchers utilized different controllers to minimize the error between the robot states and the pre-defined desired state values. However, the robustness may be poor, which means that the control strategies may not be able to handle unknown and unexpected disturbances such as unknown push or unevenness on the ground. Attempts have been made to improve the disturbance rejection ability by generating the trajectories of the robots online [14, 38]. A natural walking motion can be generated and good disturbance rejection properties may be obtained using these approaches. However, for very rough terrains such as a staircase and a steep slope, these approaches may not work well and will need to be further improved.

Compared with the above related works, the results in this thesis show that the walking performance can be improved by implementing the proposed approach in this thesis. The improvements achieved can be attributed to taking into consideration of both profile of the uneven terrain and online feedback control.

An explanation and discussion on how the proposed approach works to achieve stable bipedal robot walking on uneven terrains is given. The use of a simplified dynamic model helped in the development of a proper controller which has been shown to improve disturbance rejection.

General control architecture has been developed for the generation of suitable foot locations and control of bipedal robot to improve its stability of walking over uneven terrains. An approach, named moving ground reference map, has been proposed which takes into consideration both allowable step regions and the robot's current state balance. Furthermore, the preview controller was used which was shown to be capable of efficiently generating, through an iterative procedure, motions which accurately track the desired CoM trajectories.

6.4 Limitations and Future Work

There are several limitations in the proposed scheme for bipedal robot walking on uneven terrains in this thesis.

Firstly, the model utilized in this thesis is LIPM (Linear inverted pendulum model), which is the simplest model for bipedal robots. The simple model allows for easier designs of controllers to control the robot precisely. However, the dynamics of the humanoid robot is highly complex. Although the use of a more complex model will make the design of a good controller more difficult, trajectory tracking performance will be more accurate. However, for the control of the locomotion of bipedal robots, it is more critical to improve the stability of robot walking than to improve the accuracy of tracking the reference trajectory [1]. Therefore, in the work described in this thesis, the simple LIPM model was used to achieve a more robust control. The simplest

LIPM model used in this work may be very inaccurate and the use of the accurate complex model may lead to controller design difficulties. Perhaps a model with an accuracy, and complexity, somewhere in between can be a good compromise. This could be a topic for further research.

Secondly, the impact force during landing of the swing foot was not taken into account in this work. In practice, this impact on foot landing can significantly affect the walking performance. The dynamics of this impact is very complicated and may not be easily incorporated into any control algorithm. Since it can be treated as an unexpected disturbance while walking, it is not considered in this thesis. To address this issue, future studies can be explored.

Thirdly, in the approach discussed in this thesis, stable walking was achieved by adjusting only the step location. However, humans change not only the step length but they also use their body motion to compensate for any disturbances, such as bending the torso, controlling the hip joint or using different motions of the arm. By adjusting additional parts of the robot in bipedal motion, its walking performance may be improved.

Fourthly, in this thesis, we mainly verified the proposed approach by dynamic simulation. In future, more experimental work should be conducted. More challenging environments, such as more steep slope (30-60 degree) and stair (20-30cm with 3-5cm unknown error), may be explored by applying the approaches proposed in this thesis.

Finally, real robot experiment is not conducted due to the above mentioned constraints. In future, more experimental works may be conducted to verify the proposed approach in this thesis.

Bibliography

1. Kajita, S., Kanehiro, F., Kaneko, K., Fujiwara, K., Harada, K., Yokoi, K., and Hirukawa, H. *Biped walking pattern generation by using preview control of zero-moment point*. 2003. Taipei.
2. Diedam, H., Dimitrov, D., Wieber, P.B., Mombaur, K., and Diehl, M. *Online walking gait generation with adaptive foot positioning through Linear Model Predictive control*. in *Intelligent Robots and Systems, 2008. IROS 2008. IEEE/RSJ International Conference on*. 2008.
3. Dimitrov, D., Wieber, P.B., Stasse, O., Ferreau, H.J., and Diedam, H. *An optimized Linear Model Predictive Control solver for online walking motion generation*. in *Robotics and Automation, 2009. ICRA '09. IEEE International Conference on*. 2009.
4. Herdt, A., Perrin, N., and Wieber, P.B. *Walking without thinking about it*. in *Intelligent Robots and Systems (IROS), 2010 IEEE/RSJ International Conference on*. 2010.
5. Wieber, P.B. *Viability and predictive control for safe locomotion*. in *Intelligent Robots and Systems, 2008. IROS 2008. IEEE/RSJ International Conference on*. 2008.
6. Wieber, P.B. *Trajectory Free Linear Model Predictive Control for Stable Walking in the Presence of Strong Perturbations*. in *Humanoid Robots, 2006 6th IEEE-RAS International Conference on*. 2006.
7. Manchester, I.R., Mettin, U., Iida, F., and Tedrake, R., *Stable dynamic walking over uneven terrain*. *International Journal of Robotics Research*, 2011. **30**(3): p. 265-279.
8. de Meneses, Y.L. and Michel, O. *Vision sensors on the webots simulator*. in *Virtual Worlds*. 1998: Springer.
9. Hohl, L., Tellez, R., Michel, O., and Ijspeert, A.J., *Aibo and Webots: Simulation, wireless remote control and controller transfer*. *Robotics and Autonomous Systems*, 2006. **54**(6): p. 472-485.
10. Michel, O. *Webots: Symbiosis between virtual and real mobile robots*. in *Virtual Worlds*. 1998: Springer.
11. Sakagami, Y., Watanabe, R., Aoyama, C., Matsunaga, S., Higaki, N., and Fujimura, K. *The intelligent ASIMO: system overview and integration*. in *Intelligent Robots and Systems, 2002. IEEE/RSJ International Conference on*. 2002.
12. Kaneko, K., Kanehiro, F., Kajita, S., Hirukawa, H., Kawasaki, T., Hirata, M., Akachi, K., and Isozumi, T. *Humanoid robot HRP-2*. in *Robotics and Automation, 2004. Proceedings. ICRA '04. 2004 IEEE International Conference on*. 2004.
13. Jungho, L., Jung-Yup, K., Ill-Woo, P., Baek-Kyu, C., Min-Su, K., Inhyeok, K., and Jun-Ho, O. *Development of a Humanoid Robot Platform HUBO FX-1*. in *SICE-ICASE, 2006. International Joint Conference*. 2006.
14. Pratt, G.A., *Legged robots at MIT: what's new since Raibert?* *Robotics & Automation Magazine, IEEE*, 2000. **7**(3): p. 15-19.

15. McGeer, T., *Passive dynamic walking*. International Journal of Robotics Research, 1990. **9**(2): p. 62-82.
16. Daan G. E. Hobbelen , M.W., ed. *Limit Cycle Walking*. 2007.
17. Collins, S., Ruina, A., Tedrake, R., and Wisse, M., *Efficient Bipedal Robots Based on Passive-Dynamic Walkers*. Science, 2005. **307**(5712): p. 1082-1085.
18. Chew, C.M. and Pratt, G.A., *Dynamic bipedal walking assisted by learning*. Robotica, 2002. **20**(5): p. 477-491.
19. Weiwei, H., Chee-Meng, C., Yu, Z., and Geok-Soon, H. *Pattern generation for bipedal walking on slopes and stairs*. in *Humanoid Robots, 2008. Humanoids 2008. 8th IEEE-RAS International Conference on*. 2008.
20. Hirai, K., Hirose, M., Haikawa, Y., and Takenaka, T. *The development of Honda humanoid robot*. in *Robotics and Automation, 1998. Proceedings. 1998 IEEE International Conference on*. 1998.
21. Dunn, E.R. and Howe, R.D. *Towards smooth bipedal walking*. in *Robotics and Automation, 1994. Proceedings., 1994 IEEE International Conference on*. 1994.
22. Pratt, J.E. and Tedrake, R., *Velocity-based stability margins for fast bipedal walking*, M. Diehl and K. Mombaur, Editors. 2006. p. 299-324.
23. Khalil, H.K., *Nonlinear systems*. 2001: Prentice Hall, 3rd edition,.
24. Coleman, M.J., *A stability study of a three-dimensional passive-dynamic model of human gait*. May, 1998, Cornell University, : United States.
25. Collins, S.H., Wisse, M., and Ruina, A., *A three-dimensional passive-dynamic walking robot with two legs and knees*. International Journal of Robotics Research, 2001. **20**(7): p. 607-615.
26. Goswami, A., Espiau, B., and Keramane, A. *Limit cycles and their stability in a passive bipedal gait*. in *Robotics and Automation, 1996. Proceedings., 1996 IEEE International Conference on*. 1996.
27. Hobbelen, D.G.E. and Wisse, M., *A disturbance rejection measure for limit cycle walkers: The gait sensitivity norm*. IEEE Transactions on Robotics, 2007. **23**(6): p. 1213-1224.
28. Hobbelen, D.G.E. and Wisse, M., *A Disturbance Rejection Measure for Limit Cycle Walkers: The Gait Sensitivity Norm*. Robotics, IEEE Transactions on, 2007. **23**(6): p. 1213-1224.
29. M.VUKOBRATOVIC, *On the Stability of Anthropomorphic Systems*. Mathematical Biosciences, 1972. **15**(1): p. 1-37.
30. Vukobratovi, M., *Biped locomotion: Dynamics, stability, control, and application*. 1990 Springer-Verlag (Berlin and New York) xiv, 349 p. .
31. Yamaguchi, J., Kinoshita, N., Takanishi, A., and Kato, I. *Development of a dynamic biped walking system for humanoid development of a biped walking robot adapting to the humans' living floor*. in *Robotics and Automation, 1996. Proceedings., 1996 IEEE International Conference on*. 1996.

32. Koolen, T., De Boer, T., Rebula, J., Goswami, A., and Pratt, J., *Capturability-based analysis and control of legged locomotion, Part 1: Theory and application to three simple gait models*. The International Journal of Robotics Research, 2012. **31**(9): p. 1094-1113.
33. Pratt, J., Koolen, T., de Boer, T., Rebula, J., Cotton, S., Carff, J., Johnson, M., and Neuhaus, P., *Capturability-based analysis and control of legged locomotion, Part 2: Application to M2V2, a lower-body humanoid*. The International Journal of Robotics Research, 2012. **31**(10): p. 1117-1133.
34. Pratt, J., Carff, J., Drakunov, S., and Goswami, A. *Capture Point: A Step toward Humanoid Push Recovery*. in *Humanoid Robots, 2006 6th IEEE-RAS International Conference on*. 2006.
35. Pratt, J.E. and Drakunov, S.V. *Derivation and Application of a Conserved Orbital Energy for the Inverted Pendulum Bipedal Walking Model*. in *Robotics and Automation, 2007 IEEE International Conference on*. 2007.
36. Kajita, S., Morisawa, M., Harada, K., Kaneko, K., Kanehiro, F., Fujiwara, K., and Hirukawa, H. *Biped Walking Pattern Generator allowing Auxiliary ZMP Control*. in *Intelligent Robots and Systems, 2006 IEEE/RSJ International Conference on*. 2006.
37. Hauser, K., Bretl, T., Latombe, J.-C., Harada, K., and Wilcox, B., *Motion Planning for Legged Robots on Varied Terrain*. The International Journal of Robotics Research, 2008. **27**(11-12): p. 1325-1349.
38. Chee-Meng, C., Pratt, J., and Pratt, G. *Blind walking of a planar bipedal robot on sloped terrain*. in *Robotics and Automation, 1999. Proceedings. 1999 IEEE International Conference on*. 1999.
39. Erez, T. and Smart, W.D. *Bipedal walking on rough terrain using manifold control*. in *Intelligent Robots and Systems, 2007. IROS 2007. IEEE/RSJ International Conference on*. 2007.
40. Kajita, S., Kanehiro, F., Kaneko, K., Fujiwara, K., Yokoi, K., and Hirukawa, H., *Biped walking pattern generation by a simple three-dimensional inverted pendulum model*. Advanced Robotics, 2003. **17**(2): p. 131-147.
41. Popovic, M.B., Goswami, A., and Herr, H., *Ground reference points in legged locomotion: Definitions, biological trajectories and control implications*. The International Journal of Robotics Research, 2005. **24**(12): p. 1013-1032.
42. Vukobratović, M. and Borovac, B., *Zero-moment point—thirty five years of its life*. International Journal of Humanoid Robotics, 2004. **1**(01): p. 157-173.
43. Popovic, M. and Englehart, A. *Angular momentum primitives for human walking: biomechanics and control*. in *Intelligent Robots and Systems, 2004. (IROS 2004). Proceedings. 2004 IEEE/RSJ International Conference on*. 2004.

44. Goswami, A., *Postural stability of biped robots and the foot-rotation indicator (FRI) point*. The International Journal of Robotics Research, 1999. **18**(6): p. 523-533.
45. Borelli, G.A., *De Motu Animalium* (English translation by P. Maquet, Spring-Verlag, Berlin, 1989). 1680.
46. Elftman, H., *The measurement of the external force in walking*. Science, 1938. **88**(2276): p. 152-153.
47. Westervelt, E.R., Grizzle, J.W., Chevallereau, C., Choi, J.H., and Morris, B., *Feedback control of dynamic bipedal robot locomotion*. 2007: CRC press Boca Raton.
48. Vukobratovic, M., *Biped locomotion*. 1990: Springer-Verlag New York, Inc.
49. Vukobratovic, M. and Juricic, D., *Contribution to the synthesis of biped gait*. Biomedical Engineering, IEEE Transactions on, 1969(1): p. 1-6.
50. Nishiwaki, K. and Kagami, S. *Strategies for adjusting the ZMP reference trajectory for maintaining balance in humanoid walking*. in *Robotics and Automation (ICRA), 2010 IEEE International Conference on*. 2010.
51. Michalewicz, Z., *Genetic algorithms+ data structures= evolution programs*. 1996: springer.
52. Yang, L., Chew, C.-M., Zielinska, T., and Poo, A.-N., *A uniform biped gait generator with offline optimization and online adjustable parameters*. Robotica, 2007. **25**(5): p. 549-565.
53. Davis, L., *Handbook of genetic algorithms*. 1991.
54. Tomizuka, M. and Rosenthal, D.E., *On the Optimal Digital State Vector Feedback Controller With Integral and Preview Actions*. Journal of Dynamic Systems, Measurement, and Control, 1979/06/00/. **101**(2): p. 7.
55. Athans, M., *On the design of PID controllers using optimal linear regulator theory*. Automatica, 1971. **7**(5): p. 643-647.
56. Kajita, S., Hirukawa, H., Harada, K., and Yokoi, K., *Introduction to Humanoid Robotics*. 2014: Springer Berlin Heidelberg.

Appendix I: Realistic humanoid robot model details

A.1 Dimensions

Fig. A.1 shows the dimensions of the realistic bipedal model.

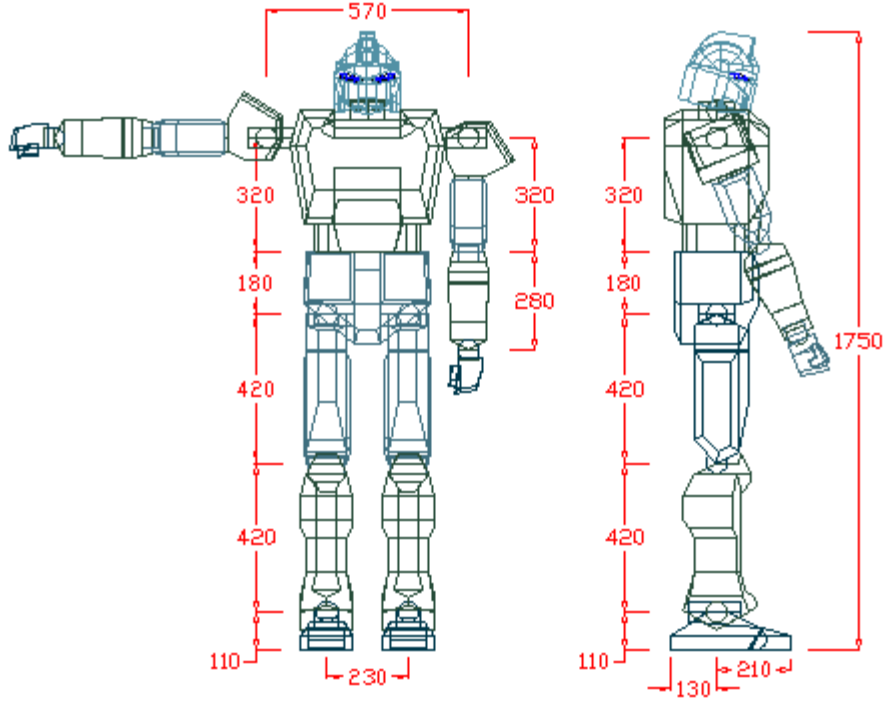
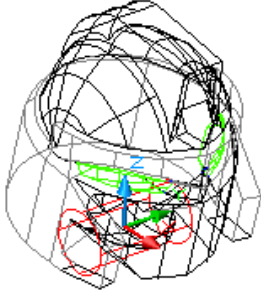
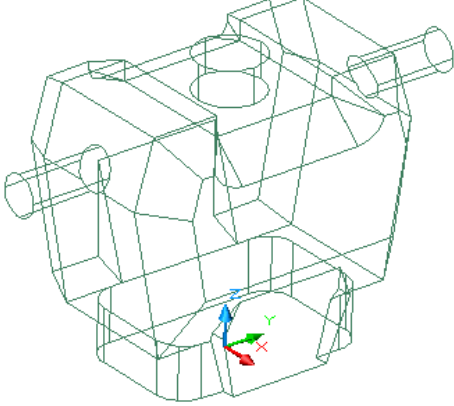
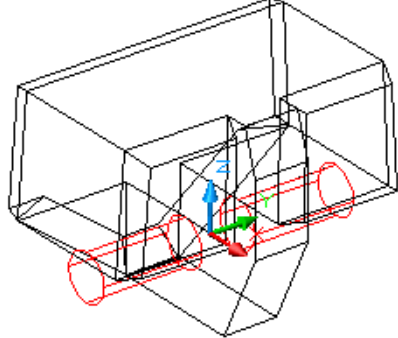


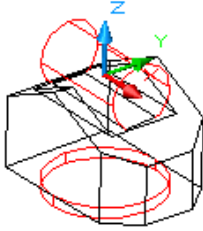
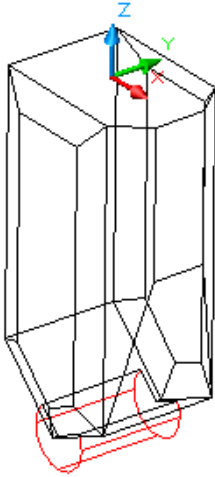
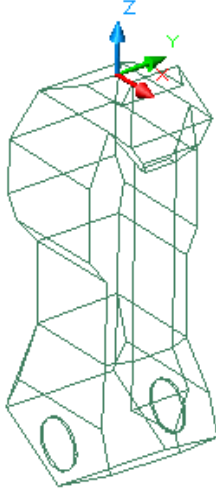
Figure A.1 Simulated bipedal robot dimensions (mm)

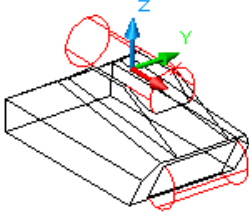
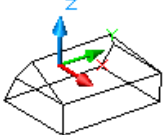
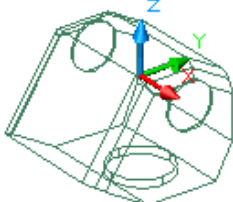
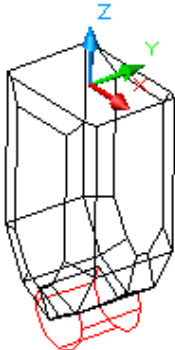
A.2 Dynamic of Model

Table A.1 shows the parts of the model and its COM location ($[x \ y \ z]$) and inertia matrices (I). The COM locations are located with respect to the origin of the part (the origin of the coordinate system on the right figure).

Table A.1 Simulated bipedal robot model

<p>Head</p> <p>$mass = 3.09Kg$</p> <p>$[x_{com} \ y_{com} \ z_{com}] = [0.01 \ 0 \ 0.13](m)$</p> <p>$I = \begin{bmatrix} 0.0178 & 0 & 0 \\ 0 & 0.0179 & 0 \\ 0 & 0 & 0.0012 \end{bmatrix} (Kg m^2)$</p>	
<p>Torso</p> <p>$mass = 13Kg$</p> <p>$[x_{com} \ y_{com} \ z_{com}] = [0 \ 0 \ 0.23](m)$</p> <p>$I = \begin{bmatrix} 1.25 & 0 & 0 \\ 0 & 0.89 & 0 \\ 0 & 0 & 0.46 \end{bmatrix} (Kg m^2)$</p>	
<p>Pelvis</p> <p>$mass = 26.44Kg$</p> <p>$[x_{com} \ y_{com} \ z_{com}] = [-0.01 \ 0 \ 0.08](m)$</p> <p>$I = \begin{bmatrix} 0.7 & 0 & 0 \\ 0 & 0.53 & 0 \\ 0 & 0 & 0.54 \end{bmatrix} (Kg m^2)$</p>	

<p>Hip</p> <p>$mass = 2.54Kg$</p> <p>$[x_{com} \ y_{com} \ z_{com}] = [0 \ 0 \ -0.01](m)$</p> <p>$I = \begin{bmatrix} 0.02 & 0 & 0 \\ 0 & 0.01 & 0 \\ 0 & 0 & 0.01 \end{bmatrix} (Kgm^2)$</p>	
<p>Thigh</p> <p>$mass = 4.69Kg$</p> <p>$[x_{com} \ y_{com} \ z_{com}] = [0 \ 0.01 \ -0.17](m)$</p> <p>$I = \begin{bmatrix} 0.19 & 0 & 0 \\ 0 & 0.19 & 0 \\ 0 & 0 & 0.01 \end{bmatrix} (Kgm^2)$</p>	
<p>Shank</p> <p>$mass = 8.63Kg$</p> <p>$[x_{com} \ y_{com} \ z_{com}] = [0.01 \ 0 \ -0.31](m)$</p> <p>$I = \begin{bmatrix} 0.95 & 0 & 0 \\ 0 & 0.95 & 0 \\ 0 & 0 & 0.03 \end{bmatrix} (Kgm^2)$</p>	

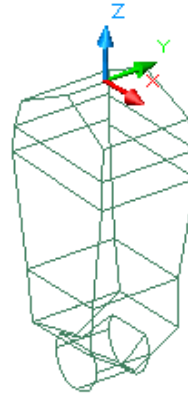
<p>Foot</p> <p>$mass = 2.2Kg$</p> <p>$[x_{com} \ y_{com} \ z_{com}] = [0.01 \ 0 \ -0.06](m)$</p> <p>$I = \begin{bmatrix} 0.02 & 0 & 0 \\ 0 & 0.02 & 0 \\ 0 & 0 & 0.01 \end{bmatrix} (Kg m^2)$</p>	
<p>Toe</p> <p>$mass = 0.53Kg$</p> <p>$[x_{com} \ y_{com} \ z_{com}] = [0.013 \ 0 \ 0.012](m)$</p> <p>$I = \begin{bmatrix} 0.0014 & 0 & 0 \\ 0 & 0.0009 & 0 \\ 0 & 0 & 0.002 \end{bmatrix} (Kg m^2)$</p>	
<p>Shoulder</p> <p>$mass = 1.09Kg$</p> <p>$[x_{com} \ y_{com} \ z_{com}] = [0.002 \ 0 \ -0.113](m)$</p> <p>$I = \begin{bmatrix} 0.0178 & 0 & 0 \\ 0 & 0.0179 & 0 \\ 0 & 0 & 0.0012 \end{bmatrix} (Kg m^2)$</p>	
<p>Upper Arm</p> <p>$mass = 0.73Kg$</p> <p>$[x_{com} \ y_{com} \ z_{com}] = [0.0002 \ 0 \ -0.0066](m)$</p> <p>$I = \begin{bmatrix} 0.0053 & 0 & 0 \\ 0 & 0.0049 & 0 \\ 0 & 0 & 0.0011 \end{bmatrix} (Kg m^2)$</p>	

Lower Arm

$$mass = 1.19Kg$$

$$\begin{bmatrix} x_{com} & y_{com} & z_{com} \end{bmatrix} = \begin{bmatrix} -0.012 & 0 & -0.165 \end{bmatrix} (m)$$

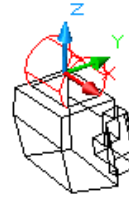
$$I = \begin{bmatrix} 0.0044 & 0 & 0 \\ 0 & 0.0439 & 0 \\ 0 & 0 & 0.0011 \end{bmatrix} (Kg m^2)$$

**Hand**

$$mass = 0.43Kg$$

$$\begin{bmatrix} x_{com} & y_{com} & z_{com} \end{bmatrix} = \begin{bmatrix} -0.061 & 0 & -0.0749 \end{bmatrix} (m)$$

$$I = \begin{bmatrix} 0.0036 & 0 & 0 \\ 0 & 0.0032 & 0 \\ 0 & 0 & 0.0005 \end{bmatrix} (Kg m^2)$$



Appendix II: Description of NUSBIP-III ASLAN

B.1 Brief History

There has been numerous bipedal robot in different sizes developed as the platforms of researches by the Legged locomotion Group (LLG) of National University of Singapore (NUS). Among the smaller platforms are the RO-PE I-VI series, which has been participating in Robocup kid size. Besides this smaller platform, LLG also has been developing the human-sized bipedal series, called NUSBIP.

The NUSBIP-III ASLAN is the latest, third generation of NUSBIP series. It has been developed since early 2008. It is developed mainly as a general platform for bipedal walking research.

B.2 Current Development

ASLAN significantly improves the existing physical bipedal robot, NUSBIP-II, especially in the physical structure and the actuator subsystem. The structure of the legs has been improved and the joints are upgraded using the harmonic drives system, which gives excellent power and accuracy with zero backlash. The servos are controlled by ELMO motor drivers, connected to the main PC 104 microprocessor via CAN bus system. By using these systems, ASLAN has achieved stable dynamic walking motions. Next, two arms and one waist joint have been added on the body, and new sensors have been added into the system. Fig. B.1 shows the mechanical design and the early realization of ASLAN.

ASLAN is a humanoid robot modeled after a teenager. It has a trunk with two legs, two arms and one waist joint. Its weight is approximately 60kg and hip height is around 0.7m when the robot is standing. The general specifications of ASLAN are shown in Table B.1.

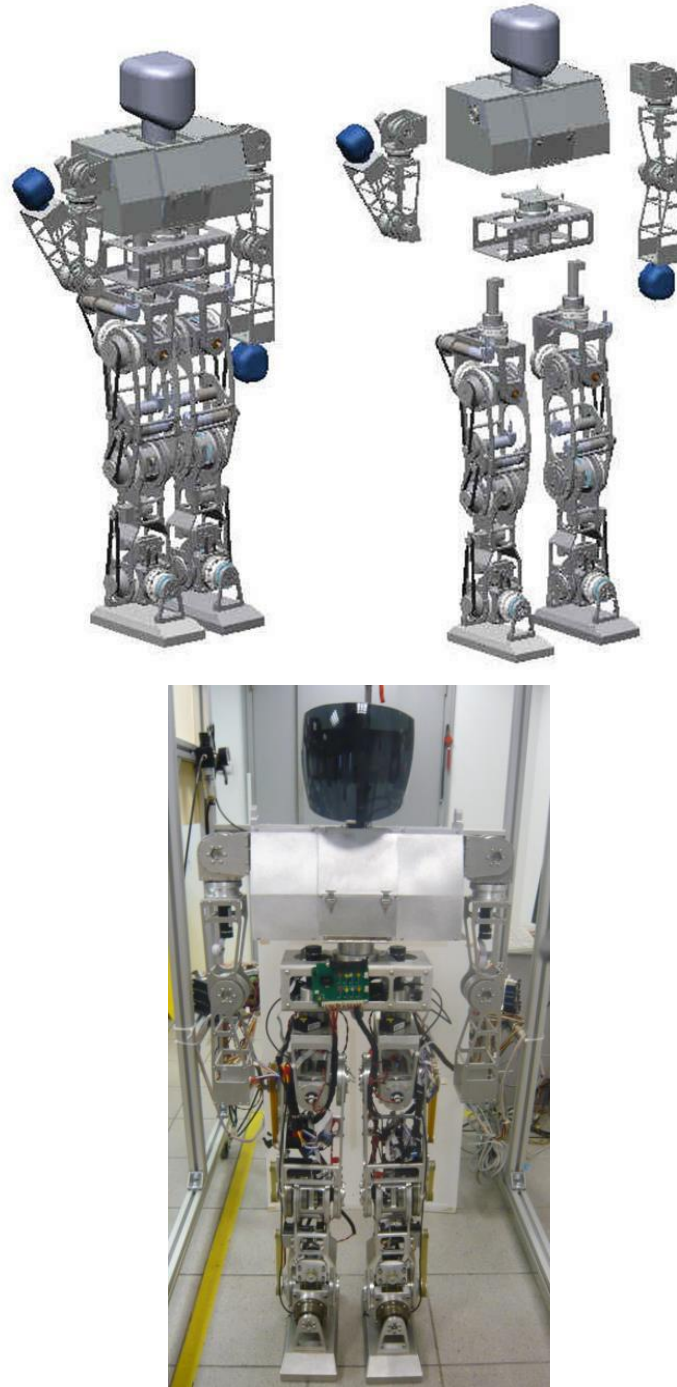


Figure B.1 Mechanical drawing and realization of NUSBIP-III ASLAN

ASLAN has six DOFs on each leg: three at the hip, one at the knee, and two at the ankle; four degrees of freedom on each arm: three at the shoulder, one at elbow. The DOFs at the hip allow the leg to twist and adduct/abduct, as well as swing forward and backward. The DOF at the knee allows the leg to flex.

The DOFs at the ankle allow the foot to pitch and roll. Fig. B.2 shows the leg configuration.

Table B.1 Specification of NUSBIP-III ASLAN

Height	1350mm
Width	550mm
Weight	60Kg
Walk speed	0.3m/s
Actuator	servomotor + harmonic gear + drive unit
Control Unit	PC/104 + ELMO + CAN bus system
Operation system	Windows XP RTX

The torso is designed with strategic sensory system, battery, and main processors placement in mind. The main processor is located at the top center section of the chest, providing ventilation from above the torso. The inertial sensory system such as gyros and accelerometers are designed to be placed in the middle chest section as well, above the COM. The battery is placed in the belly, very near to the COM, with a hatch in front of the chest for easy access. The side areas of the chest are used to storage other hardware and ELMO motor drivers. Figure B.3 shows the torso design.

Several off-line walking algorithms have been tested on ASLAN, such as the ZMP preview control by Kajita *et al.* [1]. Several task such as walking, turning, climbing a known slope and stair has been realized. However, an off-line walking algorithm is not ideal for long term robust walking development.

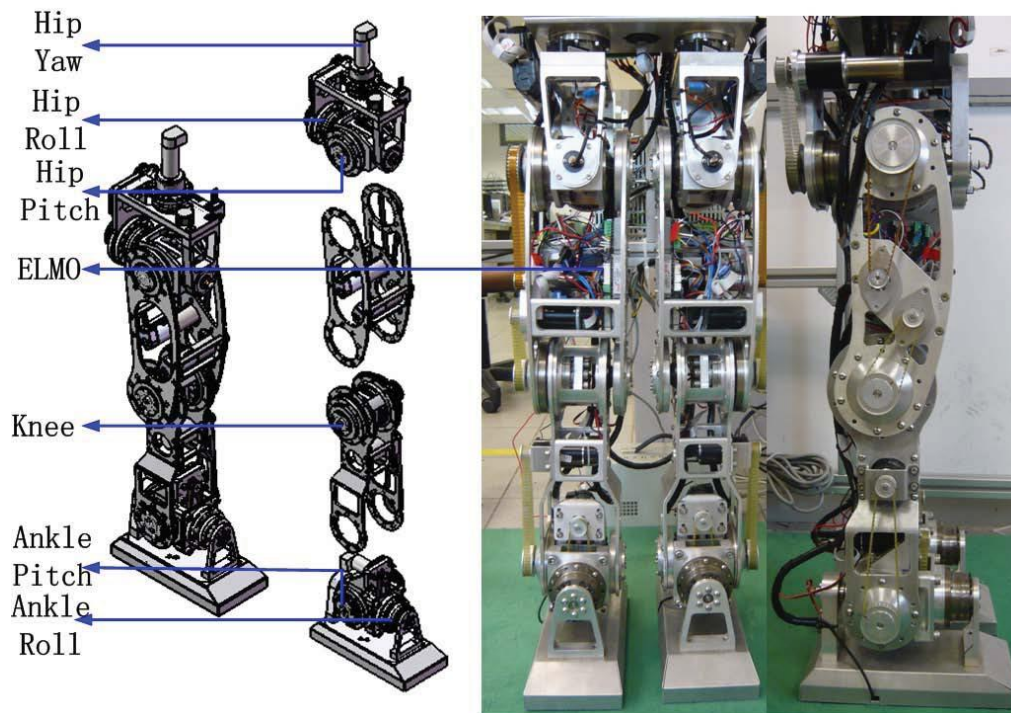


Figure B. 2 NUSBIP-III ASLAN legs.

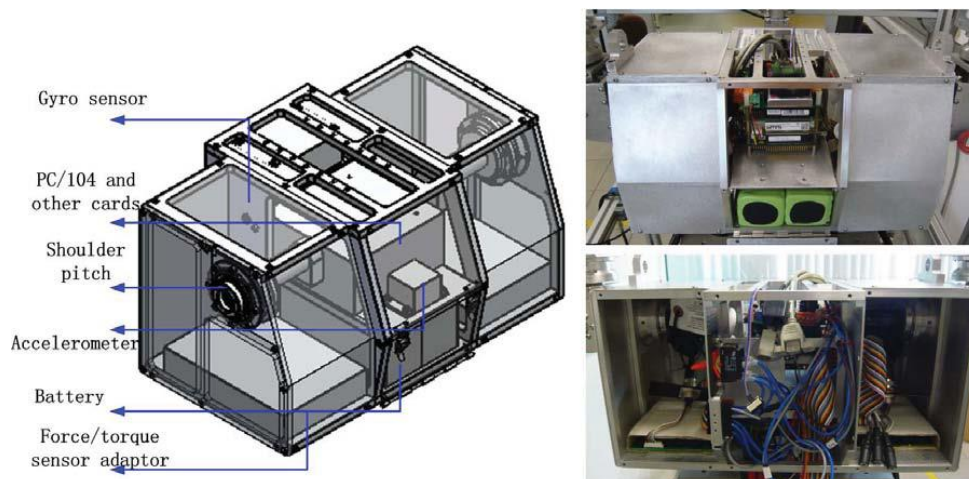


Figure B. 3: NUSBIP-III ASLAN torso design.

Some basic behavior has been successfully developed. It is able to do forward walking, backward walking, turning, side stepping, and kicking. In June 2010, ASLAN participated in the ROBOCUP humanoid adult size category, where our team, team RO-PE, manage to won the first prize for the adult size soccer competition and the adult size technical challenge. Figure B.4 shows ASLAN in a soccer match against other bipedal robot during ROBOCUP 2010.



Figure B. 4: NUSBIP-III ASLAN kicking for goal in ROBOCUP 2010 finale.

B.3 Potential future plans

Several improvements are required in order to realize the approach presented in this thesis. As discussed in section 6.2. Firstly, the implementation of a reliable sensory system, which is crucial for the calculation of the moving ground reference point. Secondly, a faster walking behavior needs to be realized. Currently, ASLAN is walking with 0.64s stepping time, which is very close to its minimum stepping time. A possible solution would be to implement the brushless motors for the knees and ankles, which could improve the maximum joint speed and acceleration. Thirdly, the weight of the legs needs to be reduced. Currently ASLAN's COM is too low, which makes fast dynamic walking with big steps very difficult. Mechanical modifications are currently in progress.